THE GENERATION AND CHARACTERIZATION OF A HUMAN INDUCED PLURIPOTENT STEM CELL MODEL FOR THE TUBEROUS SCLEROSIS COMPLEX

by:

AVERY ZUCCO

A dissertation submitted to the

School of Graduate Studies

Rutgers, The State University of New Jersey

In partial fulfillment of the requirements

For the degree of

Doctor of Philosophy

Graduate Program in Neuroscience and Cell Biology

Written under the direction of:

Gabriella D'Arcangelo

Approved by:

_____

_____

_____

_____

_____

New Brunswick, New Jersey

OCTOBER 2018

ABSTRACT OF THE DISSERTATION

The Generation and Characterization of a Human Induced Pluripotent Stem Cell Model for the Tuberous Sclerosis Complex

By AVERY ZUCCO

Dissertation Director:
Gabriella D'Arcangelo

Tuberous sclerosis complex (TSC) is an autosomal dominant disorder caused by the mutation of either the *TSC1* or *TSC2* genes and characterized by the presence of benign cortical lesions known as cortical tubers. A large proportion of patients with TSC exhibit neurological symptoms including epilepsy and intellectual disability, and a further 50% meet the diagnostic criteria for Autism. However, the appearance of this broad spectrum of neurologic manifestations does not always correlate with the neuroanatomical defects common to TSC, suggesting the possibility of underlying functional defects affecting neural development in TSC patients. Here we have utilized neural progenitor cells (NPCs) capable of fully differentiating into neurons, which carry a heterozygous *TSC2* mutation generated from patient-derived induced pluripotent stem cells (iPSCs) to investigate TSC cellular and molecular phenotypes. In these cell lines we observe that *TSC2* +/- NPCs exhibit changes in cell signaling along the Akt/mTORC1 signaling axis. This pathway is classically affected in TSC, with elevated pS6 and decreased phospho-Akt levels known as neuropathological hallmarks in knockout mouse models and studies of abnormal human tissue. Consistent with these previous findings we observed a decrease in the activity of AKT as

measured by levels of phospho-AKT Thr308 and Ser473. Evidence of increased mTORC1 signaling was seen in one patient, but not another, suggesting *TSC2* heterozygosity may produce modest signaling changes near a functional threshold for generating a molecular phenotype in NPCs. TSC2 heterozygous NPCs also exhibited a reduced capacity to produce neurons in vitro, suggesting that neural development may be impacted in TSC. Moreover, this phenotype was reproduced upon AKT inhibition of control NPC lines, but was unaffected under treatment with rapamycin, suggesting that AKT signaling may play a more prominent role in mediating the neurodevelopmental defects of TSC than previously thought.

Acknowledgements

The work contained in this thesis was supported by the efforts of numerous individuals:

Dr. Gabriella D'Arcangelo Ph.D. was the graduate mentor, project advisor and principal investigator for this project.

Dr. Ronald P. Hart Ph.D. served on the dissertation committee and provided the analysis of RNA-Seq data as well as other project advising.

Dr. Cheryl Dreyfus Ph.D., Dr. Estella Jacinto Ph.D. and Dr. Mladen-Roko Rasin M.D., Ph.D. all served on the dissertation committee and advised on this project.

Dr. John Pintar Ph.D. provided graduate student advising and mentorship.

Dr. Orrin Devinsky M.D. enrolled all subjects included in this study.

Dr. Jennifer Moore Ph.D. and Rutgers University Cell and DNA Repository (RUCDR) generated and cultured all iPSC lines used in this study.

Valentina Dal Pozzo M.S., Alina Afinogenova B.S., Beth Crowell B.A., Natalie Samper and Saad Mansuri performed experiments including cell culture, immunofluorescence staining, Western blotting, DNA sequencing and image analysis.

Dr. Noriko Goldsmith Ph.D. provided technical assistance for automated high-content microscopy and image analysis.

Joan Mordes and Lauryn Siu provided administrative assistance.

Funding was provided via grants from the National Institute of Health (NIH R21 grant NS089441), the Tuberous Sclerosis Alliance (TSA Grant #332884), the Human Genetics Institute of New Jersey (HGINJ) and Finding a Cure for Epilepsy and Seizures (FACES).

The Neuroscience and Cell Biology graduate program at Rutgers University, Robert Wood Johnson Medical School.

The Dept. of Cell Biology and Neuroscience, Rutgers University.

The W.M. Keck Center for Collaborative Neuroscience.

NeuroConnections graduate student association.

And finally, all my friends, family and peers who helped in all the many ways, every day that allowed me to see this endeavor through to completion.

Table of Contents

List of Tables

List of Figures

Chapter I: Background - Tuberous Sclerosis Pathology, Genetics and Molecular Phenotypes

Tuberous Sclerosis Complex (TSC) is a multisystem genetic disorder characterized by various neurological and neuroanatomical manifestations, and tumors. Affecting approximately 1 in 6000 live births worldwide, TSC is one of the leading genetic causes of intractable childhood epilepsy, autism, intellectual and learning disability (de Vries et al., 2015; Khwaja and Sahin, 2011; Lewis et al., 2004; Osborne et al., 1991; Sahin et al., 2016). Childhood epilepsy is present in upwards of 85% of individuals with TSC (Chu-Shore et al., 2010). Additionally, TSC and Autism Spectrum Disorder (ASD) co-morbidity rates are between 25% and 50% based on surveys of individuals with TSC and their families (Hunt and Shepherd, 1993; Smalley et al., 1992). TSC has an autosomal dominant pattern of inheritance and all known individuals with the disease have a heterozygous genotype for one of two genes: *TSC1 or TSC2*. The heterozygous mutation of these genes is the recognized etiology for TSC with nearly two-thirds of diagnoses resulting from spontaneous, de-novo mutations not found in either parent (Northrup et al., 1993).

TSC is characterized by multisystem involvement and wide phenotypic variability. Multisystem involvement can involve renal neoplasms, lung cysts similar to lymphangioleiomyomatosis (LAM), rhabdomyomas in the striated muscle of the heart, retinal lesions, facial angiofibroma, shagreen patch and other skin lesions, among the formation of various other hamartomas are often found in many cases of TSC (Crino et al., 2010b). However, the brain is one of the most commonly affected organs and neuropathologic features are present in a majority of individuals with TSC. The primary neuroanatomical features of TSC include abnormal lesions or “tubers” in the brain, which are hamartomas, as well as other noncancerous brain tumors.

It is currently understood that many of the neuroanatomical defects present in TSC such as cortical tubers and other brain lesions are the result of loss-of-heterozygosity (LOH) where one

allele carries a germline mutation and the remaining intact *TSC1* or *TSC2* allele either receives a subsequent somatic mutation or is otherwise functionally inactivated to produce a focal homozygous loss of function (Henske et al., 1997; Sepp et al., 1996). The loss of functional TSC1 (Hamartin) or TSC2 (Tuberin) protein in these abnormal regions leads to excessive cell growth and lesion formation characterized by elevated levels of mTORC1 activity. The mTORC1 complex is a critical regulatory kinase complex which promotes growth by effecting multiple processes including protein synthesis and metabolism (Jewell and Guan, 2013). Together TSC1 and TSC2 form a heterodimeric complex which regulates mTORC1 by suppressing the activity of the small GTP-binding protein Rheb. In its GTP-bound state Rheb is an important activator of mTORC1, and acts to transduce upstream pro-growth signaling through mTORC1. Within the TSC1/TSC2 complex TSC2 is the component directly responsible for regulatory activity due to the presence of a GTPase activating protein (GAP) domain near the C-terminus. The activity of TSC2 maintains Rheb in an inactive GDP-bound state. Rheb, and thus downstream mTORC1 activity is normally curtailed by the TSC complex (Huang and Manning, 2008; Inoki et al., 2003a). Due to their critical role in regulating cell growth the TSC proteins are also prominent tumor suppressors. Indeed, mTORC1 activity is elevated in TSC-associated lesions and tumors, and can be readily detected by measuring levels of phosphorylated mTORC1 targets such as S6 Kinase 1 (S6K1) or its downstream target ribosomal subunit protein S6 (S6), and the cap-dependent translation initiation factor 4E-BP1 (Chan et al., 2004; Crino, 2011). However, while mTORC1 activation is clearly elevated in TSC-associated lesions that contain homozygous *TSC1* or *TSC2* null cells resulting from LOH, it is not overtly elevated in non-lesion tissue areas which contain normally-appearing heterozygous cells. Whether mTORC1 hyperactivity in null cells is responsible for all clinical symptoms of TSC is presently unclear.

Several lines of evidence suggest that *TSC1* or *TSC2* heterozygous cells contribute to TSC neurological manifestations. For example, it has been shown that the number of cortical tubers (cortical tuber load) does not correlate well with the degree of neurological impairment in human TSC patients (Lyczkowski et al., 2007; Ridler et al., 2004). Some individuals with TSC exhibit severe neurological impairments yet have no obvious neuroanatomical defects as shown by neuroimaging studies (Erol et al., 2015). Additionally, animal studies have shown that haploinsufficiency of *Tsc1* and *Tsc2* can produce abnormal cognitive and behavioral phenotypes reminiscent of those observed in TSC in the complete absence of LOH lesions (Chevere-Torres et al., 2012; Ehninger et al., 2008; Goorden et al., 2007). These observations suggest that *TSC1* or *TSC2* heterozygous cells from non-lesion brain regions may contribute to the overall disease symptomology in TSC. Moreover, the broad behavioral and intellectual impairments present in many patients suggest the disruption of normal developmental processes responsible for brain formation and synaptic connectivity, raising the possibility that these defects may be driven by subtle, and yet unidentified molecular abnormalities in TSC heterozygous cell populations.

Neuropathological and Cognitive Hallmarks of TSC

TSC is frequently associated with the formation of noncancerous tumors which may affect any organ system in the body including the central nervous system. One of the earliest detailed descriptions of TSC by French neurologist Desire-Magloire Bourneville in 1880 described the neuropathology of a child with seizures and learning disability (Bourneville and Brissaud, 1880). He coined the term “tuberous sclerosis of the cerebral convolutions” to describe the observed CNS pathology. In 1942 the term “tuberous sclerosis complex” was first used by Sylvan Moolten to describe the multisystem disorder including involvement of skin, heart, brain, kidneys, lungs, eyes

and other organ systems (Moolten, 1942). These early observations provided some of the first descriptions of the neuroanatomical defects which have become key hallmarks used to identify TSC. Further observation and studies have led to the identification of three main types of brain malformations recognized in TSC: cortical tubers, subependymal nodules (SENs) and subependymal giant cell astrocytomas (SEGAs).

Perhaps the most prominent feature associated with TSC is the appearance of focal malformations known as cortical tubers. Cortical tubers are readily detected in older children and adults through magnetic resonance imaging (MRI) imaging where they appear as hyperintense regions in T2 weighted and FLAIR images, or low intensity regions in T1 weighted images (DiMario, 2004; Grajkowska et al., 2010). Tubers can be detected by fetal MRI as early as 20 weeks, suggesting the developmental origin of tuber formation (Levine et al., 2000; Park et al., 1997; Wortmann et al., 2008). Upon gross examination tubers appear as abnormal regions of cerebral cortex and can often be identified upon visual inspection in the human cortex where they exhibit a firmer or "tuberous" consistency than surrounding tissue. Tubers may extend deep into the subcortical white matter and can measure several centimeters across (Crino et al., 2010b; DiMario, 2004; Grajkowska et al., 2010). A minority of TSC patients may also develop cerebellar tubers, however in most cases tubers are restricted to supratentorial regions of the brain (Jay et al., 1998). Tubers tend to be restricted to a single gyrus which may become enlarged. However, in some cases they may have a lobar or hemispheric distribution. On microscopic examination there is also marked disorganization of cortical lamination within the tuber where the normal hexalaminar structure of the cortex has been lost (Crino et al., 2010b; Huttenlocher and Wollmann, 1991; Muhlebner et al., 2016a; Ruppe et al., 2014).

The tissue within cortical tubers consists of a mix of astrocytes and abnormal neurons sometimes displaying bizarre and highly aberrant characteristics. Tubers have been shown to include excessive numbers of astrocytes as detected by glial fibrillary acidic protein (GFAP) and CD44 expression (Arai et al., 2000; Sosunov et al., 2008). Interestingly, inflammatory responses are also potentially elevated in these malformations as shown by numbers of immunoreactive CD68 microglia within tubers (Boer et al., 2008a). Neurons within cortical tubers may appear as normal cortical neurons with a roughly pyramidal morphology. However, tubers are often characterized as comprising dysmorphic and highly irregular neurons which exhibit loss of orientation with respect to the pial surface of the cortex, and often exhibit enlarged cell bodies.(Crino et al., 2010b; Muhlebner et al., 2016b) These abnormal neurons have been shown to express markers similar to those expressed by pyramidal neurons such as the neurofilament protein SMI311 and glutamate receptor subunits like glutamate receptor subunits 1 and 2 (GluR1 and GluR2). However, the levels of these neuronal proteins have been shown to be dysregulated in dysplastic neurons as compared to normal cells (Crino, 2004; Talos et al., 2008).

A defining cellular feature of cortical tubers are the presence of enlarged, cytomegalic "balloon cells" (BCs) or giant cells (GCs). The maximal dimension of these cytomegalic cells can range from approximately 80μm to up to 120μm and can be found throughout the thickness of the tuber (Crino et al., 2010b; Mizuguchi, 2007). GCs extend short processes which express a highly heterogenous collection of axonal and dendrite markers. Some GCs may extend MAP2 positive processes similar to dendrites, while others extend neurofilament positive processes resembling axons. However, these projections are morphologically irregular with respect to the normal neuronal architecture (Crino et al., 2010b; Hirose et al., 1995). Interestingly, small clusters of GCs or "microtubers" have also been shown to be distributed throughout non-tuber brain areas,

suggesting a potentially unique etiology for isolated GCs separate from those found within cortical tubers (Crino, 2013; Marcotte et al., 2012; Sosunov et al., 2015).

The presence of cortical tubers can sometimes be linked to an epileptic phenotype in certain individuals with TSC. Epilepsy is a common feature of TSC, with approximately 75 to 90% of TSC patients affected (Thiele, 2010). In some of these individuals surgical resection of a tuber identified as being associated with seizure onset can ameliorate epilepsy, suggesting that cortical tubers contribute to the epileptic phenotype (Jansen et al., 2007; Koh et al., 2000). However, this link is not fully understood and in many cases of TSC seizure loci are not clearly associated with specific brain malformations. Individuals with TSC may have multiple tubers but also present a single epileptogenic focus. Even more striking is the finding that some individuals with TSC and epilepsy do not appear to have any cortical tubers as shown by MRI imaging (Erol et al., 2015; Major et al., 2009; Thiele, 2010). These data suggest that cortical malformations in TSC may be highly variable in their impact on surrounding brain tissue, and that non-tuber brain regions may contribute to TSC disease pathology as well. The degree to which non-tuber regions of the brain contribute to TSC neuropathology is poorly understood. Studies have shown subtle alterations in non-tuber brain areas such as increased neuronal excitability, suggesting that non-tuber brain tissue may contribute to TSC epileptic phenotypes (Wang et al., 2007). Additionally, microscopic structural abnormalities, radial migration lines suggesting migration defects and areas of hypomyelination have also been reported in some cases of TSC (Ruppe et al., 2014; Sosunov et al., 2015; van Eeghen et al., 2013). However, more detailed study of these non-tuber abnormalities, and their contribution to the TSC neuropathology is currently lacking.

In addition to hamartomas, other types of brain tumors can produce clinical symptoms in TSC patients. SENs are present in about 80% of TSC patients and are thought to be related to the

later formation of SEGAs, although the mechanisms underlying the transition remain largely undefined (Kim et al., 2001). SENs are nodular lesions typically less than 1cm in size located on the surfaces of the ventricles (Crino et al., 2010b). SEGAs may grow larger than SENs and can extend into the lateral ventricle, sometimes obstructing the flow of CSF causing hydrocephalus. Both SENs and SEGAs consist of abnormal, dysmorphic glial cells as well as GCs (Goh et al., 2004; Mizuguchi and Takashima, 2001).

The cellular lineage of abnormal cells in tubers and other TSC brain malformations is the subject of much discussion and has not been fully defined. Critically, determining the exact population of precursor cells from which different abnormal cells arise from has proved difficult as many cells within TSC-related lesions express markers for both neurons and glia (Crino, 2004; Mizuguchi and Takashima, 2001). Analysis of GCs revealed the expression of GFAP and S100 proteins, both markers for astrocytes (Boer et al., 2008a). However, GCs have also been demonstrated to express NESTIN, neurofilament, internexin, neuron-specific enolase, tubulin, doublecortin and MAP2 which are typically expressed in neurons or neural progenitors (Crino et al., 1996; Hirose et al., 1995; Mizuguchi et al., 2002). GCs have further been reported to express $GABA_A$ receptor subunits and synaptophysin, consistent with a neuronal phenotype (Hirose et al., 1995; Yamanouchi et al., 1997). While an explanation for the coexpression of glial and neuronal markers in the cells of TSC lesions remains undefined it has been speculated that the aberrant differentiation of neuroglial progenitors may result in the generation of abnormal cells with mixed glial and neuronal phenotypes (Crino, 2004; Ess et al., 2005; Yamanouchi et al., 1997).

During the process of cortical development projection neurons are derived from radial glial progenitor cells in the ventricular zone (VZ) of the dorsal forebrain and migrate radially to form the characteristic laminar architecture of the cortex (Kwan et al., 2012; Noctor et al., 2004).

Inhibitory interneurons are born in the ganglionic eminences (GE) of the basal forebrain and migrate tangentially into the developing cortical plate (Kriegstein and Noctor, 2004; Zhu et al., 1999). A range of markers now exists to identify cells generated from either the VZ or GE, and further subsets of cells within those populations. Using these, studies have shown that dysmorphic neurons from TSC tubers express markers consistent with an excitatory neuronal phenotype including GluR1 and GluR2, but not inhibitory neuronal markers like GAD65 for vesicular GABA transporters and parvalbumin (Talos et al., 2008; Valencia et al., 2006). Further data has demonstrated that GCs and dysmorphic neurons express brain lipid binding protein and vimentin, as well as ezrin, proteins normally expressed by radial glia, and suggestive of a VZ origin for GCs and dysmorphic neurons in TSC brain malformations (Figure 1) (Johnson et al., 2002).

Individuals diagnosed with TSC often present behavioral, psychiatric and developmental disorders. Even from very early descriptions of the disease TSC was recognized as being associated with a range of behavioral and cognitive deficits. More recent surveys in children and adolescents with TSC show rates of social communication deficits between 44 and 69% including speech and language delay. Disruptive behaviors such as self-injury have been reported in 40-50% of surveyed TSC patients, and mood-related difficulties have been shown in a further 20-50% (de Vries et al., 2007). Studies have also reported rates of Attention Deficit Hyperactivity Disorder (ADHD) between 43 and 55% in TSC patients (de Vries et al., 2007; Gillberg et al., 1994). Behavioral deficits in TSC have also been shown to correlated with intellectual ability with more intellectually impaired individuals being more likely to present more serious behavioral deficits (de Vries et al., 2007). There is a wide range of observed intellectual ability in cases of TSC from those who appear similar to the general population, to individuals with profound intellectual impairment. Around 70% of individuals with TSC fall into a normal distribution of intelligence

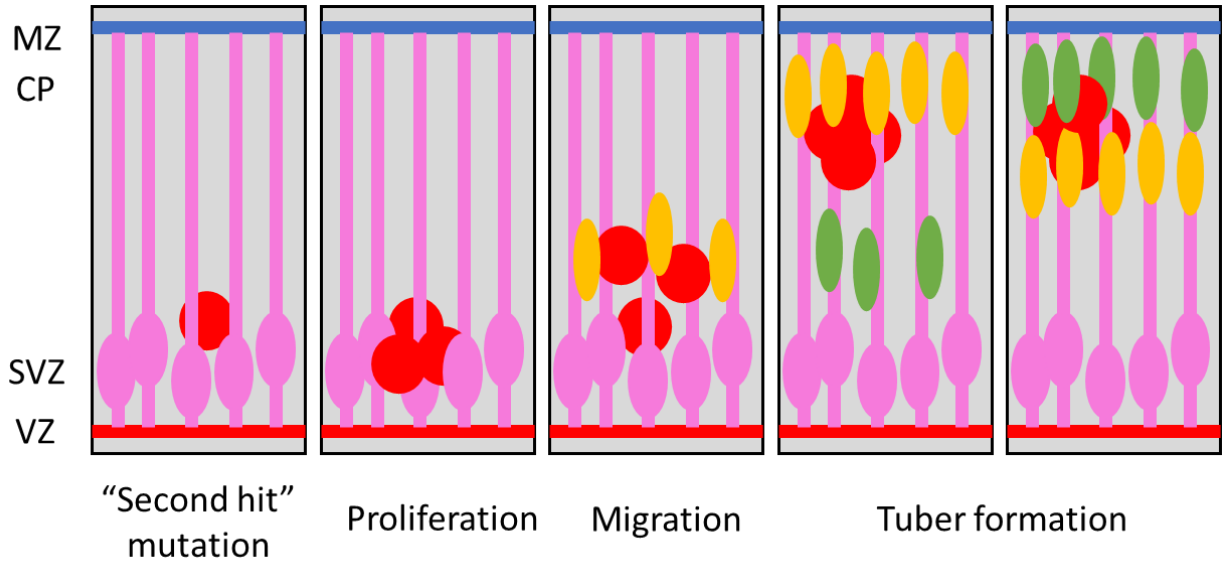

Figure 1. Diagramatic representation of cortical development. Progenitor cells in the sub-ventricular zone (SVZ) lining the ventricular zone (VZ) give rise to neurons through asymmetric division which migrate radially towards the marginal zone (MZ) of the developing brain to form the cortical plate (CP). New neurons arrive in an "inside out" fashion to establish cortical layering. Somatic mutations resulting in LOH occurring in progenitor cells give rise to abnormal and dysmorphic cells in TSC. These LOH cells proliferate and migrate along with the cortical milieu eventually giving rise to cortical tubers and TSC-related brain lesions.

scores as measured by IQ, although the mean IQ in TSC population (93) is shifted somewhat lower than the general population (100). The remaining 30% of TSC patients express profound impairment and intellectual disability, and often their performance cannot be measured directly via intelligence testing, relying instead on indirect assessment of the affected individual's intellectual abilities (de Vries and Prather, 2007; Joinson et al., 2003; Prather and de Vries, 2004). Clinical observations have indicated that many children with TSC have difficulties learning and making academic progress. One survey showed 36% of normally intelligent children with TSC were at risk of academic underperformance, suggesting that even in minimally intellectually affected individuals TSC still manifests in the form of a learning disorder (Vries, 2010). Perhaps most striking with regards to the developmental and cognitive aspects of TSC is the very strong association with Autism Spectrum Disorder (ASD). Studies have reported rates of ASD within the TSC affected population of between 25 and 50%, and TSC is known to be one of the genetic conditions most strongly associated with autism (Cass et al., 2006; Hunt and Shepherd, 1993; Smalley et al., 1992; Vignoli et al., 2015; Wiznitzer, 2004). Rates of ASD in TSC appear linked to global intellectual ability, with individuals presenting moderate intellectual disability up to 50 times more likely to fall under the diagnostic criteria for ASD than a child without TSC. Even in TSC individuals with normal intellectual ability rates of ASD may be 10 to 20 times higher than the general population, highlighting the strong association between ASD and TSC (Vries, 2010).

The link between TSC brain malformations and the observed cognitive and intellectual phenotypes is not fully understood. Perhaps the most widely cited model suggests that tuber load predicts the outcome of intellectual ability. MRI analysis of TSC patients beginning in the 1980s suggested that tuber load was correlated to intellectual disability (Roach et al., 1987). By the 1990s it was proposed that an individual with TSC who had seven or more tubers had a higher likelihood

of presenting intellectual disability than a less affected patient (Goodman et al., 1997). However, more recent analysis has brought these earlier findings into question. Recent studies have shown no correlation between IQ and tuber features, including individuals with high tuber load and normal IQ (Lyczkowski et al., 2007; O'Callaghan et al., 2004; Ridler et al., 2004). Conversely, it has been observed that some individuals with TSC display severe intellectual disability but have very few observable neuroanatomical abnormalities, suggesting that tubers are not necessary to explain the intellectual and cognitive phenotypes of TSC (Vries, 2010).

Genetics of TSC

TSC is a genetic disorder where all known individuals affected carry heterozygous mutations of either one of two genes: *TSC1* and *TSC2*. Nearly two-thirds of known cases of TSC result from spontaneous or *de novo* mutations. Early genetic studies first established that TSC is an autosomal dominant trait, and subsequent genetic linkage analysis of TSC families led to the identification of a disease-causing locus on chromosome 9q34, which was named *TSC1;* subsequent studies of additional TSC families indicated locus heterogeneity, suggesting the involvement of more than one gene. This led to the discovery of a second disease-causing locus on chromosome 16p13.3 which was called *TSC2* (Fryer et al., 1987; Kandt et al., 1992; Northrup et al., 1993).

Genetic linkage along with positional cloning studies eventually refined the *TSC1* and *TSC2* loci and led to the identification of the two TSC genes. The *TSC2* gene was in fact identified first with the aid of newly discovered markers used in the identification of other genes on chromosome 16. The newly identified *TSC2* gene was predicted to encode a 198kDa protein that

was named Tuberin (European Chromosome 16 Tuberous Sclerosis, 1993). *TSC2* lies in a gene-dense region of chromosome 16p13 and consists of 40723 nucleotides which compose 42 exons. The first exon of *TSC2* was identified after the identification of the remaining gene and is denoted 1a. The 5' UTR of *TSC2* consists of a 106-nucleotide region of exons 1a and 1. The 3' UTR consists of 101 nucleotides following the stop codon in exon 41. The remaining exons comprise the coding sequence of the gene (Kwiatkowski, 2010a; NCBI, 2018b).

The identification of *TSC1* by positional cloning occurred several years after that of *TSC2*. This was due to several factors, including that mutations in *TSC1* occur less frequently than *TSC2*, and genomic resources for the *TSC1* region were less developed at the time than those for *TSC2*. Complete genomic sequencing of a candidate region of chromosome 9q34 initiated as part of the Human Genome Project and mutation screening performed on unrelated familial TSC cases linked to *TSC1* identified mutations in an exon with a known cDNA clone. This was extended to obtain a full-length cDNA sequence, and the mRNA for this identified sequence was predicted to encode a 130kDa protein which was then named Hamartin (van Slegtenhorst et al., 1997). The *TSC1* gene consists of 53284 nucleotides containing 23 exons. The first two *TSC1* exons comprise a portion of the 5' UTR, upstream of the initiation codon in exon 3. The coding sequence of the gene comprise exons 3 through 23 (Kwiatkowski, 2010a; NCBI, 2018a).

Over 1500 different small mutations affecting one exon of *TSC1* or *TSC2* have been reported (Cheadle et al., 2000; Kwiatkowski, 2010a; Povey and Ekong, 2018). Mutations affecting larger portions of the *TSC1* and *TSC2* genes, usually involving deletions of one or more exons are rarer than small mutations, accounting for 0.5% and 6% of all TSC patients with *TSC1* and *TSC2* mutations, respectively (Kozlowski et al., 2007). Deletion and nonsense mutations are most common in *TSC1*, accounting for 37.1% and 35.5% of all *TSC1* mutations, respectively. Insertion,

splice and missense mutations are less frequent, occurring in 14.8%, 9.5% and 3.1% of cases of TSC with *TSC1* mutations. Deletion, nonsense and missense mutations occur at similar frequencies of between 22% and 27% in *TSC2*, while splice and insertion mutations are less frequent, comprising 16.2% and 8.5% of known *TSC2* mutations. Nearly half of the mutations identified in *TSC1* (48%) and *TSC2* (49%) have been reported only once (Kwiatkowski, 2010a). The distribution of mutations within *TSC1* and *TSC2* is highly nonuniform. Over a quarter of mutations in *TSC1* are found within exon 15, and exon 8 has the highest density of mutations per nucleotide. Conversely, only single mutations have been identified in *TSC1* exons 3 and 22, and no mutations have been identified in exon 23. In *TSC2* exons 16, 33 and 40 have the highest numbers of reported mutations, with exon 40 also containing the highest density of mutations. Exons 2 and 41 have mutation densities 20-fold lower than that observed in exon 40, further highlighting the non-uniform distribution of mutations within *TSC2* (Kwiatkowski, 2010a).

Interestingly, surveys undertaken to identify mutations in *TSC1* and *TSC2* have shown mutation detection rates of between 80% and 90%. These studies suggest that a proportion of TSC patients exist in which no mutation has been identified (NMI) (Au et al., 2007; Kwiatkowski, 2010a; Sancak et al., 2005). The typical TSC disease phenotype of these NMI individuals may be explained by mosaicism for mutations in *TSC1* or *TSC2*. Mosaicism refers to a genetic condition wherein not all cells within the developing embryo carry a mutation since that mutation occurred during embryogenesis, but after the fertilized egg underwent meiosis (somatic mutation). Mosaicism in TSC has been reported and shown to be relatively common in patients with large genomic mutations in *TSC2* (Kozlowski et al., 2007; Rose et al., 1999). The severity of TSC disease phenotype in these patients is generally related to the level of mosaicism present and the number of cells affected. In other words, mosaicism in which fewer cells carry a *TSC1* or *TSC2*

mutation results in a less severe TSC phenotype. However, variability has been reported where some patients with mosaicism present full and very severe TSC phenotypes perhaps due to rates of mosaicism in different tissues and frequency of second hit events during development (Kwiatkowska et al., 1999). It is also possible that in NMI patients' mutation detection fails as some mutations affecting transcription or mRNA processing can occur within intronic regions remote from coding exons. Although intronic mutations often account for small fractions of disease causing mutations, it is still possible that they may account for a proportion of TSC patients with NMI (Mayer et al., 2000; Stenson et al., 2017).

The role of *TSC1* and *TSC2* genotype in explaining TSC neuropathology, and especially neuroanatomical abnormalities is perhaps best described by the Knudson Two-Hit Hypothesis model of tumor formation (Knudson, 1971). In this model the loss of the second, normal *TSC1* or *TSC2* allele which, together with the germline mutation of the first allele drives TSC lesion formation. This "second-hit" event produces a loss of heterozygosity (LOH) in the affected cell and can be used as a marker within TSC tubers and lesions to show that the remaining *TSC1* or *TSC2* allele has been lost. Multiple studies have demonstrated LOH in SEGAs, supporting the classical two-hit model (Chan et al., 2004; Henske et al., 1997; Sepp et al., 1996). However, further analysis in cortical tubers has failed to show LOH, suggesting a different mechanism may contribute to lesion formation in TSC (Crino et al., 2010a; Niida et al., 2001). Possible explanations include inactivation of residual TSC proteins leading to complete loss-of-function or failure to detect LOH in certain TSC-related lesions due their heterogeneous cellular composition (Caban et al., 2017; Ma et al., 2005; Martin et al., 2017).

TSC1-TSC2 Protein Function, Signaling and Molecular Hallmarks of TSC

After the identification of *TSC1* and *TSC2* as the genetic loci mutated in TSC attention quickly turned towards understanding the function of their gene products. TSC1 and TSC2, also known as Hamartin and Tuberin are 140kDa and 200kDa proteins, respectively. They share no homology with each other and very little similarity with other proteins, although orthologues can be found in most eukaryotic cells (Huang and Manning, 2008). A key finding in understanding the function of TSC1 and TSC2 proteins came when it was demonstrated that the two proteins physically associate to form a heterodimeric complex (Plank et al., 1998; van Slegtenhorst et al., 1998). The association of TSC1 and TSC2 has been shown to be critical in maintaining the function of the two proteins since complex formation is required for activity and they do not appear to have independent activity. Subsequent studies demonstrated that TSC1 is required for the stabilization of TSC2, which prevents ubiquitin-mediated TSC2 degradation (Benvenuto et al., 2000). TSC1 contains no known enzymatic domain, however it does contain a TSC2 binding domain (T2BD) that interacts with the TSC1 binding domain (T1BD) near the N-terminus of TSC2 to form the TSC heterodimeric complex (Figure 2) (Hodges et al., 2001; Huang and Manning, 2008).

Early studies of the TSC1 and TSC2 proteins identified only one putative functional domain near the C-terminus of TSC2. This domain showed homology to the GTPase-activating protein domain (GAP) of Rap1GAP. Proteins containing GAP domains bind active GTP-binding proteins (G-proteins) and stimulate intrinsic GTPase activity, thereby inhibiting their signaling activity. Initial studies conducted during the search for downstream TSC2 targets revealed that TSC2 has weak GAP activity towards two small G-proteins: Rap1 and Rab5 (Wienecke et al., 1995; Xiao et al., 1997). Although these targets are not relevant in vivo, they served as important markers confirming TSC2 GAP activity. The physiological function of the TSC1-TSC2 complex

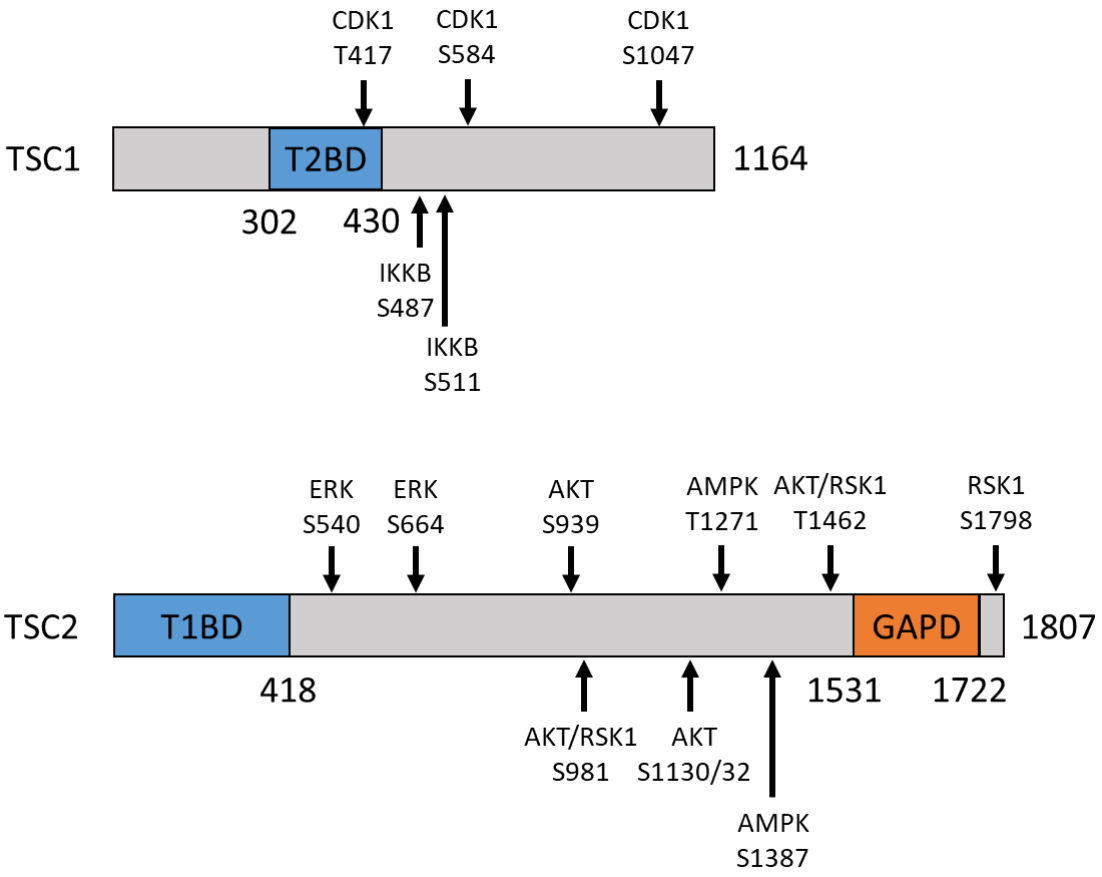

Figure 2. Diagramatic representation of TSC1 and TSC2 protein. Briefly depicted are relevant domains for the formation of the TSC1-TSC2 complex and its function. TSC1 contains a TSC2 binding domain and consensus sites for CDK1 and IKKB. TSC2 contains a TSC1 binding domain at the N-terminus and GAP domain near the C-terminus. TSC2 also contains consensus sites for AKT, ERK, RSK1 and AMPK phosphorylation.

began to be elucidated in 2001 through the study of organ growth in *Drosophila* (fruit fly). Three independent genetic screens for regulators of organ growth identified loss-of-function mutations in the *Drosophila dTsc1* gene as the causative locus for an eye-overgrowth phenotype resulting from an increase in cell size as well as cell proliferation. It was further demonstrated that *dTsc2* mutants had similar phenotypes, and that overexpression of both genes together, but not individually, resulted in organ and cell size reduction (Gao and Pan, 2001; Potter et al., 2001; Tapon et al., 2001). These studies strongly implicated a functional role for the TSC1-TSC2 complex in regulating cell proliferation and growth.

Signaling via the InR (insulin receptor/IGF1) orthologue in *Drosophila* was already known at the time to be a critical regulator of cell size, so experiments were conducted to uncover whether TSC1-TSC2 complex involvement in regulating growth was related to insulin signaling pathways (Stocker and Hafen, 2000). Findings from these genetic epistasis experiments revealed that *dTsc1* and *dTsc2* mutation or co-overexpression showed interactions with orthologous components of InR signaling, including protein kinase B (PKB, also known as AKT) and ribosomal protein S6 kinase (S6K) (Gao and Pan, 2001; Potter et al., 2001; Tapon et al., 2001). Critically, *dTsc* genes were observed to function upstream of the *Drosophila* orthologue for S6K (dS6K) in a manner that blocked the pro-growth activity of S6K, and that the lethality of *dTsc* mutations could be rescued by reducing dS6K activity, suggesting that a critical function of the TSC1-TSC2 complex is the inhibition of S6K mediated growth pathways (Radimerski et al., 2002). After these initial findings, further biochemical studies refined the placement of TSC1-TSC2 within the insulin-mediated growth signaling pathway. Screens of targets for the serine/threonine kinase AKT in mammalian cells found direct phosphorylation of two residues on TSC2 (Inoki et al., 2002; Manning et al., 2002). Perhaps most striking were findings that showed mutant TSC2 lacking AKT

phosphorylation sites blocked growth factor-mediated activation of S6K, suggesting that AKT activates S6K through the relief of the TSC1-TSC2 complex's inhibitory effect on cell growth (Manning et al., 2002). Together these data established the TSC1-TSC2 complex as acting directly downstream from AKT, but upstream of S6K. Furthermore, these early findings showed the first evidence of the direct regulatory activity AKT exerts on the TSC1-TSC2 complex to stimulate growth via an S6K-dependent signaling pathway.

Direct regulation of TSC1-TSC2 was thus shown to be mediated by AKT. However, AKT has multiple targets besides TSC2. This protein kinase is a key signaling factor within insulin-mediated growth pathways, and AKT-mediated networks have a wide range of pro-survival, pro-growth and cell cycle promoting targets (Figure 3) (Manning and Toker, 2017). In the 1990s it was shown that AKT is activated by many growth factors in a manner that was dependent on phosphoinositide 3-kinase (PI3K) (Burgering and Coffer, 1995; Franke et al., 1995; Kohn et al., 1995). These findings established AKT as a critical downstream effector for PI3K-mediated growth signaling. The mechanisms underlying PI3K/Akt signaling were further refined when it was demonstrated that lipid second messengers produced by PI3K, i.e. phosphoinositol (PI) 3-phosphates, can bind and activate AKT at the plasma membrane. Binding occurs via a pleckstrin homology (PH) domain at AKT's amino terminus (Franke et al., 1997; Frech et al., 1997; James et al., 1996; Klippel et al., 1997). PI3K recruitment and activation is achieved via stimulation of receptor tyrosine kinases such as insulin-like growth factor 1 receptor (IGF1R) or growth factor receptors, and also G-protein coupled receptors (Manning and Toker, 2017). In this manner AKT responds by integrating growth factor and insulin signaling. Insulin receptor substrates IRS1 and IRS2 serve as scaffolding adaptors linking IGF1 receptors to PI3K ac tivation. Interestingly, S6K activity promotes the degradation of IRS1 and IRS2 via direct phosphorylation of the IRS proteins

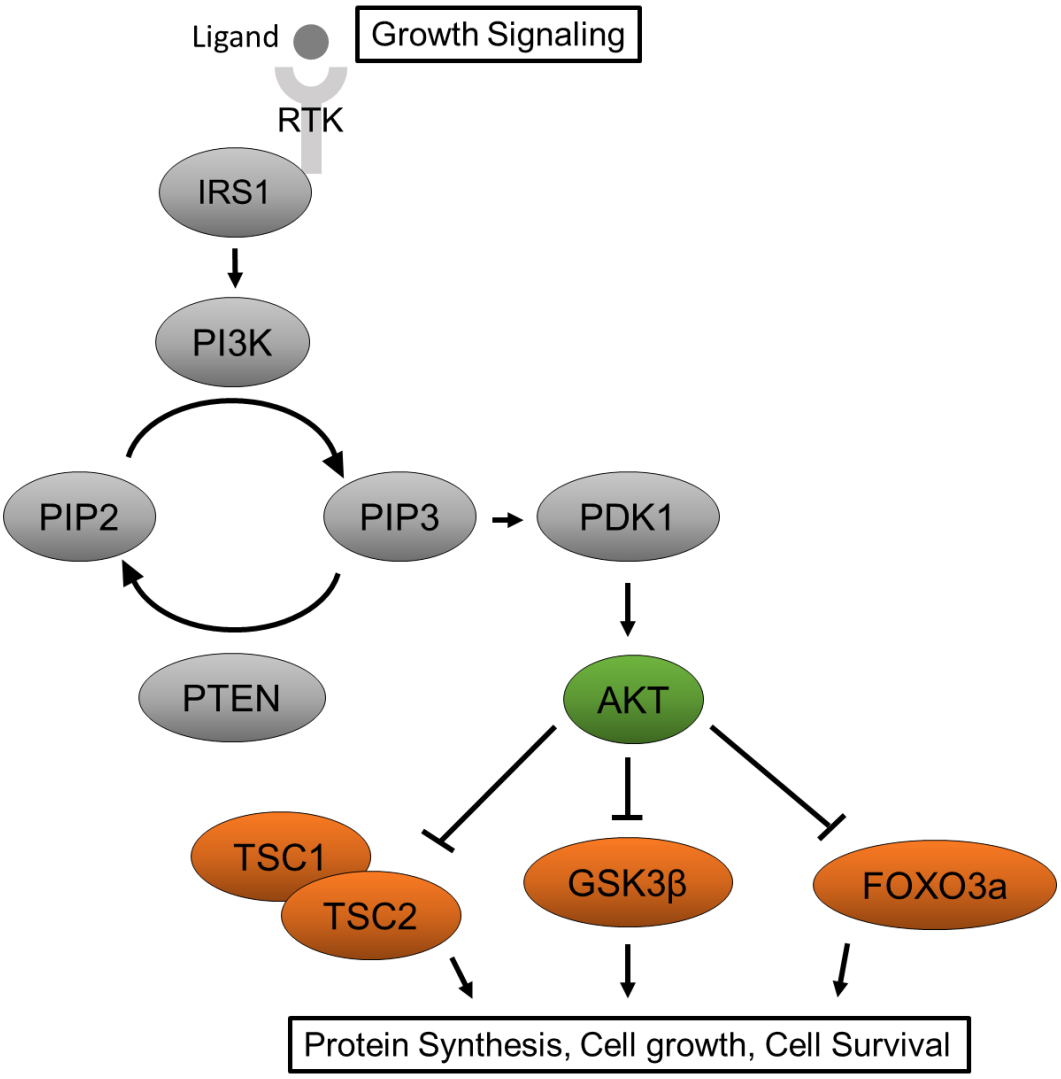

Figure 3. Diagramatic representation of PI3K/AKT signaling. Briefly, upstream stimulation of this pathway via growth signaling ligand binding to receptor tyrosine kinases (RTK) leads to the activation of PI3K which promotes the conversion of PIP2 to PIP3 and is counteracted by PTEN inhibition. PIP3 and PDK1 activation effects AKT leading to its activation and subsequent kinase activity on downstream targets which promote cell growth and survival. This action occurs via inhibition of factors such as TSC1-TSC2, GSK3β and FOXO3a.

thereby limiting PI3K activation. This negative feedback mechanism therefore dampens downstream activation of S6K by PI3K/AKT (Harrington et al., 2004; Hiratani et al., 2005; Manning and Toker, 2017; Zhang et al., 2008).

The main targets of AKT activity besides TSC2 are glycogen synthase 3β (GSK3β) and the forkhead box O family of transcription factors (FOXOs). GSK3β was the first AKT substrate identified, has been shown to participate in Wnt-β-catenin signaling, and regulates a number of downstream targets which are inhibited or degraded upon GSK3β-mediated phosphorylation (Cross et al., 1995; Kaidanovich-Beilin and Woodgett, 2011). AKT-mediated phosphorylation of GSK3β positively regulates these factors via the inhibition of GSK3β. Substrates of GSK3β are involved in cell survival, proliferation and metabolism. Thus, by inhibiting GSK3β in this manner AKT acts to promote these pro-survival and proliferation pathways (Manning and Toker, 2017).

FOXO transcription factors, including FOXOs 1, 3, 4 and 6 control a variety of gene targets involved in mediating stress responses to low insulin and IGF1 signaling, metabolism, proliferation, cell growth and survival (Webb and Brunet, 2014). AKT regulates FOXO activity by phosphorylating the transcription factors at three conserved sites. Two of these sites generate recognition motifs for 14-3-3 proteins which lead to the translocation of FOXO out of the nucleus, preventing its transcriptional activity. The expression of FOXO targets have been shown to trigger the induction of apoptosis, cell cycle arrest and growth inhibition pathways (Manning and Toker, 2017; van der Vos and Coffer, 2011). In a manner similar to that shown in GSK3β inhibition, the translocation of FOXOs and the cessation of their transcriptional program by AKT phosphorylation acts in a positive capacity to promote cell survival and growth signaling pathways. Taken together, these data show a convergence of pro-growth and survival activities mediated by PI3K/AKT signaling.

While GSK3β and FOXOs were shown to be important substrates of AKT, a direct link between the TSC1-TSC2 complex, AKT activity and the observed downstream effects on S6K remained to be established. Significant biochemical research was conducted to further refine the role of the TSC1-TSC2 complex which had been shown to involve the regulation of S6K-mediated cell growth. S6K plays a role as an important downstream target of the growth regulating complex that includes the mammalian target of rapamycin (mTOR) kinase (Figure 4) (Wullschleger et al., 2006). mTOR was initially discovered through the study of the antibiotic rapamycin, which had been shown to act as a potent immunosuppressant in organ transplants (Collier, 1989; Vezina et al., 1975). Genetic screens of rapamycin resistant yeast identified two genes which were called the targets of rapamycin 1 and 2 (TOR1 and TOR2) (Heitman et al., 1991). Later studies in mammalian cells identified a homologue now known as mTOR (Brown et al., 1994; Sabatini et al., 1994). The structure of the mTOR protein consists of a C-terminal kinase domain resembling the lipid kinase domain of PI3K. Despite this mTOR is not known to possess significant lipid kinase activity, instead acting as a serine/threonine kinase. Interestingly, mTOR has been shown to be sensitive to certain PI3K inhibiting compounds, highlighting its structural resemblance to other members of the phosphatidylinositol 3-kinase-related kinase (PIKK) family of protein kinases (Brunn et al., 1996). Adjacent to the kinase domain in mTOR is the FKBP12-rapamycin binding domain (FRB). The FRB domain found exclusively in mTOR is responsible for rapamycin binding (Chiu et al., 1994; Stan et al., 1994) and it was mutations within this FRB domain which led to the original identification of TOR1 and TOR2 in rapamycin resistant mutant yeast. mTOR proteins possess two further domains of unknown function called the FAT (focal adhesion kinase targeting) and FATC domains. These domains are also found in other PI3K-related proteins. Finally, at the N-

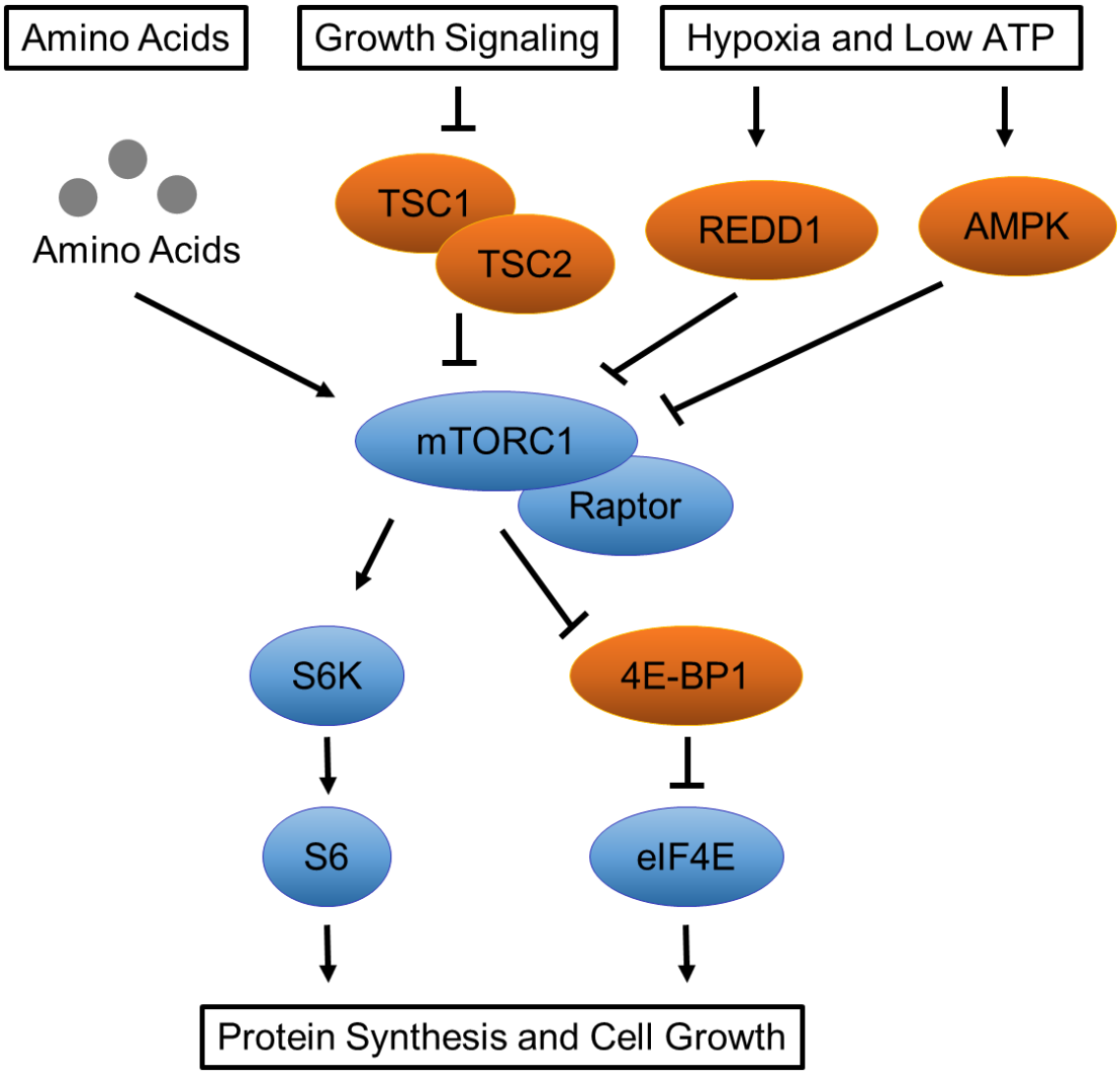

Figure 4. Diagramatic representation of mTORC1 signaling. mTORC1 responds to amino acid levels, growth signaling via AKT/TSC1-TSC2, hypoxia and energy level pathways. Downstream effectors of mTORC1 S6K and 4E-BP1 initiate cell growth and protein synthesis via phosphorylation of ribosomal subunit protein S6 and the cap dependent translation initiator eIF4E.

terminus of mTOR lies a large region of tandem HEAT repeats, again of unknown or undefined function (Manning, 2010; Wullschleger et al., 2006).

Investigation into the functions of TOR proteins in yeast led to the surprising observation that not all TOR activities were sensitive to inhibition by rapamycin (Helliwell et al., 1994; Zheng et al., 1995). This finding led to the discovery that mTOR proteins exist in two distinct protein complexes, only one of which is sensitive to rapamycin. mTOR complex 1 (mTORC1) is readily inhibited by rapamycin and contains mTOR along with the proteins Raptor and mLST8 (Hara et al., 2002; Kim et al., 2002; Kim et al., 2003). mTORC1 is responsible for the direct phosphorylation of S6K, which in turn phosphorylates and activates the ribosomal subunit p70S6 (S6) and eIF4B. Another major target of mTORC1 is the cap-dependent translation initiation factor 4E-BP which is phosphorylated and inhibited by mTORC1 activity (Shimobayashi and Hall, 2014; Wullschleger et al., 2006). The substrate binding activity of mTORC1 with S6K and 4E-BP appears to be mediated by Raptor, and knockdown of Raptor has been shown to mimic rapamycin treatment or mTOR depletion (Burnett et al., 1998; Hara et al., 2002; Kim et al., 2002; Nojima et al., 2003). Together these phosphorylation events promote protein translation and cell growth, a major process which are dysregulated in models where the TSC1-TSC2 regulatory complex is mutated (Gao and Pan, 2001; Manning et al., 2002; Potter et al., 2001; Tapon et al., 2001). mTORC2 consists of mTOR along with Rictor, SIN1 and mLST8 (Jacinto et al., 2006; Sarbassov et al., 2004; Yang et al., 2006). The function of mTORC2 is less clearly defined than mTORC1, although it has been shown that mTORC2 targets AKT for phosphorylation, and is also involved in Actin polymerization and cell spreading (Jacinto et al., 2004; Sarbassov et al., 2004; Wullschleger et al., 2006).

As mentioned previously, mTORC1 activity self-regulates through negative feedback mechanisms. mTORC1-mediated activation of S6K leads to phosphorylation of IRS proteins, mediating their degradation and resulting in reduction of PI3K/AKT signaling and thus reduced mTORC1 activity (Manning and Toker, 2017). Another mechanism involves the growth factor receptor-bound protein 10 (GRB10), an adaptor protein that is phosphorylated directly by mTORC1 to suppress insulin and IGF signaling and plays a central role in restoring normal levels of cell growth (Ramos et al., 2006; Taniguchi et al., 2006). Interestingly, dysregulation of mTORC1 due to lack of TSC1-TSC2 complex regulatory activity has been shown to strongly induce these negative feedback pathways (Figure 5). However, these mechanisms fail to normalize mTORC1 activity if TSC2 is completely absent, emphasizing the critical role of this protein in mediating AKT-induced mTORC1 activation. These data suggest that mTORC1 feedback signaling may also play a role in mediating TSC cellular and molecular pathology (Ozcan et al., 2008; Shah et al., 2004).

Downstream targets of mTORC1 activity have been shown to regulate cap-dependent protein translation not only over an acute timescale, but also through prolonged increases in the synthetic capacity of the cell by up regulating ribosome biogenesis (Wullschleger et al., 2006). Both acute and prolonged effects on protein synthesis place mTORC1 as the key regulator of the most energy intensive process within eukaryotic cells. Because of this critical function mTORC1 has evolved to be sensitive to multiple upstream signaling pathways which sense changes in cell growth conditions. Much of this signal integration has been shown to be mediated by the TSC1-TSC2 complex, which had previously been identified as having inhibitory actions on downstream effectors of mTORC1 activity (Gao et al., 2002; Potter et al., 2001; Radimerski et al., 2002; Tapon et al., 2001). This integration includes insulin and growth factor signaling transduced via PI3K/Akt

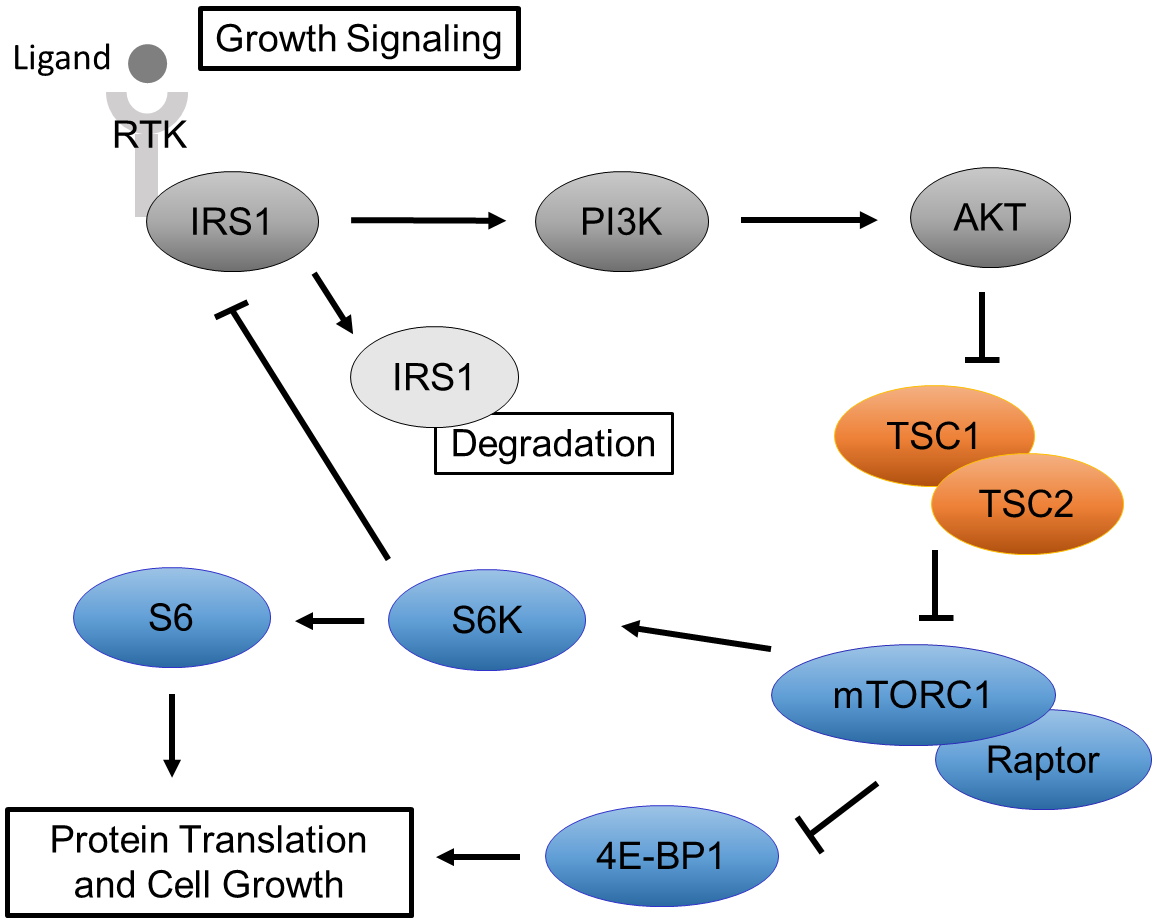

Figure 5. Diagramatic representation of the PI3K/AKT/mTORC1 signaling axis including TSC1-TSC2. Growth factor signaling via RTKs and mediated by IRS1 activates PI3K/AKT leading to the release of TSC1-TSC2 inhibition of mTORC1. Downstream growth pathways activated by mTORC1 are mediated by S6K and 4E-BP1. mTORC1 activity initiates feedback signaling via S6K inactivation and degradation of IRS1, attenuating AKT activity and self-limiting activation of mTORC1 by restoring TSC1-TSC2 inhibitory effects.

as described previously, as well as other pathways which transduce signals for growth factor signaling, cytokines, energy, oxygen and amino acid levels (Huang and Manning, 2008; Jewell and Guan, 2013).

Apart from the PI3K/AKT pathway, TSC1-TSC2 signal integration has also been shown to be sensitive to ERK pathway activation. ERK-mediated activation of mTORC1 has been shown to occur in a manner dependent on the phosphorylation of TSC2 by the ribosomal s6 kinase (RSK) complex (sometimes called MAPKAP K1) and subsequent dissociation of TSC1 from TSC2 (Roux et al., 2004; Tee et al., 2003a). The identification of two ERK consensus sites on TSC2 also demonstrated that TSC2 could be phosphorylated directly by ERK to mediate mTORC1 activity (Figure 2) (Ma et al., 2005). Cytokine signaling through the PI3K/AKT pathway has also been shown to stimulate mTORC1, although specifically tumor necrosis factor α (TNFα) was found to stimulate mTORC1 independent of AKT through inhibitory kinase kB kinase β (IKKβ) phosphorylation of TSC1 (Huang and Manning, 2008; Lee et al., 2007).

The TSC-TSC2 complex is also known to be influenced cyclin-dependent kinases (CDKs), and several CDK consensus sites have been identified on TSC1 which appear to be the target of phosphorylation by CDK1-cyclin B complexes (Figure 2). Overexpression of mutant TSC1 lacking these CDK phosphorylation sites was shown to be more efficacious at suppressing mTORC1 activity, indicating that CDKs can influence mTORC1 activity via modulating TSC1-TSC2 (Astrinidis et al., 2003). Additionally, cyclin D has been shown to associate with TSC2, and CDK6-cyclin D complexes appear to increase phosphorylation of both TSC1 and TSC2, although at which sites remains unclear (Zacharek et al., 2005). While mTORC1-mediated effects on protein synthesis have been linked to cell cycle regulation, the exact relationship between TSC1-TSC2, mTORC1 and the regulation of protein synthesis across the progression of the cell cycle is not

entirely understood, although mTORC1 appears to have a positive effect on cell proliferation (Huang and Manning, 2008).

In addition to growth factor signaling mTORC1 activity is very responsive to energy levels within the cell. Protein synthesis requires energy in the form of ATP, and mTORC1 signaling has evolved in a manner which incorporates energy-sensing pathways to regulate this activity (Huang and Manning, 2008; Wullschleger et al., 2006). One primary pathway through which mTORC1 is sensitive to levels of available intracellular ATP is via the phosphorylation of TSC2 by AMP-dependent protein kinase (AMPK). Under conditions of energy depletion an increase in AMP levels leads to AMP binding with AMPK. Once active, AMPK phosphorylates targets leading to the inhibition of anabolic processes such as protein synthesis. Phosphorylation of TSC2 by AMPK leads to TSC2 activation and mTORC1 inhibition, although the exact molecular mechanism by which AMPK activates TSC2 remains unclear (Inoki et al., 2003b; Shaw, 2009). mTORC1 is further inhibited under conditions of oxygen depletion, or hypoxia. Since oxygen is required for aerobic respiration and ATP production via mitochondrial oxidative phosphorylation, oxygen depletion leads to energy depletion and activation of AMPK (Liu et al., 2006). Another AMPK-independent pathway for mTORC1 inhibition has also been identified which involves the transcriptional target of hypoxia inducible factor α (HIFα) known as REDD1. It has been proposed that REDD1 inhibits mTORC1 by reversing AKT-mediated inhibition of TSC2 (Brugarolas et al., 2004; DeYoung et al., 2008; Sofer et al., 2005). Taken together these findings indicate the critical integrative role of the TSC1-TSC2 complex. By sitting at the juncture of numerous energy sensing and growth signaling pathways the TSC1-TSC2 complex serves as a key regulatory switch controlling mTORC1 activity.

Like studies which showed loss of dS6K activity in *Drosophila* prevented the lethality of *dTsc1* or *dTsc2* mutations, concurrent findings revealed that loss of function mutations in the *Drosophila* orthologue *dTor* also rescued lethality of *dTsc1* and *dTsc2* mutations (Gao et al., 2002; Radimerski et al., 2002). Likewise, overexpression of TSC1 and TSC2 reduces the mTORC1-dependent phosphorylation of S6K and 4E-BP1 (Inoki et al., 2002; Kwiatkowski et al., 2002; Manning et al., 2002; Tee et al., 2002). These data suggested that the TSC1-TSC2 complex acts upstream of mTOR to regulate mTOR-dependent S6K and 4E-BP1 activity. The key mechanism in joining the activity of the TSC1-TSC2 and mTOR complexes came with the identification of a member of the Ras superfamily of small GTPases called Rheb, or Ras-homologue enriched in brain (although it is ubiquitously expressed) (Li et al., 2004; Yu et al., 2005). Like the original breakthroughs establishing the TSC1-TSC2 complex within the PI3K/AKT/mTOR pathway, the function of Rheb was discovered during screens for regulators of cell and organ growth in *Drosophila*. However, conversely to dTsc1 and dTsc2, dRheb was identified as a promoter of cell growth. Subsequent epistasis analysis revealed dRheb to be downstream of dAkt, but upstream of dTor (Patel et al., 2003; Saucedo et al., 2003; Stocker et al., 2003). These findings provided the potential answer for a longstanding question regarding TSC1-TSC2 function: what is the target of the GAP activity of TSC2? Finally, a potential target was presented and several independent research groups searching for the target of TSC2 identified Rheb GTPase activity as strongly elevated by the TSC1-TSC2 complex in vitro (Inoki et al., 2003a; Tee et al., 2003b; Zhang et al., 2003b). Furthermore, these biochemical studies showed that Rheb is a potent activator of mTORC1 signaling and that the TSC1-TSC2 complex can block this activation (Castro et al., 2003; Garami et al., 2003). With the inclusion of Rheb a full picture of the TSC1-TSC2 signaling pathway could finally be constructed. In what is now the currently agreed upon pathway TSC2

stimulates the GTPase activity of Rheb, converting it from an active GTP-bound state into an inactive GDP-bound state (Figure 6). Since GTP-bound Rheb is required for mTORC1 activation, the GAP activity of TSC2 effectively serves as a molecular switch regulating the activity of mTORC1 in response to upstream mitogenic stimuli and growth signaling pathways (Huang and Manning, 2008; Manning, 2010).

While TSC1 and TSC2 are generally recognized as the primary components of the TSC1-TSC2 regulatory complex, recent biochemical studies have identified a third component of this complex. This protein has been named TBC1D7 and is predicted to bind to TSC1. Knockdown of TBC1D7 has also been shown to reduce TSC1-TSC2 association, suggesting it works to stabilize the complex and may play a role in supporting TSC1-TSC2 complex activity (Dibble et al., 2012; Gai et al., 2016). Genetic analysis of TSC patients described previously had identified a population of affected individuals with no obvious mutation in TSC1 and TSC2, and the possibility of a mutation in a third TSC gene has been hypothesized as a potential explanation for these cases of TSC (Kwiatkowski, 2010a). However, sequencing analysis of TSC patients does not suggest TBC1D7 is the hypothetical “TSC3” protein which might account for these incidences of TSC, although other studies have shown disruptions of TBC1D7 related to intellectual disability (Alfaiz et al., 2014; Capo-Chichi et al., 2013; Dibble et al., 2012).

The alteration in mTORC1 signaling due to TSC1/TSC2 mutations has been recognized as contributing to many of the major features of TSC (Crino, 2011; Crino et al., 2010b; Grajkowska et al., 2010; Marcotte and Crino, 2006). In addition to promoting increases in cell size, mTORC1 activity has been linked to increased cell proliferation, both processes linked to tumor formation and the appearance of dysplastic cells in TSC brain lesions (Nelsen et al., 2003). Loss of TSC1-TSC2 regulatory activity in TSC was predicted to lead to increased mTORC1 activity, and indeed

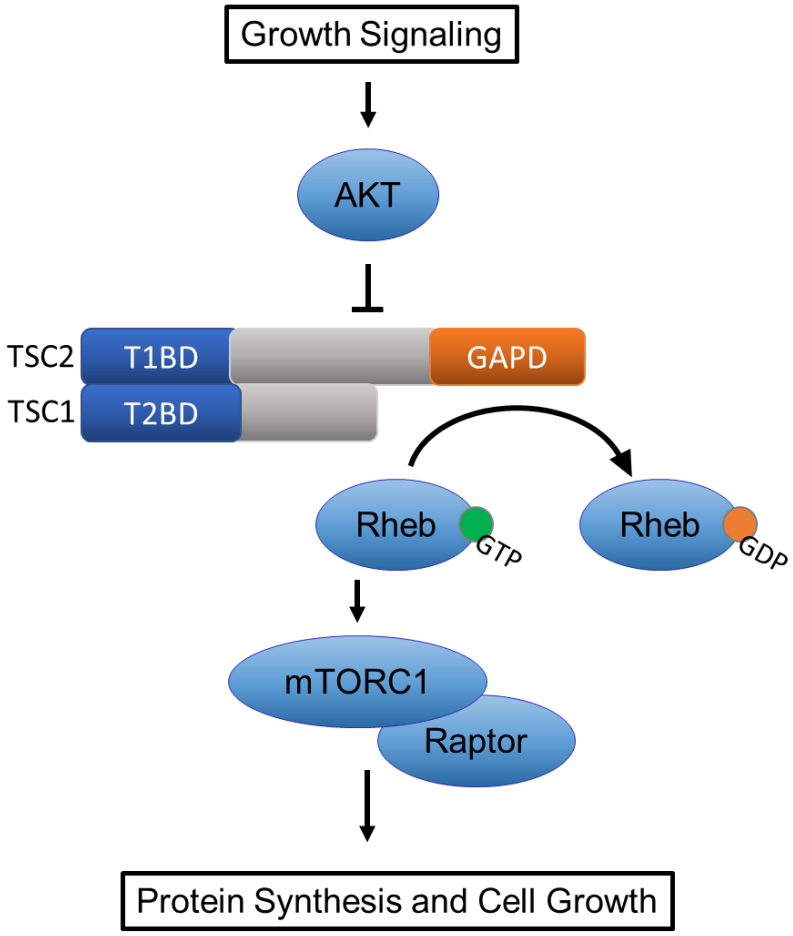

Figure 6. Diagramatic representation of the TSC1-TSC2 complex and its interaction with the small GTPase Rheb. TSC1-TSC2 modulates activity of Rheb via the GAP domain of TSC2 which activates Rheb GTPase activity converting GTP-bound active Rheb into inactive Rheb-GDP. Active Rheb interacts with mTORC1 to stimulate that complex's downstream cell growth and translation actions. TSC1-TSC2 inhibitory activity on Rheb is attenuated by upstream growth signaling via AKT.

increased phosphorylation of downstream targets for mTORC1 have been observed in neoplastic or dysplastic lesions in TSC mouse models and human tissues (Baybis et al., 2004; Crino, 2011; Kwiatkowski et al., 2002; Meikle et al., 2007). Likewise, upstream indicators of mTORC1 dysregulation, such as attenuated AKT signaling due to negative feedback, have also been demonstrated in TSC animal models (Manning et al., 2005; Meikle et al., 2008; Ozcan et al., 2008; Zhang et al., 2006). Strikingly, it was shown that cell culture models of mTORC1 over activation developed insulin resistance attributable to S6K mediated feedback of IRS proteins, demonstrating the wide effects of mTORC1 pathway dysregulation (Harrington et al., 2004; Ozcan et al., 2008; Shah and Hunter, 2006). Moreover, lesion formation is thought to be driven at least in part by over-activation of mTORC1 in TSC1 or TSC2 deficient cells (Crino, 2011). Studies in mouse embryonic fibroblasts (MEFs) have demonstrated the increased proliferative capacity of *Tsc2* null cells under conditions where wild-type controls normally undergo cell cycle arrest, suggesting that TSC1 or TSC2 LOH underlies tumor formation of abnormally proliferating cells in TSC (Zhang et al., 2003a; Zhang et al., 2006). Additionally, the mTORC1 inhibitor rapamycin and its analog RAD001 have been shown to be effective at reducing TSC lesion volume in TSC patients (Franz et al., 2010; Franz et al., 2006). These observations further highlight the relationship between mTORC1 signaling and TSC pathology.

Elevated mTORC1 activity has also been associated with the abnormal morphology of dysplastic neurons and GCs (Crino, 2013; Mizuguchi and Takashima, 2001). Phosphorylation of downstream mTORC1 targets has been used to identify GCs in microtubers and abnormal cells throughout the TSC brain, demonstrating that these abnormal cells exhibit elevated mTORC1 activity relative to surrounding TSC gene haploinsufficient tissue (Chan et al., 2004; Crino et al., 2010b; Miyata et al., 2004). This phenomenon was classically explained by the loss of

heterozygosity (LOH) resulting from a "second-hit" mutation event which inactivates the remaining *TSC1* or *TSC2* allele in the affected cell (Henske et al., 1997; Sepp et al., 1996). Interestingly, while LOH has been proposed as the trigger for mTORC1 cascade activation in abnormal cells and tuber formation other studies have described neuroanatomical defects in TSC without observable LOH (Niida et al., 2001). This may be explained by functional inactivation of the TSC1-TSC2 complex through other mechanisms and suggests that tuber formation and mTORC1 signaling dysregulation may occur in certain haploinsufficient cells independent of a second-hit event. However, normal staining for mTORC1 phospho-targets in non-tuber brain regions suggests that signaling alterations in haploinsufficient tissue may exist below a threshold for detection, or involve components of the PI3K/AKT/TSC2 signaling axis other than mTORC1 (Crino et al., 2010b).

Animal Models of TSC

Animal models are a common tool used in the investigation of human disease and provide insights which would otherwise be difficult or impossible to obtain from human studies. This is especially relevant in the investigation of brain diseases including TSC, since only very limited sampling of the brain tissue can be sometimes obtained from affected patients undergoing epilepsy surgery. Studies of TSC using animal models have been pursued since the introduction of the Eker rat model in 1954. More recent work has focused on the development of mouse models of TSC using genetic engineering techniques.

The first reported animal model of TSC was the Eker rat which was described by Reidar Eker as being affected by an autosomal dominant, hereditary predisposition to renal adenoma and

carcinoma (Eker, 1954). While Eker reported the phenotype of these animals, the genetic evidence linking Eker rats with TSC did not come until the 1980s when Alfred Knudson began using them to validate the two-hit hypothesis. Knudson's research led to the identification in 1994 of a spontaneous germline mutation in the rat *Tsc2* gene (Yeung et al., 1994). Following this discovery, the Eker rat model has been used in many studies of TSC and tumor biology and has provided strong evidence that TSC2 acts as a tumor suppressor. Eker rats exhibit LOH consistent with second-hit deletion of the wild type *Tsc2* allele in a large proportion of renal and pituitary adenomas (Kubo et al., 1995; Yeung et al., 1995). Moreover, transgenic Eker rats with an additional wild type *Tsc2* gene were shown to have increased rates of survival and reduced tumor size and number, further solidifying the role of TSC2 as a critical tumor suppressor (Kobayashi et al., 1997). Interestingly, brain lesions identified in Eker rats are very rare and do not appear to involve *Tsc2* LOH (Mizuguchi et al., 2004; Yeung et al., 1997). GCs have occasionally been shown to be present in the brains of aged Eker rats following prenatal carcinogen treatment. These GCs appear to express a mixture of neuronal, astrocytic and neural progenitor markers like those found in humans including NeuN, EAAC1, GFAP and Nestin (Takahashi et al., 2004). However, the presence of Tsc2 in these cells again suggests TSC brain lesions may originate in the absence of second-hit genetic events (Tschuluun et al., 2007). Regardless of the presence of abnormal neurons, Eker rats display altered synaptic plasticity as shown by altered paired-pulse plasticity and decreased long-term potentiation (LTP) at Schaffer collateral-CA1 synapses (von der Brelie et al., 2006). These observations suggest that Tsc2 heterozygosity adversely affects brain function independently of lesion formation or neuronal overgrowth.

The first genetically engineered mouse models of TSC were developed in the late 1990s with two different *Tsc2* constitutive knockout alleles being independently reported in 1999,

followed by two *Tsc1* constitutive knockout alleles reported in 2001 and 2002 (Kobayashi et al., 1999; Kobayashi et al., 2001; Kwiatkowski et al., 2002; Onda et al., 1999). These heterozygous *Tsc1* and *Tsc2* mouse models developed renal and liver tumors and provided early *in vivo* evidence of the role of the TSC1-TSC2 complex in regulating mTORC1 when it was shown that phosphorylated levels of ribosomal subunit S6 protein (pS6) were increased and phosphorylated Akt (pAkt) was decreased in *Tsc1* -/- mouse embryonic fibroblasts and the renal tumor lysates of *Tsc1* +/- mice (Kwiatkowski et al., 2002). However, no evidence of a neuropathological phenotype similar to that seen in human TSC patients was observed in these models (Kwiatkowski, 2010b; Wong and Roper, 2016).

In order to fully recapitulate TSC neuropathology researchers next turned to generating animal models with homozygous inactivation of the *Tsc1* and *Tsc2* genes. Since constitutive homozygous *Tsc* gene KO mice are embryonically lethal it became necessary to generate mice with conditional homozygous ablation of *Tsc* genes targeted to specific cell types in the brain. The first conditional knockout of a *Tsc* gene was established in 2002 using a GFAP-Cre transgene and a LoxP flanked "floxed" *Tsc1* conditional allele to excise *Tsc1* specifically in astrocytes. The resulting mice lacked astrocytic *Tsc1* expression and exhibited progressive astrogliosis, abnormal neuronal organization in the dentate region of the hippocampus, and seizures suggesting that abnormal astrocytes as well as neurons can significantly contribute to epilepsy in TSC (Uhlmann et al., 2002). A conditional neuronal-specific knockout of *Tsc1* in *ex-vivo* hippocampal slices followed in 2005 which showed enlarged *Tsc1* -/- neurons. Interestingly, the same study showed that loss of just one *Tsc1* allele was sufficient to cause an enlargement of dendritic spine structures in the absence of gross neuronal soma hypertrophy (Tavazoie et al., 2005). These observations

suggest that non-dysmorphic heterozygous neurons can contribute to TSC neurological symptoms due to altered synaptic activity.

Since these models were first described numerous studies utilizing conditional knockouts of *Tsc1* or *Tsc2* in different brain cell types have been reported contributing a great deal to our understanding of TSC neuropathology. Conditional gene inactivation of *Tsc1* or *Tsc2* has since been shown to produce mice with a range of neuropathological defects reminiscent of those observed in human TSC, including seizures, Autistic-like behavior, the appearance of dysplastic neurons, disruptions of cortical neuron positioning, altered neural stem cell proliferation and differentiation, astrocytosis and myelination defects. Studies using *Tsc* conditional knockouts have also confirmed the presence of hallmark signaling defects related to TSC, including elevated mTORC1 activity and attenuated Akt signaling in the mutant brain (Crowell et al., 2015b; Feliciano et al., 2011; Hernandez et al., 2007; Magri et al., 2011; Meikle et al., 2007; Wang et al., 2007; Wong and Roper, 2016). Moreover, many of these abnormal phenotypes were shown to be rescued by the administration of rapamycin, reinforcing the role of TSC1-TSC2's regulatory activity on mTORC1 and highlighting mTORC1's position in driving certain aspects of the TSC disease pathology, such as epilepsy, astrogliosis and neuronal hypertrophy (Cambiaghi et al., 2013; Crowell et al., 2015b; Meikle et al., 2008).

While conditional homozygous knockout mouse models were being developed for *Tsc1* and *Tsc2*, concurrent studies of *Tsc1* and *Tsc2* heterozygous mice made surprising findings which suggested homozygous loss of the *Tsc* genes is not necessary for producing other aspects of the TSC disease phenotype, especially cognitive impairment. While it had previously been shown that *Tsc1* and *Tsc2* heterozygous models failed to recapitulate TSC neuroanatomical defects, behavioral studies showed the heterozygous genotype was sufficient to produce an abnormal

neurocognitive phenotype. It was demonstrated that *Tsc1* +/- and *Tsc2* +/- mice exhibited impaired learning and displayed behavioral abnormalities, and that these effects may be due to recognizable neural mechanisms when it was further shown that *Tsc2* haploinsufficiency was linked to aberrant axon guidance. Additionally, *Tsc2* +/- mice displayed a lowered threshold for late-phase LTP further suggesting underlying cellular abnormalities persist in *Tsc* heterozygous neurons (Ehninger et al., 2008; Goorden et al., 2007; Nie et al., 2010; Tsai et al., 2012). These data raise the question of whether neurocognitive defects in TSC patients are due to the local effects of brain lesions driven by second-hit events or other loss of function mechanisms, or whether they result from haploinsufficiency of TSC1 and TSC2 in non-lesion brain areas. Moreover, such findings in heterozygous mouse models are consistent with clinical data indicating that some patients exhibit neurocognitive defects or seizures with little or no tuber load (Crino et al., 2010b; Vries, 2010).

Induced Pluripotent Stem Cell Models of Disease

Diseases such as TSC with prominent neuropathological aspects have proven to be among some of the most difficult to study in the laboratory. While animal models provided researchers with an important preclinical tool which has been used to study disease mechanisms they have led to few novel therapies successfully translating to the human condition. Many drugs which have shown promise in treating various disorders in mice have failed in humans, underlining the difficulty in using mouse models due to species specific differences. Likewise, studies of post mortem tissue from human TSC patients, while useful at describing TSC pathophysiology in the brain, cannot be used as a test platform for new therapeutic targets and cannot be used to study the neurodevelopmental aspects of the disease. Filling this role for a model system which can be used to study disease mechanisms, identify novel therapeutic targets in a high throughput manner and

recapitulate neurodevelopment in a way that is highly translatable to human disease are induced pluripotent stem cells (iPSCs) (Figure 7) (Dolmetsch and Geschwind, 2011; Tiscornia et al., 2011). Given these qualities iPSCs have the potential to change the way in which human disease, and especially neurodevelopmental and neuropsychiatric disorders such as TSC are studied *in vitro*.

iPSCs are pluripotent stem cells generated from adult somatic cells which have been reprogrammed via specific sets of transcription factors. The landmark findings of Kazutoshi Takahashi and Shinya Yamanaka in 2007 that human fibroblasts could be reprogrammed directly to a pluripotent stem cell state through forcing the expression of four transcription factors: Oct4, Sox2, Klf4 and c-Myc opened this new avenue of disease modeling, and overcame obstacles present in earlier *in vitro* disease models such as human embryonic stem cells (hESCs) which were hindered by ethical concerns and a lack of available hESC lines for most diseases (Takahashi et al., 2007; Tiscornia et al., 2011). iPSCs can be obtained from multiple somatic cell types taken directly from individuals with the disease of interest, or more recently from cell repositories. To date multiple human genetic disorders, including neurological diseases have been modeled *in vitro* using iPSCs. Models of amyotrophic lateral sclerosis (ALS), Rett's syndrome, Down syndrome, schizophrenia, Parkinson's disease and Alzheimer's disease among others have all been successfully produced (Marchetto et al., 2011; Tiscornia et al., 2011; Yu et al., 2013). Cells differentiated from iPSCs in these models have been shown to reproduce cellular and molecular hallmarks of the disease relevant to humans *in vitro*, and in many cases have been used as a platform for therapeutic testing either through drug treatment or genetic manipulation. Additionally, due to their source iPSCs can address genetic variability within human disease populations as different patients may express dramatically different disease phenotypes. TSC, for example has a spectrum of affected individuals from mild to severe (Vries, 2010). The concept

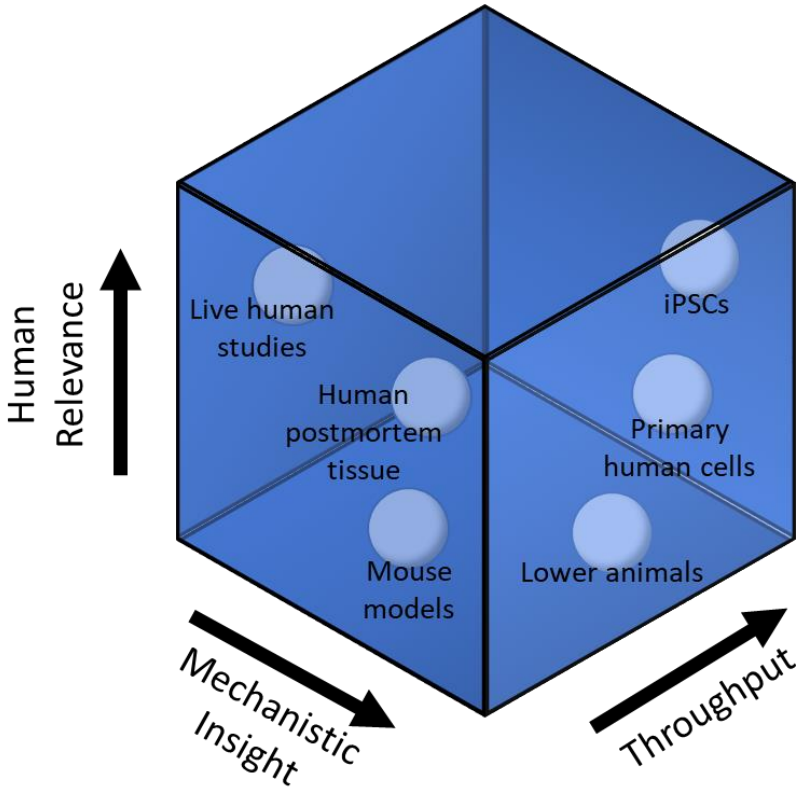

Figure 7. Diagramatic representation of disease models in relation to their relative levels of throughput, mechanistic insight and human relevance. Live human studies, human postmortem studies, mouse models, lower animal models, primary human cell cultures and iPSC culture systems are depicted relative to one another. iPSCs provide a unique combination of human relevance, mechanistic insight and high throughput relative to these other model systems. Adapted from Dolmetsch and Geschwind (Dolmetsch and Geschwind, 2011).

of personalized medicine relies heavily on the ability for disease models like iPSCs to allow for the formation of tailored treatments and medical decision making based on individually predicted risk and response (Chun et al., 2011; Yu et al., 2013). While iPSC-derived disease models are still in their infancy, the field is likely to grow in importance as more diseases are successfully modeled adding to its clinical as well as scientific application.

One of the primary strengths of iPSCs is their ability to be differentiated into cells of any three germ layers: endoderm, mesoderm and ectoderm. Protocols for producing many different cell types exist, with robust methods for generating neurons and glia having been developed over the past several years (Dimos et al., 2008; Hu et al., 2010; Mariani et al., 2012; Zhao et al., 2010). More recently, directed differentiation of iPSCs to specific subtypes of neurons has been achieved (Hu et al., 2016; Liu et al., 2013; Shi et al., 2012a; Yan et al., 2013). The differentiation of neurons from iPSCs can also be directed to reproduce the sequence of *in vivo* neurodevelopmental events in terms of timing of exposure to specific combinations of growth factors and signaling molecules. Indeed, early work on recapitulating cortical development *in vitro* as a proof of principle showed that neuronal differentiation of iPSCs could be induced following the application of certain signaling factors known to play critical roles in mediating neuronal differentiation *in vivo*. Studies have shown the effectiveness of combinations of Noggin, brain derived neurotrophic factor (BDNF), glial derived neurotrophic factor (GDNF), Wnt inhibitors, bone morphogenic protein (BMP) inhibitors and transforming growth factor beta (TGF-β) among others factors in the differentiation of neurons *in vitro* (Gunhanlar et al., 2017; Mariani et al., 2012; Shi et al., 2012a; Shi et al., 2012b; Yan et al., 2013; Yu et al., 2013). The differentiation of iPSCs using viral vectors or synthetic RNA constructs to transduce pro-neuronal differentiative transcription factors has also been demonstrated with a variety of combinations of transcription factors showing high efficacy

for neuronal differentiation (Goparaju et al., 2017; Goto et al., 2017; Pang et al., 2011; Soldner et al., 2009). Additionally, multiple independent groups have demonstrated the direct reprogramming of somatic cells into neurons, further highlighting the expanding capability of cellular reprogramming methods to leverage the critical links between cell identity and gene expression (Pfisterer et al., 2011; Thier et al., 2012; Vierbuchen et al., 2010).

iPSC-derived neurons have been shown to express markers stereotypic of neuronal identity including βIII Tubulin, Doublecortin (DCX) and MAP2. These iPSC-derived neurons have also been shown to differentiate and organize *in vitro* in a manner which recapitulates *in vivo* development with early born neurons expressing deeper layer cortical markers such as T-box 1 (Tbr1) and later born neurons expressing upper layer markers including Cux1 and Special AT-rich sequence binding protein 2 (SATB2) (Mariani et al., 2012; Nicholas et al., 2013; Shi et al., 2012b; Stein et al., 2014). The generation of multilayered structures resembling the neural tube has been demonstrated with iPSC-based *in vitro* culture systems. Interestingly, substructures in these culture systems displayed zones of radially arranged cells similar in appearance to radial glia, and which express glial fibrillary acidic protein (GFAP) along with other markers of neuronal progenitors (Nicholas et al., 2013; Shi et al., 2012b). The production of populations of lineage restricted neural progenitors in the subventricular zone of the developing cortex which give rise to neurons via asymmetric division form critical steps during mammalian cortical development (Kwan et al., 2012; Noctor et al., 2004). Techniques for differentiating neurons from iPSCs have also been shown to produce neural progenitors intermediately between iPSC and neuronal differentiation. These cells typically express markers characteristic of neural progenitors such as Paired box protein 6 (PAX6), the neuroectodermal stem cell marker NESTIN and the neuroepithelial

transcription factors SOX1 and SOX2 (Hu et al., 2010; Mariani et al., 2012; Shi et al., 2012b; Yan et al., 2013).

More recently 3D culture systems such as cerebral organoids developed using specialized bioreactors have allowed researchers to further recapitulate cortical development *in vitro* (Chambers et al., 2013; Fatehullah et al., 2016). These organoid models have shown evidence for differentiation between forebrain and hindbrain neuronal identity in individual cerebral organoids, as well as radial migration and the production of Reelin expressing cells in a marginal zone-like apical layer (Lancaster et al., 2017; Lancaster and Knoblich, 2014). During normal mammalian cortical development, the Cajal-Retzius cells of the MZ secrete the extracellular matrix protein Reelin, which has been shown to act as an important positional cue for radially migrating neurons (Lee and D'Arcangelo, 2016; Stranahan et al., 2013). The reproduction of this process *in vitro* reinforces the immense potential of iPSC-based systems in the modeling of cortical development. 3D culture systems have also moved beyond the proof of concept phase towards modeling neurological disease with an organoid model of microcephaly being successfully produced in 2013 (Lancaster et al., 2013).

As researchers first began differentiating neurons from iPSCs the question arose as to the level of similarity between iPSC-derived neurons *in vitro* and functional neurons *in vivo*. The applicability of *in vitro* findings to *in vivo* systems has been a point of contention in the scientific community for as long as research using either system has existed. However, fundamental questions about the functional characteristics of iPSC-derived neurons were well placed. Since the ability for neurons to form synaptic connections and neural circuits is their critical function, and many neurological diseases specifically affect these processes, the formation of mature neurons capable of synaptic communication *in vitro* became an important early goal in iPSC research.

Studies of mature iPSC-derived neurons showed the expression of markers such as post-synaptic density protein 95 (PSD95), Synaptophysin, Synapsin I and Homer suggesting the formation of synapses does occur *in vitro* (Mariani et al., 2012; Shi et al., 2012b). The observation that neurons produced from iPSCs could fire action potentials strongly indicated that these cells were functionally like neurons *in vivo* as they exhibited characteristic neuronal electrical properties. Moreover, small excitatory and inhibitory post-synaptic potentials (EPSPs and IPSPs) have been observed in iPSC-derived glutamatergic excitatory and GABAergic inhibitory neurons, respectively (Nicholas et al., 2013; Shi et al., 2012b). These findings provide further evidence that these neurons produce synapses *in vitro,* and that their synapses are functional as shown by their electrical activity. The authenticity of iPSC-derived neurons was perhaps most clearly illustrated in 2012 when differentiated neurons were plated on cultured mouse cortical slices and were observed to survive and integrate into the mouse cortex, extending neurites and positioning themselves in the proper radial orientation (Shi et al., 2012b). The transplantation of human neurons derived from iPSCs into a neonatal mouse brain was demonstrated on year later, with human neurons integrating and establishing functional circuitry within the host brain (Espuny-Camacho et al., 2013). Taken together these data demonstrated that iPSC-based models of cortical development can produce mature, functional neurons and reinforces the validity of iPSC-based models as a suitable system for modeling neurologic diseases.

Human iPSC and Stem Cell Based Models of TSC

To date there are currently only three studies using iPSC or stem cell-based systems to model TSC *in vitro*. Only two of these studies utilized TSC patients, while another used genetic manipulation techniques to generate *TSC2* +/- and *TSC2* -/- cell lines. The first study using a stem

cell-based model to study neurodevelopment in the context of TSC utilized zinc-finger nuclease-mediated targeted gene disruption to generate *TSC2* +/- and *TSC2* -/- cell lines from human embryonic stem cells. Findings in heterozygous *TSC2* edited lines showed more modest changes to mTORC1 pathway activation which was only readily apparent after neuronal differentiation, although deficits in neuronal differentiation were still transiently observed in some heterozygous cell lines. This finding is consistent with the subsequent observation that neural progenitors from a TSC patient had a decreased capacity to differentiate into Purkinje cells, suggesting neuronal differentiation may be one process which is affected during brain development in TSC, although this phenotype may be sub-type specific to certain types of neuron (Sundberg et al., 2018). Neural progenitor cell proliferation appeared to be unaffected in heterozygous cell lines, however increased proliferation was shown in homozygous *TSC2* null lines. Neurons produced from *TSC2* heterozygous neural progenitors also expressed alterations in synaptic function as measured by the frequency of spontaneous excitatory post-synaptic currents (sEPSCs). This synaptic phenotype, but not the deficit in neuronal differentiation, could be rescued by long term treatment of rapamycin. These data suggest that some cellular abnormalities observed in TSC may be more directly dependent on mTORC1 pathway hyperactivation than others. As expected, more dramatic effects were shown in lines with full *TSC2* gene inactivation, suggesting that abnormal cellular and molecular phenotypes observed in human TSC are dose dependent with respect to the affected gene, and that more severe abnormalities are expressed in *TSC* null cells. However, some cellular and molecular alterations are also present in *TSC* heterozygous cells reinforcing the hypothesis that full gene inactivation may not be required to produce all aspects of TSC neurological phenotype. (Costa et al., 2016; Grabole et al., 2016).

Of the two subsequent studies using TSC patients one assayed only a single TSC patient and a control, and the other differentiated specifically cerebellar Purkinje cells. Both studies of TSC patients showed alterations in molecular phenotype with evidence of elevated mTORC1 signaling. The assay of primitive neural progenitors and neurons in one patient showed an increased proliferative tendency in *TSC2* heterozygous neural progenitor cells along with morphological abnormalities in differentiated neurons including reduced neurite length. An increased proliferative capacity was also observed in iPSC-derived neural progenitors of three other TSC patients before differentiation into Purkinje cells. Interestingly, these effects were observed despite the heterozygous *TSC* genotype of the patient cell lines, in contrast to the earlier findings in isogenic *TSC2* heterozygous cell lines which did not exhibit obvious cellular effects in neural progenitor cultures. Abnormalities in neuronal differentiation, neuronal morphology and hypoexcitability were also observed in TSC patient Purkinje cell cultures. Neural progenitors from these TSC patient studies also showed an increased tendency for TSC neural progenitors to differentiate to an astroglial fate and were more susceptible to oxidative stress and cell death. In both studies many of the observed abnormalities in TSC patient cultures could be rescued with rapamycin treatment (Li et al., 2017; Sundberg et al., 2018).

Due to the relatively recent adoption of iPSCs as a model system for neurologic disease there are still significant gaps regarding which diseases have been successfully modeled to date. Even where an iPSC disease model exists data will often be incomplete and further research will be needed to fully explore the phenotype in the new model. Furthermore, individual variability in disease phenotype and genetic background may produce different results between studies, highlighting the importance of individualized approaches to understanding disease mechanisms where there is high variability in neuropathologic or neurocognitive severity of the affected

population. Given the paucity of data on TSC using iPSC-based models, more research will be needed to explain many remaining questions about the human disease. Specifically, studies exploring the nature of the heterozygous cellular and molecular TSC disease phenotype will be needed to explain observed disease phenotypes in human iPSC models of TSC which are heterozygous in nature and most likely do not rely on any large-scale second-hit gene inactivation events which produce LOH.

Project Rationale

The observation that certain aspects of TSC symptomology have been reported in model systems without LOH suggests that the classic second-hit model is insufficient to fully explain the diverse neuropathological and neurocognitive phenotypes in TSC (Niida et al., 2001). This observation is further supported by surveys of intellectual disability which show no correlation between tuber load and severely affected individuals for intellectual disability (Vries, 2010). Critically, heterozygous animal models of TSC do not express neuroanatomical defects but do show evidence of neurocognitive and behavioral phenotypes (Ehninger et al., 2008; Goorden et al., 2007). Taken together these findings suggest that an abnormal phenotype persists in non-tuber brain regions which are heterozygous for either TSC gene, and that alterations in non-tuber cell function may underlie part of TSC disease pathology.

Animal models, and especially transgenic mouse models have provided useful insight into TSC molecular mechanisms and the function of the TSC1-TSC2 tumor suppressor complex. However, these models provide limited translatability and fail to fully recapitulate TSC neurological phenotypes in Tsc1 and Tsc2 heterozygous animals. In order to study cellular and molecular alterations in TSC progenitors and neuronal differentiation we have used iPSCs to generate an *in vitro* model of TSC. This will provide a platform to study neuronal progenitors and neurons in a manner with high translatable relevance to the human disease and will allow for the investigation of key neurodevelopmental processes *in vitro*.

Hypothesis

We hypothesize that TSC1 or TSC2 haploinsufficiency, or the expression of an abnormal phenotype resulting from the loss of 50% of a gene's function is present in cells which are heterozygous for the TSC genes. This hypothesis is based on observations of TSC cortical malformations which lack LOH, the expression of neurocognitive defects in heterozygous animals missing obvious neuroanatomical defects and the neurocognitive and behavior hallmarks of TSC including Autism which suggest broad neurodevelopmental abnormalities may be driven by abnormal phenotypes in heterozygous neural progenitors and neurons. We predict that molecular signaling abnormalities characteristic to TSC will be present in heterozygous cells, but that this effect will be intermediate to that observed after LOH or homozygous gene inactivation. We further predict that normal neurodevelopmental and cellular phenotypes will be altered in a manner that is influenced by TSC signaling pathway alterations.

Generation and Characterization of Neural Progenitors and Neurons from Tuberous Sclerosis Complex Patients

Chapter 2: Methods and Materials

Human Subjects and iPSC Generation

Four human subjects were recruited for our study through the Comprehensive Epilepsy Center, NYU Medical School after obtaining informed written consent from the subjects or their guardians. Our subject group includes two clinically diagnosed TSC patients who carry *de novo* heterozygous mutations in the *TSC2* gene that are predicted to cause loss of function of the mutant allele, and two unaffected controls consisting of one gender and age-matched sibling, and one age-matched individual (Table 1). Mutation sites are based on human *TSC2* mRNA variant 1 sequence (GenBank NM_000548.3). Peripheral blood samples from each subject was collected and processed at the Rutgers Cell and DNA Repository (RUCDR) where CD4+ hematopoietic progenitor cells were isolated and transduced with Sendai viruses expressing reprogramming factors to generate iPSCs according to an established protocol (Loh et al., 2010). Multiple iPSC clones were derived from each individual, and clones were subjected to a standardized set of quality control services including assays for microbiological contamination and pluripotency as defined by the expression of markers determined via immunofluorescence and fluorescence-activated cell sorting (FACS) analysis. This study was conducted as described in protocols approved by the Institutional Review Board (IRB) at NYU and Rutgers University.

	Subject	**Age**	**Gender**	***TSC2* genotype**	**Mutation site**	**TSC features**
Same family	TSC #1	32	male	4bp deletion causing frame-shift	Nucleotides 4650-4653 (ACAA)	Refractory epilepsy, tubers, low IQ
	CTR #5	30	male	Normal	none	None
Different family	TSC #6	18	male	Point mutation causing premature stop	Nucleotide 2427 (C->T)	Controlled epilepsy, SEGAs, low IQ
	CTR #8	19	female	Normal	none	none

Table 1. Summary of subjects included in study. Subjects included two pairs of patient-control individuals from the same and different families. Briefly included information reports subject age, gender, *TSC2* genotype including mutation type and site for TSC patients and major TSC features reported in each TSC patient.

Neural Progenitor Cell Induction

iPSC colonies were maintained in mTESR hPSC media (STEMCELL Tech) (Table 2) and were passaged onto matrigel coated six well plates. To generate neural progenitor cell (NPC) lines the iPSC culture medium was replaced with a neural expansion medium (NEM) containing a defined Neural Induction Supplement containing a proprietary cocktail of factors, and equal parts Neurobasal and Advanced DMEM +F12 media (Table 2) according to the manufacturer's instructions (Gibco). The NEM was changed every other day for four days, after which it was changed every day until day seven. Newly generated NPCs were detached using Accutase (STEMCELL Tech), plated in matrigel coated cell culture flasks, and expanded in NEM. NPC cultures were maintained in NEM with medium being changed every 2-3 days. Cells were passaged to new matrigel coated flasks (Cell Star) after reaching ~70 - 90% confluence. During passaging NPCs were seeded at 2×10^7 cells per $75cm^2$ cell culture flask. NPCs were counted for seeding by manual counting with a hemocytometer. Cell counts from four hemocytometer fields were averaged per culture during passaging and the cell count was then calculated for the total volume of detached cells in suspension. At least three NPC lines per subject were generated and used in this study.

Neuronal Differentiation

Expanded NPC lines were expanded and allowed to reach ~70 - 90% confluence in Cell Star 500 mL cell culture flasks before being detached with Accutase. Dissociated NPCs were then seeded at 1×10^6 cells per well in a 24 well cell culture plate (Falcon) coated with 10 µg/mL laminin and poly-D-lysine in order to support neuronal growth. NPCs were induced to differentiate

Media Type	Cell Culture	Media Components
Feeder-free iPSC maintenance medium	iPSCs	mTeSR1 basal medium (STEMCELL Technologies) 5X mTeSR1 supplement (STEMCELL Technologies)
Neural expansion medium	NPCs	Neurobasal medium (Gibco) Advanced DMEM/F12 medium (Gibco) 50X Neural induction supplement (Gibco)
Neural differentiation medium	neurons	Neurobasal medium (Gibco) BDNF (Pepro Tech) GDNF (Pepro Tech) 50X B27 supplement without vitamin A (Gibco) Non-essential amino acids

Table 2. Summary of media used for relevant cell culture systems. Briefly included are medium type and the appropriate cell culture type in which that media was used, the components included in each medium type and manufacturer. Supplements used may include factor cocktails not disclosed by the manufacturer.

by replacing the NPC-maintaining NEM with a neural differentiation medium (NDM) comprised of Neurobasal medium, 1X B-27 supplement without vitamin A, 1X GlutaMAX supplement, 1X nonessential amino acid supplement, 20 µg/mL BDNF, and 20 µg/mL GDNF (Table 2). Cultures were differentiated for 7 to 21 days depending on assay requirements. NDM was refreshed every 2-3 days through the course of differentiation.

Sanger Sequencing

NPCs generated from control and affected TSC patients were seeded at a density of 5 x 10^6 per well in 6 well cell culture plates (Falcon). NPCs were allowed to reach ~70% confluence before lysis and RNA extraction with a commercially available kit (ThermoFisher). cDNA was then generated from RNA samples via reverse transcription using reverse transcriptase (ThermoFisher). Sequences surrounding each known mutation site in each patient was amplified via polymerase chain reaction (PCR).

Oligos for *TSC2:*

Set 1 - 5’-GGAACCTGGTGCCTCACTTG-3’ (forward);

Set 1 - 5’-GCTGCCACAGGGAGCTTAG-3’ (reverse);

Set 2 - 5’-CACAGGCATTCAGGGACTTG-3’ (forward);

Set 2 - 5’-TGAGCTTCACCACCAGAAC-3’ (reverse).

Primers from set 1 were used to amplify sequences from subject lines CTR #5 and TSC #1, surrounding the patient 4bp deletion mutation. Primers from set 2 were used to amplify sequences from subject lines CTR #8 and TSC #6, surrounding the patient nonsense mutation. PCR products

were then purified and sequenced via Sanger Sequencing (Genewiz). Sequences were analyzed with Chromas Lite software to view trace files (Technelysium).

Immunofluorescence Staining

iPSCs or NPCs were seeded at 5 x 10^5 or 1 x 10^6 per well either on glass coverslips or directly onto 24 well cell culture plates coated with either matrigel or laminin/poly-D-lysine (as appropriate for either pluripotent, progenitor or neuronal cultures). Dissociated iPSC colonies and NPCs were cultured for 48 hours whereas neurons were differentiated for 1-3 weeks before staining. Media was then removed, and cells were gently washed twice with cold 1X phosphate buffered saline (PBS) and fixed with 4% paraformaldehyde. Fixed cells were washed twice with PBS before permeabilization with 0.1 % Triton X-100, and then washed three times in PBS before blocking in 10% normal goat serum. Cells were incubated overnight at 4°C with appropriate primary antibodies (Table 3) in an antibody buffer containing 0.1% Triton X-100 and 10 % normal goat serum. After primary incubation cells were washed three times in PBS then incubated with an appropriate secondary antibody in a secondary antibody buffer containing 0.1% Triton X-100 in 1X PBS. Cells were incubated in secondary antibody for one hour and washed again three times in PBS before mounting coverslips on glass slides with Vectashield (Vector Laboratories) mounting medium containing DAPI nuclear stain. Cells fixed directly onto plates were counterstained with either RedDot2 (Biotium) or Hoechst nuclear stain (ThermoFisher). Images were captured using an Olympus microscope equipped with a Yokogawa CSU-10 spinning disk confocal head and/or an inverted epifluorescence microscope (Olympus). Images were cropped and corrected for brightness and contrast using ImageJ analysis software.

Antigen	Antibody Type	Manufacturer	Catalog #	Application	Working Dilution
4E-BP1	Rabbit IgG	Cell Signaling	9452	WB	1:2000
p4E-BP1	Rabbit IgG	Cell Signaling	2855	WB	1:2000
ACTIN	Mouse IgG2b	Millipore	MAB1501	WB	1:2000
AKT	Rabbit IgG	Cell Signaling	4961	WB	1:2000
pAKT (Ser473)	Rabbit IgG	Cell Signaling	9271	WB	1:2000
pAKT (Thr308)	Rabbit IgG	Cell Signaling	9275	WB	1:2000
βIII TUBULIN	Mouse IgG2a	Bio Legend	MMS-435P	IF/WB	1:250
BrdU	Rat IgG2a	Abcam	ab6326	IF	1:250
DOUBLECORTIN	Rabbit IgG	Abcam	ab18723	WB	1:2000
HuC/D	Mouse IgG2b	Thermofisher	A-21271	IF	1:250
IRS1	Rabbit IgG	Cell Signaling	2382	WB	1:2000
KI67	Rabbit IgG	Cell Signaling	9129	IF	1:250
MAP2	Rabbit IgG	Millipore	AB5622	IF	1:250
NESTIN	Mouse IgG1	Millipore	MAB5326	IF	1:250
OCT4	Mouse IgG1	Millipore	AB4401	IF	1:500
PAX6	Mouse IgG1	DSHB	AB_528427	IF	1:250
S6	Mouse IgG1	Cell Signaling	2317	WB	1:2000
pS6	Rabbit IgG	Cell Signaling	4858	WB	1:2000
SOX2	Rabbit IgG	Millipore	AB5603	IF	1:250
TRA-1-60	Mouse IgM	Millipore	AB4360	IF	1:500
TSC2	Rabbit IgG	Cell Signaling	4308	WB	1:2000

Table 3. List of primary antibodies used in all included studies. Briefly, antigen, antibody type, antibody manufacturer and catalog number, relevant immune-linked applications and working dilution are included.

High Content Analysis of Microscopy Images

Cells stained on coverslips or plates using the previously described immunofluorescence protocol were loaded into an INCell Analyzer 6000 (GE Healthcare) for high-content analysis of fluorescence microscopy images. Multiple image fields were selected at random and analyzed using Workstation software (GE Healthcare). For coverslips twelve fields across four wells per experiment were imaged, whereas 4-9 fields per well were captured from cells plated on 24 well plates. Fields containing less than 30 cells were excluded from analysis.

Total cell count per image field was measured by counting total nuclei as shown by nuclear counter staining. INCell Workstation multi-target analysis was used to identify nuclei and cellular objects. Nuclei were identified via top-hat segmentation and thresholding for minimum object size ($50\mu m^2$) to discard non-nuclear objects. Total cell count of either RedDot2, Hoechst or DAPI was attained in this manner. HuC/D positive neurons were counted utilizing the same object identification protocol. Cell size was measured from HuC/D-stained cultures using top-hat segmentation and minimum size thresholding to identify and measure immunolabeled objects and discard non-cell objects. The percentage of HuC/D-positive cells was determined by counting all identified objects in each image field of the HuC/D channel and dividing by the total number of objects in the nuclear (total cell) channel (HuCD+ cell count/Total nuclei) (Figure 8). FOXO3a distribution was measured via multi-target analysis using cellular measurements. Collar analysis was used to describe an area extending for 5μm immediately surrounding nuclei identified using the previously described nuclear counting protocol. Collar area was then analyzed for staining intensity in the FOXO3a channel in order to determine relative levels of cytoplasmic FOXO3a localization.

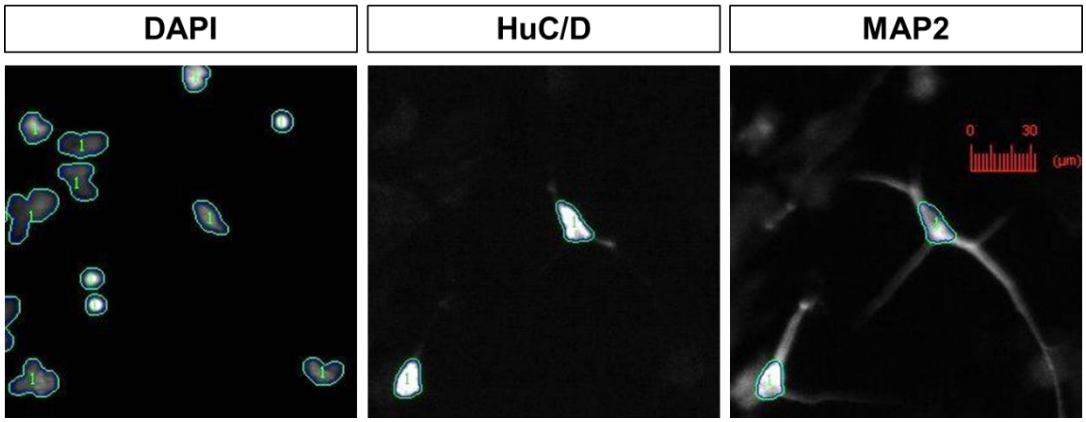

Figure 8. Representative immunofluorescence images taken with an GE INCell 6000 automated confocal microscope and analyzed with the INCell Workstation image analysis program using the nuclear counting protocol. Recognized objects to be counted are highlighted in green. DAPI and HuC/D labeled objects are identified via top-hat segmentation. HuC/D expression used for counting post-mitotic neurons is highly neuron-specific as shown by colocalization with MAP2. Scale bar = 30µm.

BrdU Staining of Cells in S-Phase

Neural progenitor cell cultures were incubated for four hours in neural expansion media containing 10uM bromodeoxyuridine (BrdU) labeling solution (Abcam). After incubation cells were treated with 2N HCl for 30 minutes at 37C. HCl was then removed and neutralized with 0.1M sodium borate for ten minutes at room temperature. Next, treated cells were fixed with 4% paraformaldehyde and prepared for immunofluorescence staining as detailed previously. Cells were incubated overnight with a primary antibody against BrdU, then prepared for imaging using the same steps for the standard immunofluorescence staining protocol described above. Images of cultures were obtained and analyzed using the GE INCell Analyzer 6000 and INCell Workstation software as outlined previously. The total number of BrdU labeled cells was divided from the total number of cells as counted by Hoechst nuclear stain to obtain the fraction of cells actively replicating DNA in S-phase within each culture.

Cell Death Assay

Cell death was assayed by seeding NPCs at a density of 5×10^5 in matrigel coated 24 well cell culture plates. After 48 hours of growth in NEM the medium was removed, and cells were incubated with 1:1000 2mM Hoechst and 30nM SYTOX Green dead cell (Invitrogen) nuclear stains in 1X PBS for ten minutes. Cells were then washed twice quickly with 1X PBS and imaged live immediately using the INCell Analyzer 6000. Cultures were subjected to high content analysis for nuclei counting as described previously for high content microscopy. To calculate the percentage of dead cells the number of Sytox stained dead cells was divided by the number of the total cell population labeled by Hoechst nuclear staining (Sytox cell count/Hoechst cell count).

Sytox staining exclusively labels dead nuclei in live cultures, while Hoechst labels all nuclei of dead and living cells.

FOXO3a Localization Assay

NPCs were seeded at a density of $5x10^4$ cells per well in a 24 well cell culture plate and cultured for 48 hours before fixation in 4% paraformaldehyde and preparation for immunofluorescence staining as outlined previously. Prepared cells were incubated with an antibody against total FOXO3a. After the completion of immunofluorescence staining cells were imaged using the GE INCell Analyzer of confocoal microscopy to obtain representative images and images for high content analysis. INCell Analyzer Workstation high content analysis of microscopy images were used to determine relative nuclear and peri-nuclear distributions of FOXO3a staining. Briefly, the total cellular fluorescence, nuclear fluorescence and the fluorescence detected in a 10um peri-nuclear collar cellular region were measured and these data were used to calculate relative nuclear and cytoplasmic distributions of FOXO3a.

Whole Transcriptome Analysis

Two independently generated NPC lines from each of the related subjects (TSC #1 and sibling CTR #5) were seeded at a density of $5x10^6$ cells per well in 6 well cell culture plates and cultured for 48 hours before dissociation with Accutase. Dissociated NPCs were then spun down (5 minutes at 1200rpm) to form a dry pellet to be harvested for RNA extraction. Total cellular RNA was prepared using a Zymo Direct-Zol kit and delivered to RUCDR Infinite Biologics (Piscataway, NJ) for sequencing. Libraries were prepared with Illumina Tru-Seq kits and run as

paired-end, 75nt/end on Illumina NextSeq. RNA-Seq reads were pseudoaligned to hashed k-mers built from the UCSC Reference Sequence library of mRNAs using the Kallisto RNA-seq quantification program (Bray et al., 2016). Estimated counts were imported into the Sleuth package for differential analysis of gene expression data in R/Bioconductor, where differential expression was assessed using a Wald test (Gentleman et al., 2004; Pimentel et al., 2017). Gene ontology analysis utilized the DAVID website (Huang da et al., 2009). RNA-Seq data are available from the NIH GEO archive (accession GSE111584).

Western Blotting

Dissociated NPC lines were seeded in triplicate for expansion or individually for differentiation onto six well cell culture plates coated with Matrigel or poly-d-lysine/laminin, respectively at densities of 5 x 10^6 cells per well. NPCs were allowed to differentiate for 7-21 days in NDM or expand for 48 hours in NEM before lysing with radioimmunoprecipitation assay buffer (RIPA) cell lysis buffer containing phosphatase and protease inhibitors. Lysates were cleared via centrifugation at 12,000 x g for 10 minutes and the supernatant was collected. Soluble protein samples were combined in a 1:1 solution with loading buffer containing sodium dodecyl sulfate (SDS) and loaded into Tris-Glycine gels for gel electrophoresis for 1.5 hours. Proteins were then transferred for 2.5-3 hours at 450-500 milliamps onto nitrocellulose membranes and blocked in a blocking buffer consisting 3 % nonfat dry milk in 1X Tris-buffered saline containing 0.1% Tween (TBST) for one hour before incubation overnight with primary antibodies (Table 3) in a primary antibody buffer solution of 1X TBST and 0.1% sodium azide (for antibody storage). Membranes were then washed three times in 1X TBST and incubated for one hour in an HRP-conjugated secondary antibody solution in 1X TBST, then washed a further 3 times in 1X TBST. Membranes

were then coated with ECL Western Blotting Substrate for chemiluminescence (ThermoFisher) and images of protein bands were obtained using radiographic film. Image scanning and band densitometry was performed using AlphaImager band analysis software.

Small Molecule Treatments

For drug treatments NPCs were plated in either 24 well or 6 well cell culture plates at a density of 1 x 10^6 or 5 x 10^6, respectively. Cells were expanded for 48 hours then treated with NEM containing either 0.1 % DMSO (Sigma), 5 µM RAD001, 5ug/mL SC79, 1 µM MK2206 or 10uM LY294002 (all Selleckchem). After 24 (MK2206) or 48 (RAD001, SC79 and LY294002) hours samples in 6 well plates were collected for Western blotting. Cells plated for immunofluorescence staining in 24 well cell culture plates were differentiated by changing medium from NEM to NDM containing DMSO, RAD001, SC79, MK2206 or LY294002 as needed. Cells were cultured for 7 days before fixation, staining and imaging via high content analysis of microscopy imaging protocol as described previously.

Statistics

Sample size (*n*) was determined by the number of independent experiments conducted using at least 2 different lines per subject and, where indicated, additional replicate experiments using the same NPC lines cultured at a different time and after a different number of passages. Comparisons between TSC patient and control groups were conducted pairwise between one sibling-matched pair (CTR #5 and TSC #1) and non-sibling pair (CTR #8 and TSC #6). All statistical analysis was conducted using GraphPad Prism7 software. For proliferation (KI67 and

BrdU staining) experiments at multiple time points significance was determined using ordinary or repeated measure two-way ANOVA with Sidak's multiple comparisons tests. For cell death and soma size measurements statistical significance between genotypes was determined using unpaired nonparametric *t* tests (Mann-Whitney). To compare neuronal differentiation between control and TSC cell lines at different time points statistical significance was determined using multiple unpaired *t* tests corrected using the Holm-Sidak method and □= 0.05. To determine the effect between control and TSC genotypes in Western blot experiments statistical significance was determined using either unpaired *t* tests or one-sample *t* tests, depending on the data structure. When multiple independent samples from each TSC and the corresponding control subject were analyzed simultaneously on the same gel using nonparametric unpaired *t* tests (Mann-Whitney) to compare the means of the two groups. When independent samples were analyzed in technical triplicates and run at different times on different gels data was normalized to the mean of the control value (set to 1). In this case comparison was made using one-sample *t* tests. For drug treatment experiments that were performed at different times with different drugs the mean percentage of HuC/D+ cells in the CTR + DMSO sample was normalized and the internal control set to 1. Values from experimental groups were expressed as fold change from control. Significance was determined via one-way ANOVA with Dunnett's post-hoc analysis. For gene expression analysis results obtained from 2 independent NPC lines/subject in the CTR #5, TSC #1 pair were compared. Transcripts having a False Discovery Rate (FDR; *p* value adjusted by the Benjamini-Hochberg method) of 1% or less and a beta value estimating at least a two-fold change were selected for analysis.

Chapter 3: Results

Generation of NPCs from TSC patient and control subjects

In order to study *TSC2* heterozygous phenotypes, we developed an *in vitro* model of TSC by generating iPSCs from two individuals with *de novo TSC2* mutations who had epilepsy, low IQ and neuroanatomical defects, and two genetically normal controls. Patient designated TSC# 1, the sibling of unaffected CTR# 5, carries a heterozygous deletion in the *TSC2* gene (hg38 chr16:2,085,001-2,085,004, del ACAA) predicting a frameshift beginning at Asn1515, that results in termination after 1573 amino acids, according to the reference isoform (NM_000548). The patient designated TSC #6 has a single base change (chr16:2,074,224; rs45517233), causing premature termination of *TSC2* mRNA translation (Gln794->Stop). iPSCs were generated from peripheral blood cells and reprogrammed using Sendai viruses expressing the Yamanaka cocktail of transcription factors following a previously reported protocol for cellular reprogramming for iPSCs (Figure 9A) (Loh et al., 2010). Newly generated patient- and control-derived iPSC colonies expressed the factors OCT4 and TRA-1-60 confirming their pluripotent state (Figure 9B).

We next generated primitive, lineage restricted NPCs from iPSC cultures using commercial reagents and following previously described methods for NPC induction (Figure 10A) (Yan et al., 2013). After seven days of differentiation in neural expansion medium, NPCs were isolated and assayed. This protocol was repeated multiple times to obtain at least 3 independently-generated NPC lines per subject. Direct sequencing results of NPC lines from each subject confirmed that TSC patient-derived NPCs carried the expected heterozygous *TSC2* mutations consisting of a frame-shift in TSC #1 and a nonsense mutation in TSC #6. Both mutations occur before the TSC2 GAP domain and are predicted to result in a deficit of functional TSC2 protein (Figure 10B-C).

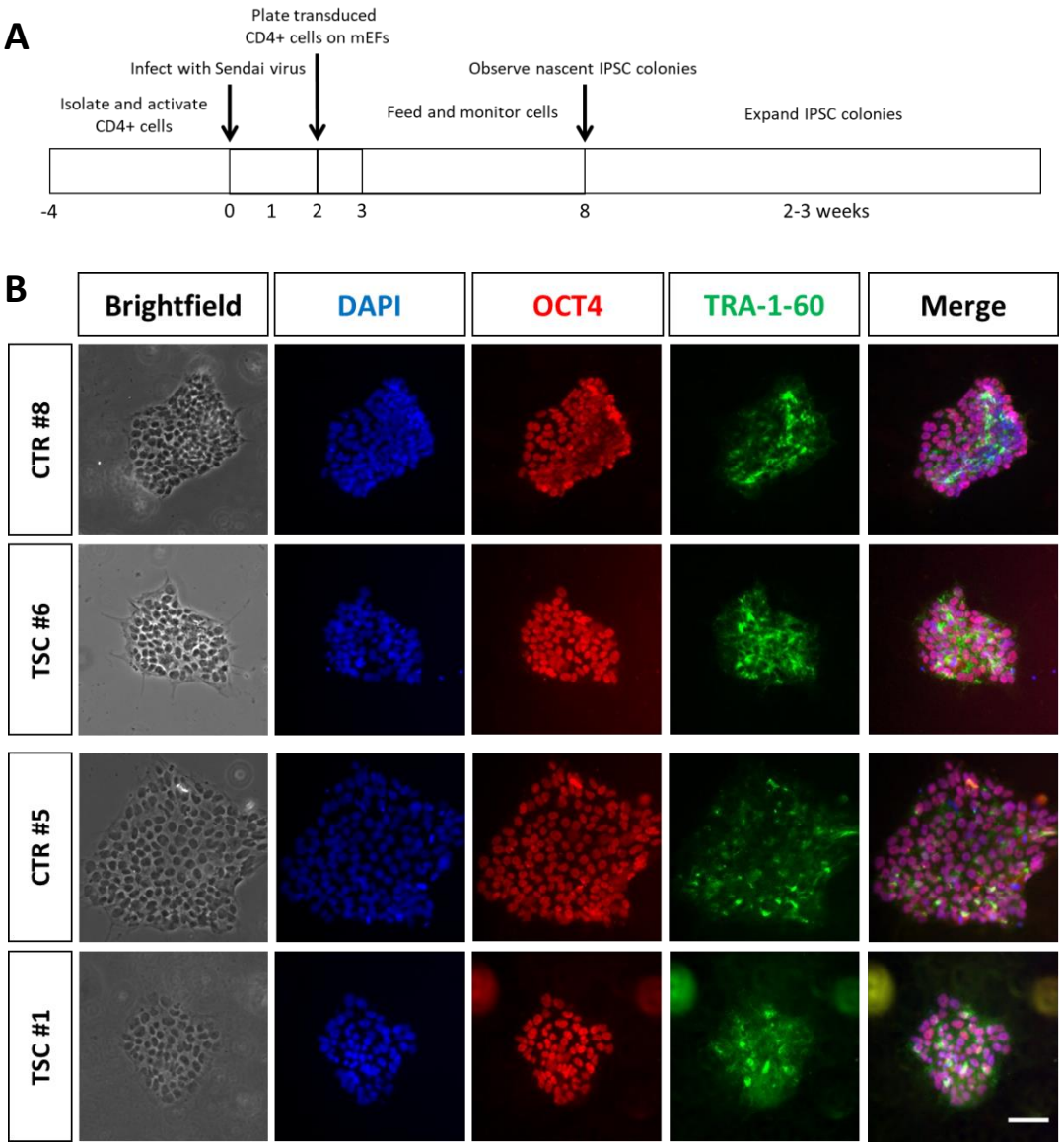

Figure 9. (A) Protocol timeline of iPSC induction from activated CD4+ cells via infection with Sendai viruses carrying Yamanaka factors. (B) Brightfield and immunofluorescence microscopy images of iPSC colonies. Transduced cells expressed markers of pluripotency OCT4 and TRA-1-60 in cultures derived from both TSC-CTR subject pairs. Cell nuclei were counterstained with DAPI. Scale bar = 100µm.

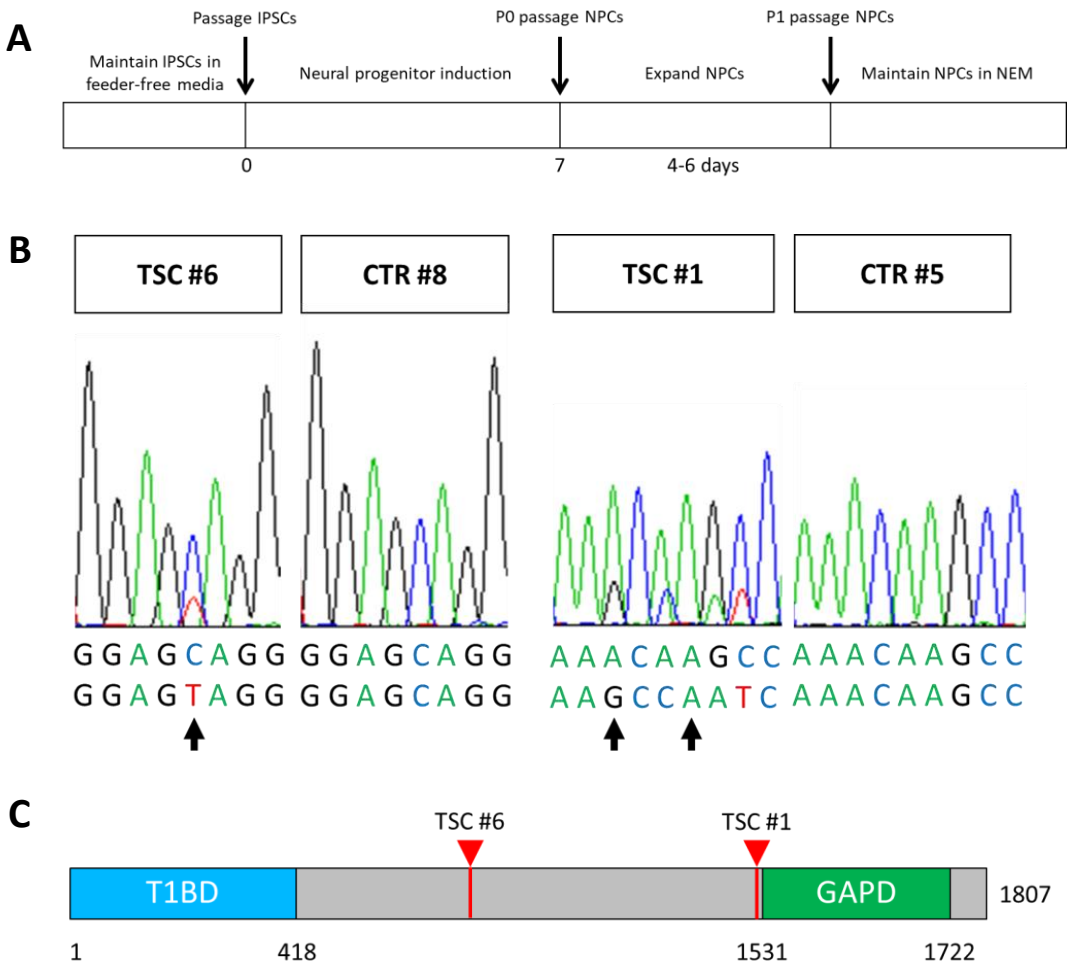

Figure 10. (A) Workflow depicting the generation of lineage restricted NPCs from subject-derived iPSCs. (B) Sanger targeted sequencing confirms the heterozygous *TSC2* genotype of TSC patient NPC lines. Arrows point to double peaks in patient cells showing the presence of a point mutation resulting in a nonsense mutation in the *TSC2* gene of subject TSC #6, and a four base pair deletion resulting in frameshift in subject TSC #1. (C) Schematic representation of the TSC2 protein indicating the approximate position of each TSC patient mutation.

TSC2 protein levels may also be reduced due to nonsense-mediated RNA decay (NMD) which is known to degrade mRNAs carrying premature termination codons (Maquat, 2002). Immunofluorescence staining confirmed the robust expression of Nestin (NES), SOX2 (>80%) and PAX6 (>70%) markers in both patient and control NPCs, consistent with a neural progenitor identity (Figure 11A-E). We also demonstrated that NPC cultures derived in this manner did not show expression of iPSC markers OCT4 and TRA-1-60 (Data Not Shown), confirming that these cells successfully differentiate from a pluripotent to a lineage-restricted neural progenitor state.

Characterization of NPC proliferation and viability

Since TSC signaling and mTORC1 activity have been demonstrated to play key roles in regulating cell growth and survival (Gan et al., 2008; Hartman et al., 2013; Lee et al., 2003; Ozcan et al., 2008; Wu et al., 2009) we sought to determine the effect of *TSC2* haploinsufficiency on NPC proliferation and viability *in vitro*. Here we utilized high-content analysis of microscopy images in order to quantify a large number of cells from multiple technical replicate samples and multiple independent experiments in an unbiased manner. NPC proliferation was assayed at two and ten days *in vitro* (DIV) by labeling cells actively replicating DNA in S phase using bromodeoxyuridine (BrdU) or in all active phases of the cell cycle (G_1, S, G_2 and M) with an antibody against the proliferative marker KI67 (Figure 12A-B). The total cell number was determined using a common nuclear stain, either Hoechst or RedDot2. The percentages of KI67 positive or BrdU positive proliferating cells over the course of two and ten DIV was not significantly altered between patient and control progenitor lines in both subject sets analyzed, although a small increase in both BrdU positive and KI67 positive proliferating cells at DIV10 was noted in one patient (TSC #6) relative to control at that time point. However, this difference was not significant (Figure 12C-F).

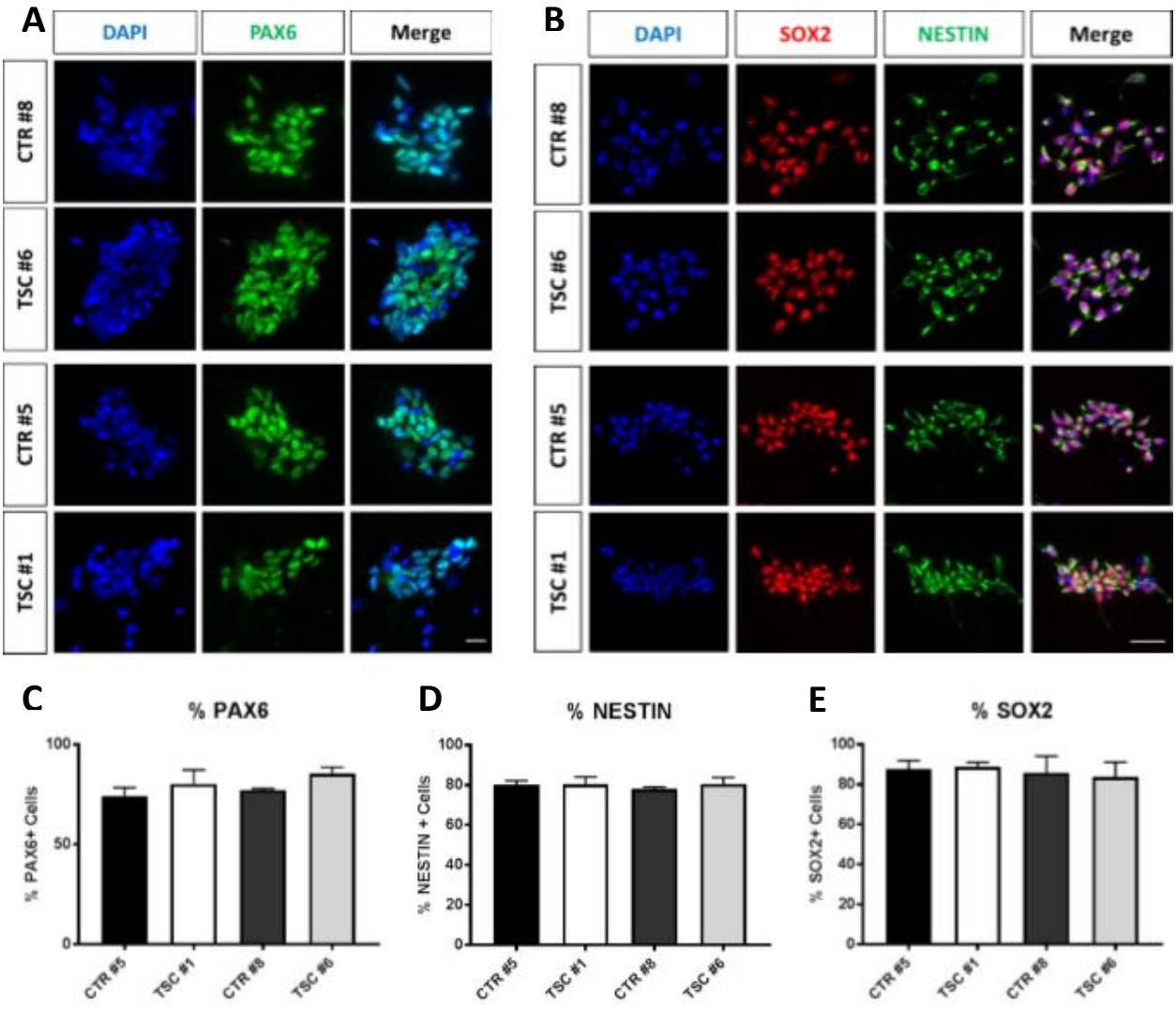

Figure 11. (A-B) Immunofluorescence images of induced NPCs. NPC lines show expression of neural stem cell markers PAX6, SOX2 and NESTIN. Cells are counterstained with DAPI nuclear stain (C-E) Quantification of the percentage of cells expressing each NPC marker relative to the total number of cells (DAPI-labeled nuclei). Data obtained from n = 3 independent experiments per subjects. A total of nine fields were analyzed per experiment. Data are plotted as mean values ± SEM. Scale bars = 20µm (A) and 50µm (B).

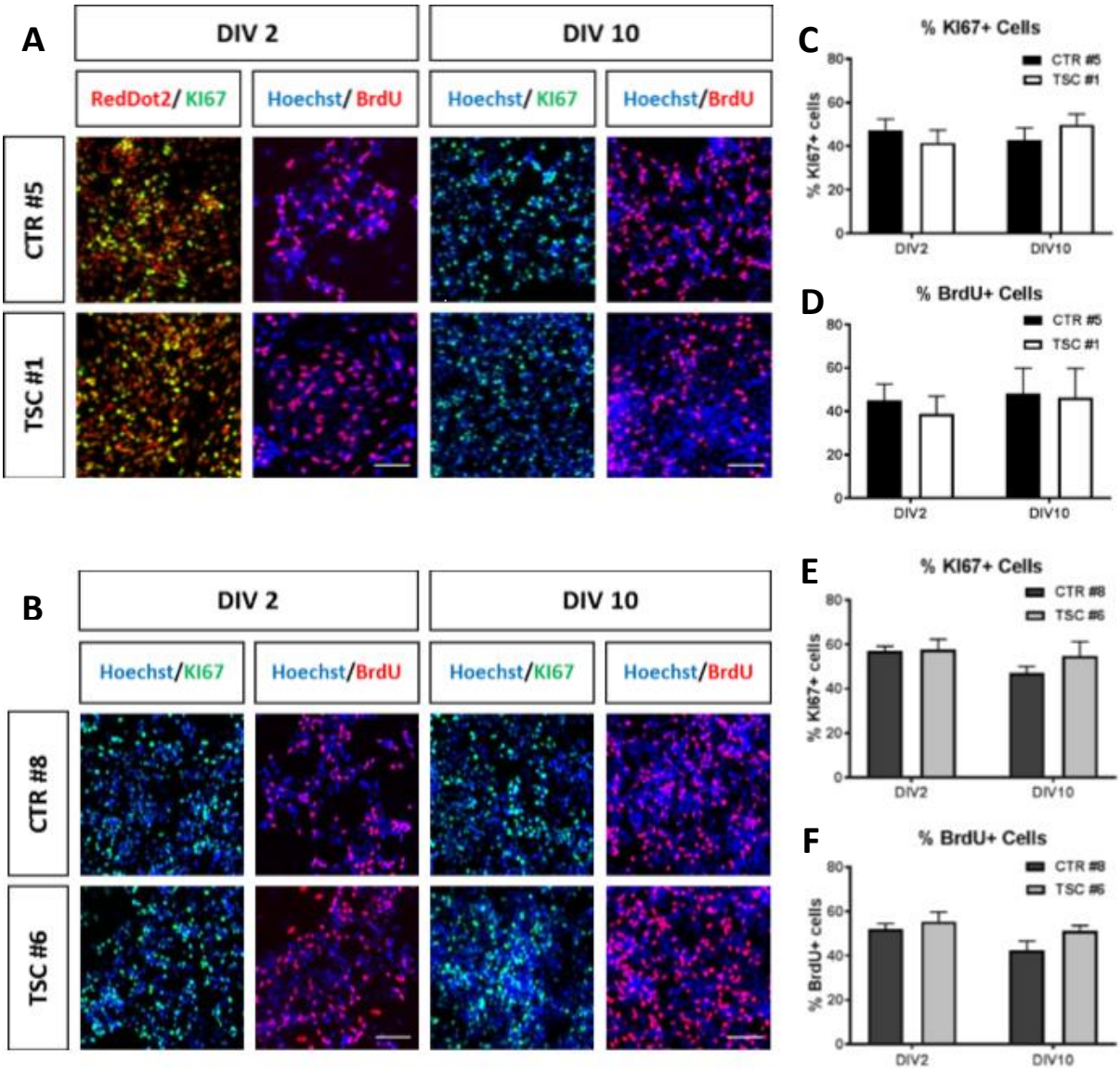
A
DIV 2
DIV 10
RedDot2/ KI67
Hoechst/ BrdU
Hoechst/ KI67
Hoechst/BrdU
CTR #5
TSC #1
B
DIV 2
DIV 10
Hoechst/KI67
Hoechst/BrdU
Hoechst/KI67
Hoechst/BrdU
CTR #8
TSC #6
C
% KI67+ Cells
CTR #5
TSC #1
% KI67+ cells
DIV2
DIV10
D
% BrdU+ Cells
CTR #5
TSC #1
DIV2
DIV10
E
% KI67+ Cells
CTR #8
TSC #6
% KI67+ cells
DIV2
DIV10
F
% BrdU+ Cells
CTR #8
TSC #6
% BrdU+ cells
DIV2
DIV10

Figure 12. Analysis of patient and control NPC proliferation. (A-B) Representative confocal images of DIV2 and DIV10 NPC cultures for the active cell cycle marker KI67 or an antibody against previously incorporated BrdU to label proliferating cells in S-phase, and counterstained with RedDot2 or Hoechst. (C-F) Automated high content analysis of randomized image fields of control and patient cultures labeled on DIV2 or DIV10 for KI67 and BrdU showed no significant change in the percentage of proliferating cells between TSC and control cultures at either time point using either proliferative marker. n = 6 independent cultures (CTR #5 and TSC #1 DIV2 KI67), n = 4 independent cultures (CTR #5 and TSC #1 DIV2 BrdU), n = 3 independent cultures (CTR #5 and TSC #1 DIV10 KI67 and BrdU), n = 4 independent cultures (CTR #8 and TSC #6 DIV2 and DIV10 KI67 and BrdU). Data was analyzed using repeated measures two-way ANOVA with Sidak's multiple comparison test, $p>0.05$ for all comparisons. Data are plotted as mean values ± SEM. Scale bars = 100 µm.

To assay NPC viability, we measured the percentage of cells stained with SYTOX Green in similar 48-hour culture experiments (Figure 13A). The data here indicates that there is no significant increase in cell death in TSC cell lines as measured by the proportion of dead cells counted in each culture, although both patient-derived cultures showed a trend towards increased cell death (Figure 13B). Together these data show that the viability and proliferative background of TSC2 haploinsufficient NPCs remain mostly unchanged.

Signaling abnormalities in TSC neural progenitors

To investigate potential molecular defects in *TSC2* heterozygous cells derived from TSC patients we analyzed TSC2 protein expression levels and signal transduction pathways likely to be affected by *TSC2* mutations. Protein lysates from 3 independent NPC lines per subject were analyzed through Western blotting using an antibody against the C terminus of TSC2. The levels of this protein were significantly reduced by approximately 50% in both patients compared to control cell lines (Figure 14A-B). These data demonstrate that both patient mutations result in observable *TSC2* haploinsufficiency. The TSC1/TSC2 complex is a key regulator of mTORC1 activity in response to growth factor signaling, and mTORC1 upregulation has been observed in numerous homozygous animal or cellular models of TSC (Goto et al., 2011; Huang and Manning, 2008; Inoki et al., 2003a; Magri et al., 2011; Meikle et al., 2007). mTORC1 kinase activity is readily inferred by the levels of phosphorylation of downstream targets such as the ribosomal protein S6 and the translation initiation factor 4E-BP1. Western blotting data showed that *TSC2* haploinsufficiency in patient progenitor cells affected mTORC1 activity, resulting in an increase in S6 phosphorylation relative to total S6 protein levels (Figure 14A, C). The phosphorylation of

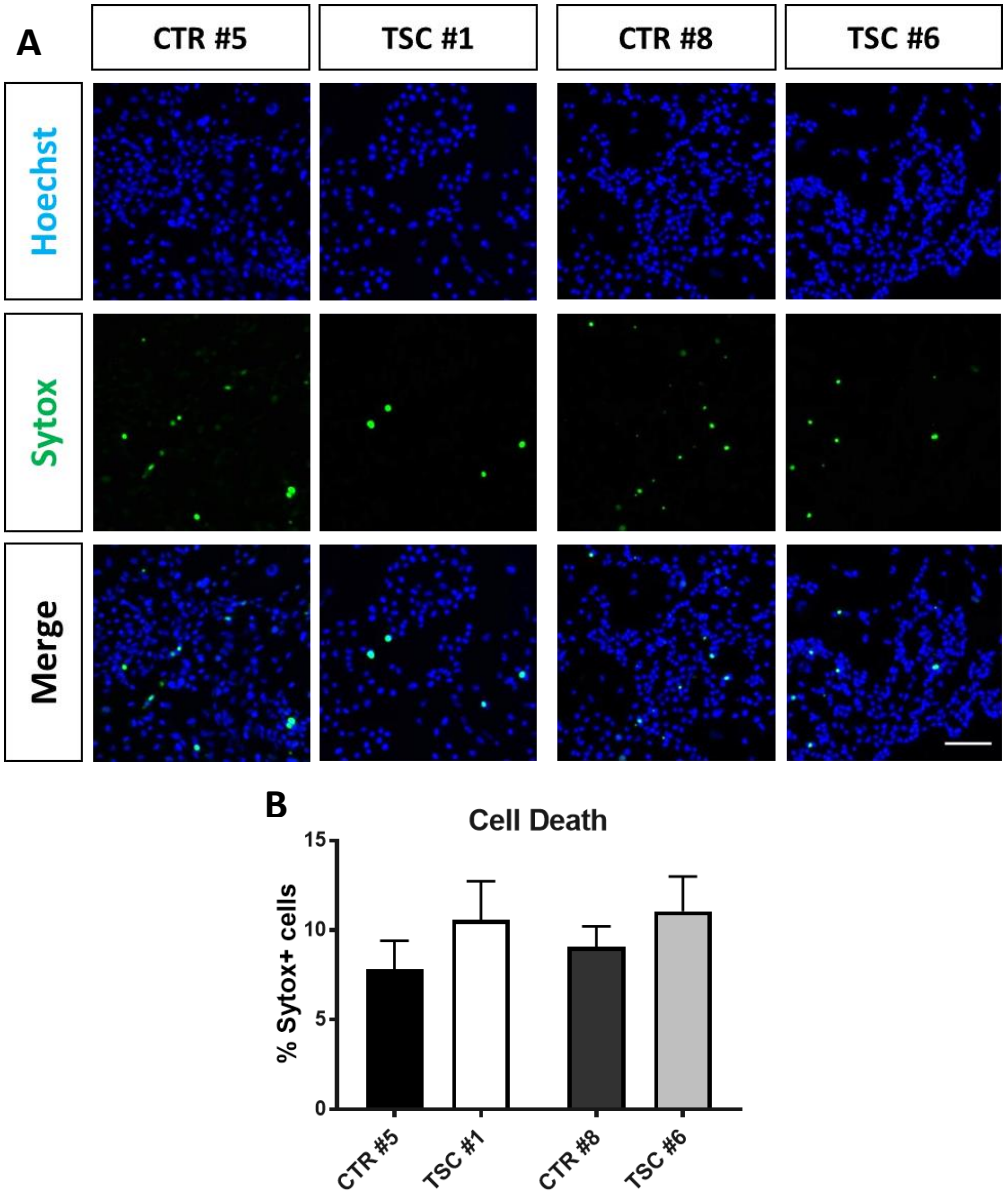

Figure 13. (A) Representative confocal images of NPC cultures stained with Sytox Green to visualize dead cells and counterstained with Hoechst nuclear stain. (B) Automated high content analysis of Sytox Green staining shows no significant difference between either TSC patient group and its respective control. *n* = 5 independent cultures (CTR #5 and TSC #1) and *n* = 4 independent cultures (CTR #8 and TSC #6). Significance was determined via unpaired nonparametric t test (Mann-Whitney). Data are plotted as mean values ± SEM. Scale bar = 100µm.

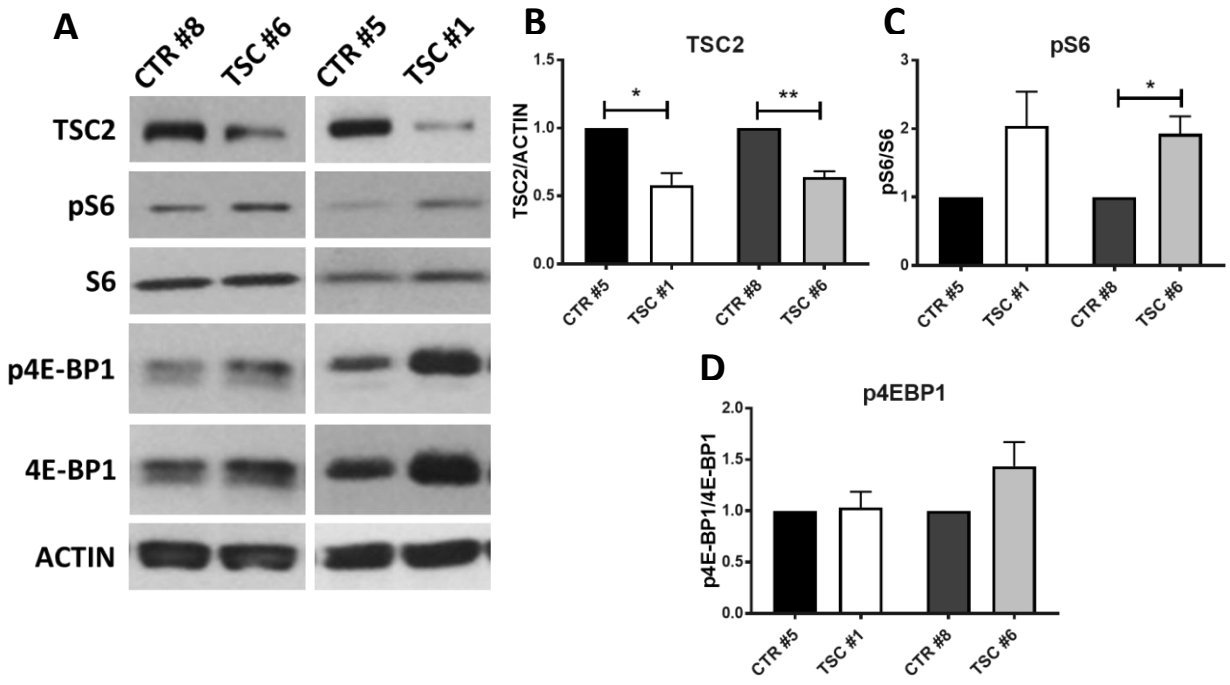

Figure 14. (A) Western blotting for TSC2 and phosphorylated proteins downstream of mTORC1: ribosomal protein S6 and 4E-BP1. (B-D) Quantification of Western blot data showed significantly decreased levels of TSC2 protein in both TSC patients (*$p<0.05$, **$p<0.01$), significantly increased phosphorylation of S6 in one TSC patient (TSC #6) (*$p<0.05$) and a trending increase in the second TSC patient (TSC #1) ($p=0.13$). Levels of phospho-4E-BP1 relative to total protein were not significantly altered in either patient samples. Significance determined via one-sample *t*-test. n = 4 independent cultures from three independently generated NPC lines. Data are plotted as mean values ± SEM.

4E-BP1 was not significantly altered when levels of phospho-4E-BP1 were normalized to levels of the total protein (Figure 14A, D). However, relative levels of total 4E-BP1 appeared to be elevated in TSC cells derived from one patient (TSC #1), potentially confounding the interpretation of these results. Interestingly, levels of total 4E-BP1 relative to the translation initiation factor eIF4E have been suggested as part of one mechanism regulating levels of cap-dependent protein translation mediated by mTORC1 activity (Alain et al., 2012). Western blotting of total 4E-BP1 and eIF4E showed the same patient with elevated 4E-BP1 also expressed higher relative levels of 4E-BP1 when compared to eIF4E (Figure 15A-C). These effects suggest the possibility of alternative pathways involved in the regulation of protein synthesis which may be affected by TSC2 haploinsufficiency. However, how these changes relate to TSC2 haploinsufficiency directly remains unclear. Overall, these data suggest that *TSC2* heterozygosity in NPCs increases mTORC1 activity, albeit to a more modest degree than which is observed in *TSC2* LOH cells.

Upstream regulation of TSC function occurs by PI3K/Akt signaling in response to mitogenic stimuli and insulin or growth factor receptors via the insulin receptor substrate IRS1, an adapter protein which mediates PI3K activation. In the presence of pro-growth stimuli, the PI3K/Akt pathway acts to phosphorylate and inhibit TSC2, resulting in the downstream activation of mTORC1 and the increase in protein translation and cell growth (Huang and Manning, 2009; Manning and Cantley, 2003). A negative feedback loop involving S6K has been shown to suppress PI3K/Akt signaling via inhibition and degradation of IRS1 (Pederson et al., 2001; Shah and Hunter, 2006; Shah et al., 2004). Consistent with the observed activation of mTORC1 we found that IRS1 levels were significantly reduced in both patient NPC lines (Figure 16A-B). Reduced AKT phosphorylation has been shown in homozygous models of TSC where mTORC1 activity,

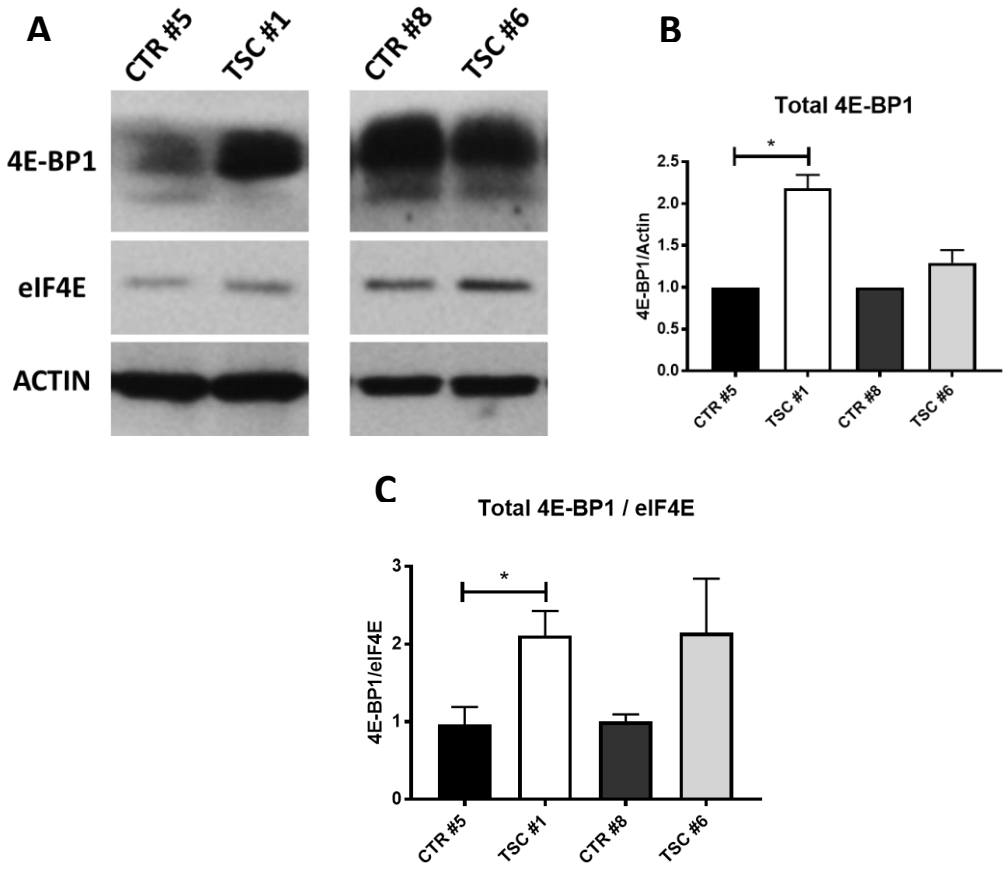

Figure 15. (A) Western blotting for total 4E-BP1 and the cap dependent translation initiation factor eIF4E in TSC patient and control NPCs. (B-C) Quantification of Western blot data shows an increased in the total levels of 4E-BP1 protein relative to sibling control in one TSC patient (TSC #1) (*$p<0.05$). Significance was determined via one sample *t*-test. Levels of 4E-BP1 protein relative to eIF4E were also increased in the same patient (TSC #1) (*$p<0.05$). This 4E-BP1/eIF4E ratio also trended upwards in the other TSC patient but was not significant. Significance was determined by unpaired parametric *t*-test. n = 3 independent cultures. Data are plotted as mean values ± SEM.

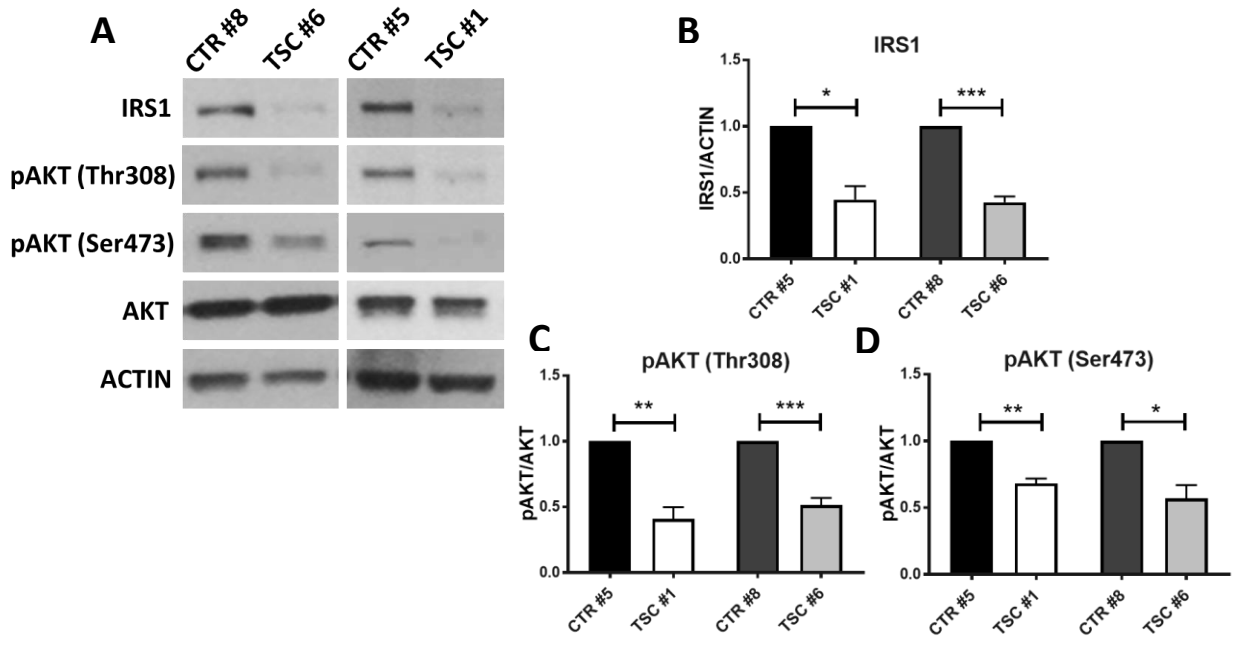

Figure 16. (A) Western blotting for IRS1 and phosphorylated levels of AKT as shown by immunoblotting against two phosphorylation sites: Thr308 and Ser473. (B-D) Quantification of Western blot data shows a decrease in total IRS1 protein in both TSC patients (*p<0.05, ***p<0.001). n = 4 independent cultures. Levels of phospho-AKT was also reduced at both Thr308 and Ser473 consensus sites in both TSC patients (*p<0.05, **p<0.01, ***p<0.001). n = 5 independent cultures (Thr308), and 4 independent cultures (Ser473). Significance was determined via one-sample *t*-test. Data are plotted as mean values ± SEM.

and the activity of S6K is robustly elevated (Jaeschke et al., 2002; Meikle et al., 2008; Zhang et al., 2003a). Consistent with these findings we observed that *TSC2* heterozygous NPCs exhibited significantly decreased levels of phosphorylated AKT protein (Figure 16A). Additionally, AKT in *TSC2* heterozygous cell lines showed reduced phosphorylation at both Ser473 and Thr308 phosphorylation sites, both of which are required for AKT activation (Figure 16C-D). The Thr308 site of AKT is phosphorylated by PI3K via 3-Phosphoinositide-dependent kinase 1 (PDK1), and reduced levels of phosphorylation at that site are indicative of reduced PI3K activity. The Ser473 site, on the other hand, is known to be phosphorylated by the mTOR-containing complex mTORC2, although the regulation of this kinase complex activity is not well understood it has been shown that phosphorylation of Ser473 may not be necessary for Akt activation, and so Thr308 is a more reliable biomarker of Akt activity (Vadlakonda et al., 2013; Vincent et al., 2011). Together, our findings suggest that the S6K-mediated negative feedback triggered by mTORC1 upregulation is responsible for the downregulation of IRS1 and the attenuation of PI3K/AKT activity observed in *TSC2* heterozygous cells.

Analysis of FOXO3a activity in TSC neural progenitors

Given the marked reduction in PI3K/AKT signaling observed in TSC2 heterozygous NPCs we next sought to ascertain whether other downstream targets of AKT activity were noticeably dysregulated. AKT has multiple downstream targets involving pro-growth and survival pathways and the attenuation of AKT signaling could impact NPC function through these pathways (Manning and Toker, 2017). We focused on the Forkhead Box family of transcription factors, specifically FOXO3a, which are primarily responsible for the promotion of factors involved in pro-apoptotic and cell-cycle arrest responses to cellular stress (Lam et al., 2013). The localization

of FOXO3a under normal circumstances when AKT is active and phosphorylates FOXO3a has been shown to be mainly cytoplasmic, becoming nuclear when AKT activity decreases and de-phosphorylated FOXO3a translocates into the nucleus to carry out its transcriptional program. Immunofluorescence staining of control and patient NPC cultures showed examples of differences in FOXO3a localizations between *TSC2* genotypes. However, automated high content analysis of microscopy images revealed only very modest changes in FOXO3a localization in TSC2 heterozygous NPCs (Figure 17A). Cytoplasmic FOXO3a immunofluorescence intensity as measured within a peri-nuclear collar region was slightly reduced in *TSC2* heterozygous cultures from one patient (TSC #1), however this difference was not significant. Nuclear FOXO3a intensity was unchanged between genotypes, and the proportion of cytoplasmic, peri-nuclear FOXO3a from total immunofluorescence intensity was very mildly and not significantly reduced (Figure 17B-D). These data suggest that downstream effects of AKT attenuation may be more modest and involve convergent effects of multiple pathways, or that other downstream targets of AKT activity are differentially affected by changes in AKT activity. However, three independent experiments from only one patient were analyzed. More experiments including additional TSC patients should be conducted to fully elucidate the effect of TSC2 haploinsufficiency on FOXO activity and other downstream effectors of AKT signaling.

Differential expression of mRNA transcripts in TSC2 heterozygous NPCs

While the TSC1 and TSC2 proteins themselves are not known to possess any transcription factor activity, the PI3K/AKT/mTORC1 pathway includes cross-talk and interaction with numerous transcription factors. mTORC1 has been linked to the activity of the signal transducer and activator of transcription 3 (STAT3), Transcription Factor EB (TFEB) and Hypoxia-inducible

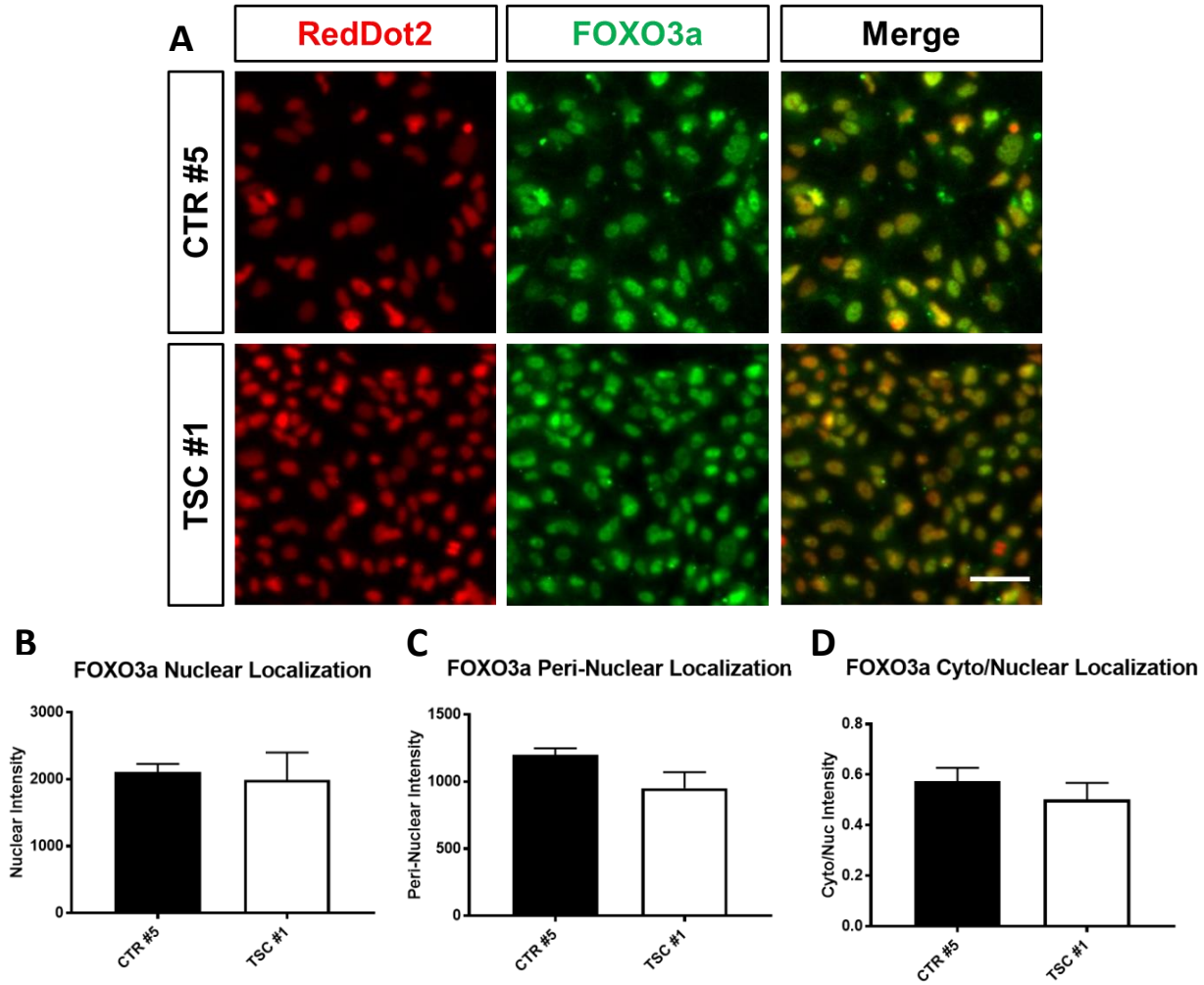

Figure 17. (A) Representative confocal immunofluorescence images of FOXO3a expression in DIV2 NPC cultures from one TSC patient and sibling control pair (CTR #5 and TSC #1). Cells are counterstained with RedDot2 nuclear stain (B-D) Automated high content analysis of FOXO3a staining intensity showed no significant effect of *TSC2* genotype on FOXO3a localization in either the nucleus or a 5µm peri-nuclear collar region immediately surrounding the nucleus. The proportion of FOXO3a staining detected in the peri-nuclear region relative to nuclear staining was likewise not significantly affected. n = 3 independent cultures. Significance determined via unpaired non-parametric *t*-test. Data are plotted as mean values ± SEM. Scale bar = 50µm.

factor 1-alpha (HIF1A), while Akt activity is known to impact the FOXO family of transcription factors as well as the cAMP response element-binding protein (CREB) (Finkbeiner, 2000; Laplante and Sabatini, 2013; Webb and Brunet, 2014). Given this wide range of interaction with various transcription factor pathways we next sought to determine whether TSC2 haploinsufficiency altered patterns of gene expression in *TSC2* heterozygous NPCs. Here we chose to perform high-throughput whole transcriptome sequencing, or RNA-Seq to obtain a snapshot of the transcriptome of subject NPCs. We performed RNA-Seq analysis of two independent NPC lines derived from one patient (TSC #1) and sibling control (CTR #5) and identified 513 transcripts as differentially expressed between genotypes (Figure 18A). Gene ontology (GO) analysis of transcripts that were depleted in TSC2 haploinsufficient NPCs enriched two biological processes relating to neuronal migration and development (Table 4, Figure 18B). These data suggest that TSC2 haploinsufficiency may be linked to effects on certain processes underlying neuronal differentiation and cortical development. RNA-Seq reads aligning with the *TSC2* gene also exhibited evidence of allelic imbalance, since a synonymous SNP (rs34012042) in TSC #1 was heterozygous but unequal (28% C, 72% T). This supports the prediction that the frameshifted mRNA may be destabilized.

Neuronal differentiation of NPCs derived from TSC and control subjects

While progenitors derived from iPSCs express stereotypical NPC markers, we also sought to assess their capability as neural progenitors to differentiate into neurons *in vitro*. Here we tested whether TSC patient- and unaffected control-derived NPC cultures were able to produce neurons using a neuronal differentiation medium containing specific growth factors to induce neuronal differentiation. Medium was changed from neural expansion media to a differentiative media

Up/ Down	Term	Count	%	p-value	Fold Enrich-ment	FDR	Genes
Down	GO:0001764 neuron migration	12	6.56	7.52E-09	11.42	1.20E-05	CDK5R1, FGF13, FYN, GPM6A, MDGA1, NAV1, NR2F2, NRCAM, SATB2, SOX1, SPOCK1, TUBB2B
Down	GO:0007399 nervous system development	14	7.65	6.05E-06	4.88	9.64E-03	ADGRV1, APBA1, APBA2, ARHGAP26, CHRDL1, DPYSL5, FGF13, GBX2, GPM6B, JAG1, PAX3, SPOCK1, ST8SIA2, ZIC5
Up	GO:0009952 anterior/posterior pattern specification	14	5.71	2.14E-11	13.80	3.53E-08	HOXB4, HOXB5, HOXB6, HOXB7, HOXB8, HOXB9, HOXC10, HOXC4, HOXC6, HOXC8, HOXC9, PBX1, RARG, TSHZ1
Up	GO:0007155 cell adhesion	22	8.98	3.82E-07	3.78	6.29E-04	BCAM, CASK, CD9, COL15A1, COL6A6, DSC3, DSG2, EDIL3, EGFL6, GPNMB, LAMA3, LRRN2, MFGE8, OLR1, PCDH10, POSTN, PTPRK, S1PR1, SIRPA, SPON1, VTN, WISP1
Up	GO:0030198 extracellular matrix organization	13	5.31	7.48E-06	5.23	1.23E-02	CDH1, COL8A2, CRISPLD2, DCN, EGFL6, FOXF1, HPSE2, KDR, LAMA3, LOXL1, NPNT, POSTN, VTN

Table 4. Gene ontology analysis in DAVID identified two major groups of neuronal development and neuronal migration genes that were stringently-enriched in the down-regulated transcripts (≥10 transcripts per term, ≤5% FDR). Terms enriched in the up-regulated transcripts were less focused, and included anterior/posterior patterning, cell adhesion, and extracellular matrix organization.

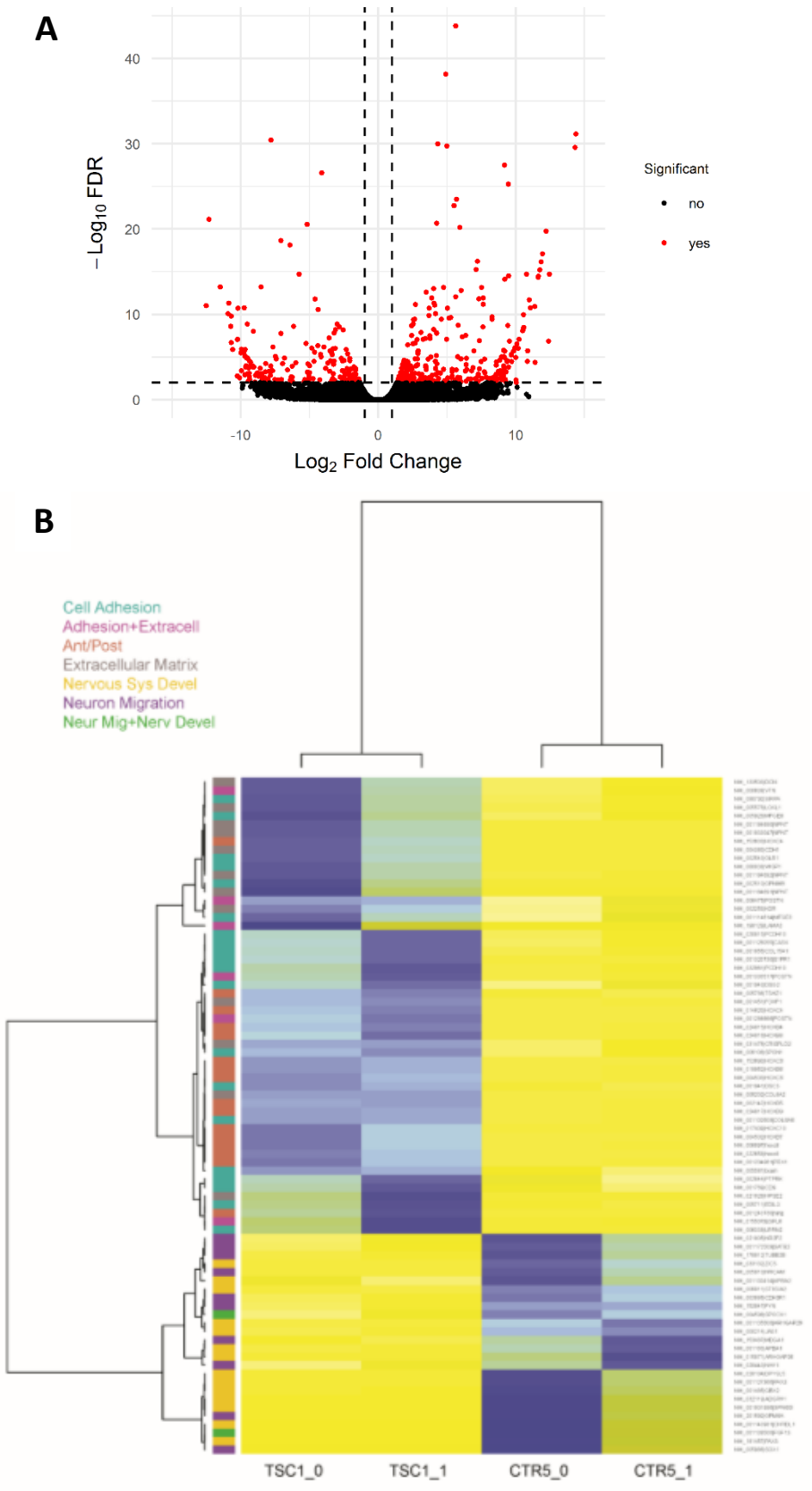
A
40
30
20
10
0
−Log10 FDR
-10
0
10
Log2 Fold Change
Significant
no
yes
B
Cell Adhesion
Adhesion+Extracell
Ant/Post
Extracellular Matrix
Nervous Sys Devel
Neuron Migration
Neur Mig+Nerv Devel
TSC1_0
TSC1_1
CTR5_0
CTR5_1

Figure 18. (A) A volcano plot shows the range of transcripts with significantly different transcripts highlighted in red. Of 38,027 transcripts detected, there were a total of 513 transcripts meeting the criteria for significance using this filter, with 208 that were reduced in TSC patient NPCs and 305 that were increased. (B) Differentially expressed transcripts enriched GO biological processes listed in Table S2. Genes included in the enriched GO terms are displayed in a heatmap. Heatmap colors indicate expression levels relative in each sample relative to overall mean expression, with blue indicating high expression and yellow indicating low expression. A sidebar (left) indicates membership for each transcript in one or more GO term (identified with colored labels).

containing BDNF and GDNF, and NPCs were moved to cell culture plates coated with poly-d-lysine and laminin to support neuronal growth. After two weeks in differentiation media all subject NPC cultures produced cells with stereotypical branched neuronal morphologies. Many of these cells expressed the neuronal markers βIII TUBULIN (TUJ1) and MAP2, which could be readily detected in cell bodies and branching processes (Figure 19A-B). We detected no significant differences in the proportion of MAP2 or βIII TUBULIN positive cells between matched sets of patient and control subjects, although interestingly the proportion of βIII TUBULIN positive post-mitotic neurons in cultures from one patient (TSC #1) appeared decreased compared to a sibling control (Figure 19C-D). However, this effect was not significant. We further detected no signs of enlarged soma size in TSC2 deficient neurons, showing that TSC2 haploinsufficiency is not sufficient to produce hypertrophy in neurons (Figure 19E).

Next, the molecular phenotype of *TSC2* heterozygous neurons was assayed via western blotting analysis of neuronal cultures from one patient and control pair (TSC #6, CTR #8) taken after two weeks of differentiation (Figure 20A). *TSC2* heterozygous neuronal cultures showed alterations in mTORC1 signaling like that observed in TSC2 haploinsufficient NPCs. Elevated levels of phospho-S6 persisted after two weeks of differentiation, while conversely levels of phospho-Akt Thr308 appeared to be only very minorly, and not significantly affected as neuronal differentiation progressed (Figure 20B-C). These data suggest that mTORC1 remains over-active in *TSC2* heterozygous cells through the process of neuronal differentiation, but that signaling feedback via IRS1 and PI3K/AKT becomes less pronounced as neural progenitor cells transition into post-mitotic neurons.

Neurons differentiated from one TSC patient and control pair also expressed the synaptic marker Synaptophysin after DIV28 which was observed to co-localize with dendrites and cell

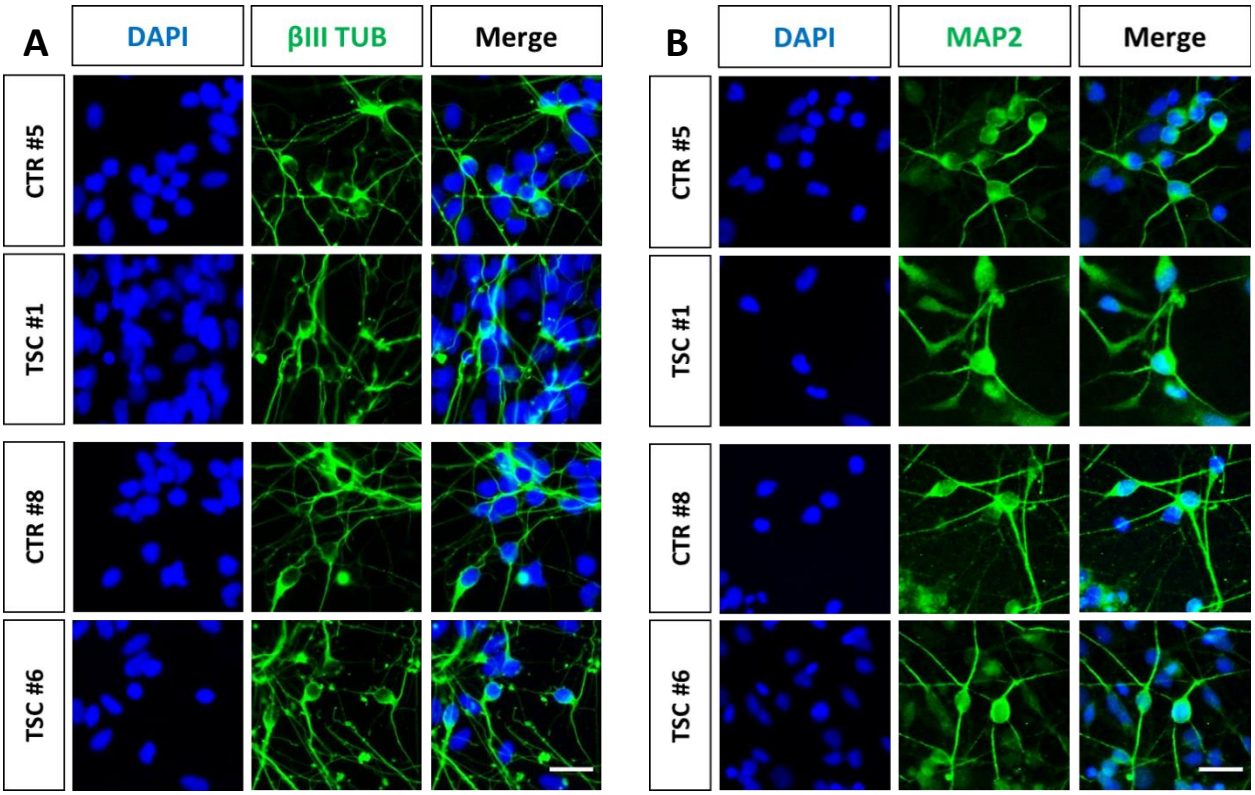
A
DAPI
βIII TUB
Merge
CTR #5
TSC #1
CTR #8
TSC #6
B
DAPI
MAP2
Merge
CTR #5
TSC #1
CTR #8
TSC #6

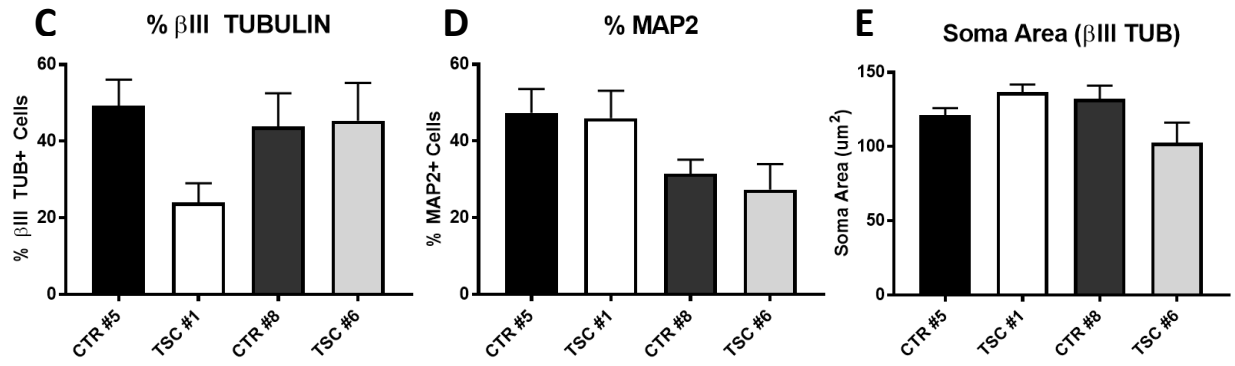
C
% βIII TUBULIN
% βIII TUB+ Cells
60
40
20
0
CTR #5
TSC #1
CTR #8
TSC #6
D
% MAP2
% MAP2+ Cells
60
40
20
0
CTR #5
TSC #1
CTR #8
TSC #6
E
Soma Area (βIII TUB)
Soma Area (um2)
150
100
50
0
CTR #5
TSC #1
CTR #8
TSC #6

Figure 19. (A-B) Representative immunofluorescence images of DIV14 neuronal cultures from all subjects show expression of the neuronal markers βIII TUBULIN and MAP2. Cells were counterstained with DAPI nuclear stain. (C-D) Quantification of the proportion of total cells expressing each neuronal marker showed no significant difference by *TSC2* genotype. (E) DIV14 TSC patient neurons also show no sign of hypertrophy as measured by βIII TUBULIN soma area. n = 3 independent differentiations from three independently generated NPC lines per subject. Significance was determined via unpaired non-parametric *t*-test. Data are plotted as mean values ± SEM. Scale bars = 25μm.

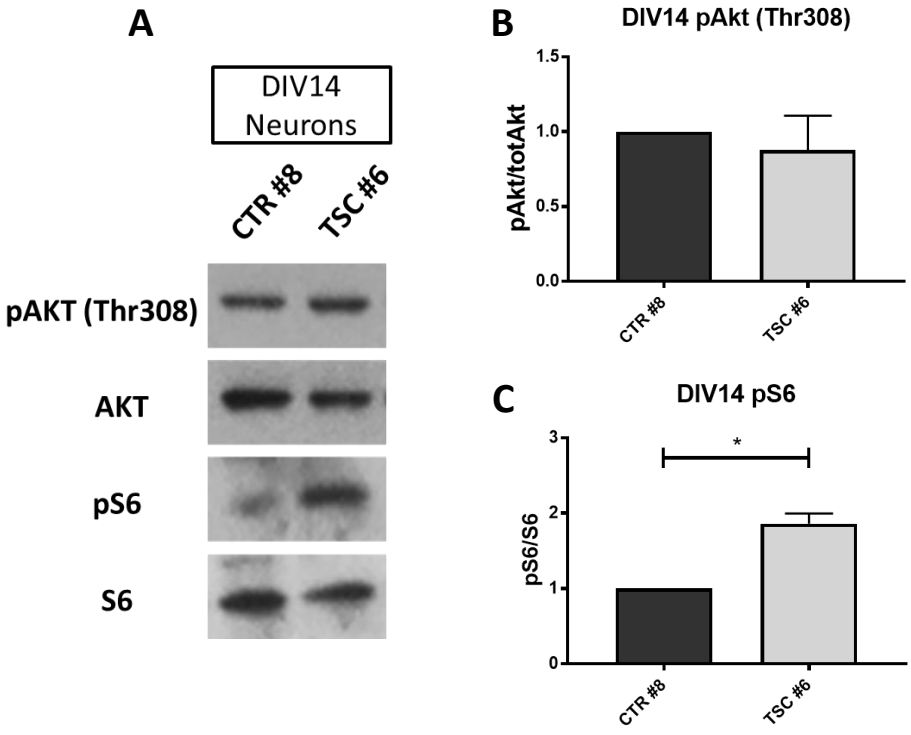

Figure 20. (A) Western blotting for phospho-AKT (Thr308) and phospho-S6 proteins in DIV14 neuronal cultures from one TSC patient and control pair (TSC #6 and CTR #8). (B-C) Western blot analysis shows relative levels of pospho-AKT (Thr308) are not significantly affected in TSC patient cells after 14 days of differentiation, but levels of phospho-S6 remain elevated (*$p<0.05$). Significance was determined via one sample *t*-test. $n = 3$ independent differentiations. Data are plotted as mean values ± SEM.

bodies as shown by immunostaining for the dendritic marker MAP2 (Figure 21). The observation of Synaptophysin puncta in these cultures strongly suggests that neurons generated from iPSC-derived NPCs are capable of forming synapses *in vitro*. Together these data further confirm the neural progenitor identity of our NPC lines by showing their capacity to generate neurons *in vitro* and demonstrates that iPSC-derived NPCs can provide a suitable platform for studying the effects of *TSC2* heterozygosity on processes related to neuronal differentiation and brain development.

TSC2 heterozygous NPCs exhibit abnormal neuronal differentiation

The appropriate schedule of neuronal differentiation is critical during the process of brain development, and aberrations in the temporal regulation of differentiation could have profound impacts on the developing brain. The previously identified molecular abnormalities in patient-derived NPCs next led us to determine whether these cells may be impaired in their ability to undergo neuronal differentiation. While we detected no significant changes using the post-mitotic neuronal markers βIII TUBULIN and MAP2 at two weeks, we then sought to track the process of differentiation in multiple control and TSC NPC lines from both subject sets over a time course of three weeks. Neuronal induction was achieved in the same manner by changing cell culture media from an NPC supporting neural expansion media to a differentiative media containing BDNF, GDNF and B-27 without vitamin A. To identify the cell bodies of differentiated neurons we immunostained differentiating cultures with antibodies against HuC/D, an RNA-binding protein that is specifically expressed in post-mitotic neurons. This antibody clearly detected neuronal nuclei and cell bodies, and co-labeled cells that expressed the classic neuronal marker MAP2 (Figure 22A). We then conducted high-content analysis of microscopy images and measured neuronal differentiation by calculating the overall percentage of HuC/D positive cells over the total

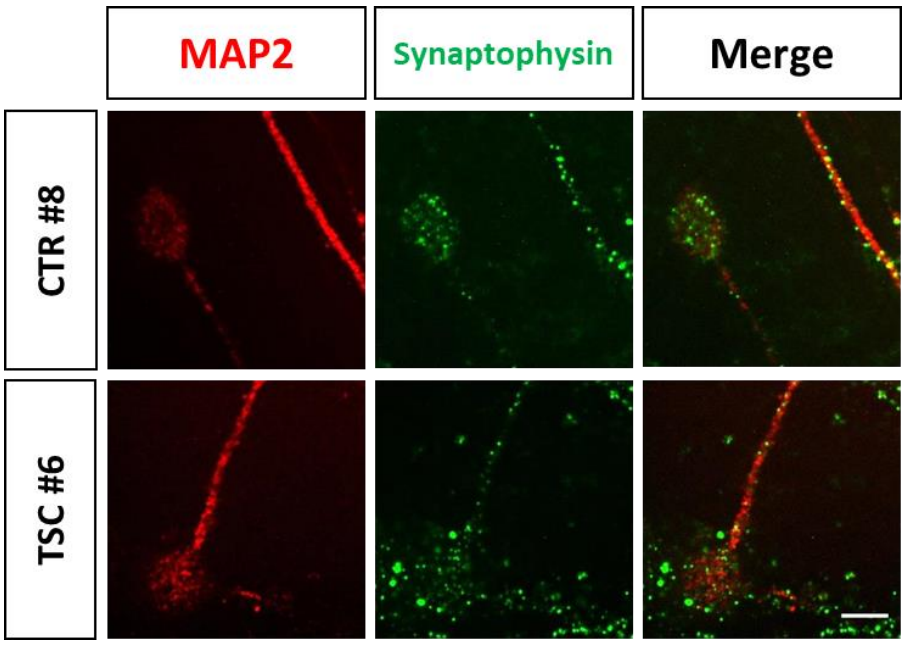

Figure 21. Representative confocal immunofluorescence images of MAP2 and the synaptic marker Synaptophysin taken of DIV28 neurons from one pair of TSC patient and control neuronal cultures. Neurons from both genotypes express the pre-synaptic marker Synaptophysin in puncta that colocalize with dendrites and neuronal cell bodies as labeled with MAP2, indicative of nascent synapses *in vitro*. Scale bar = 10µm.

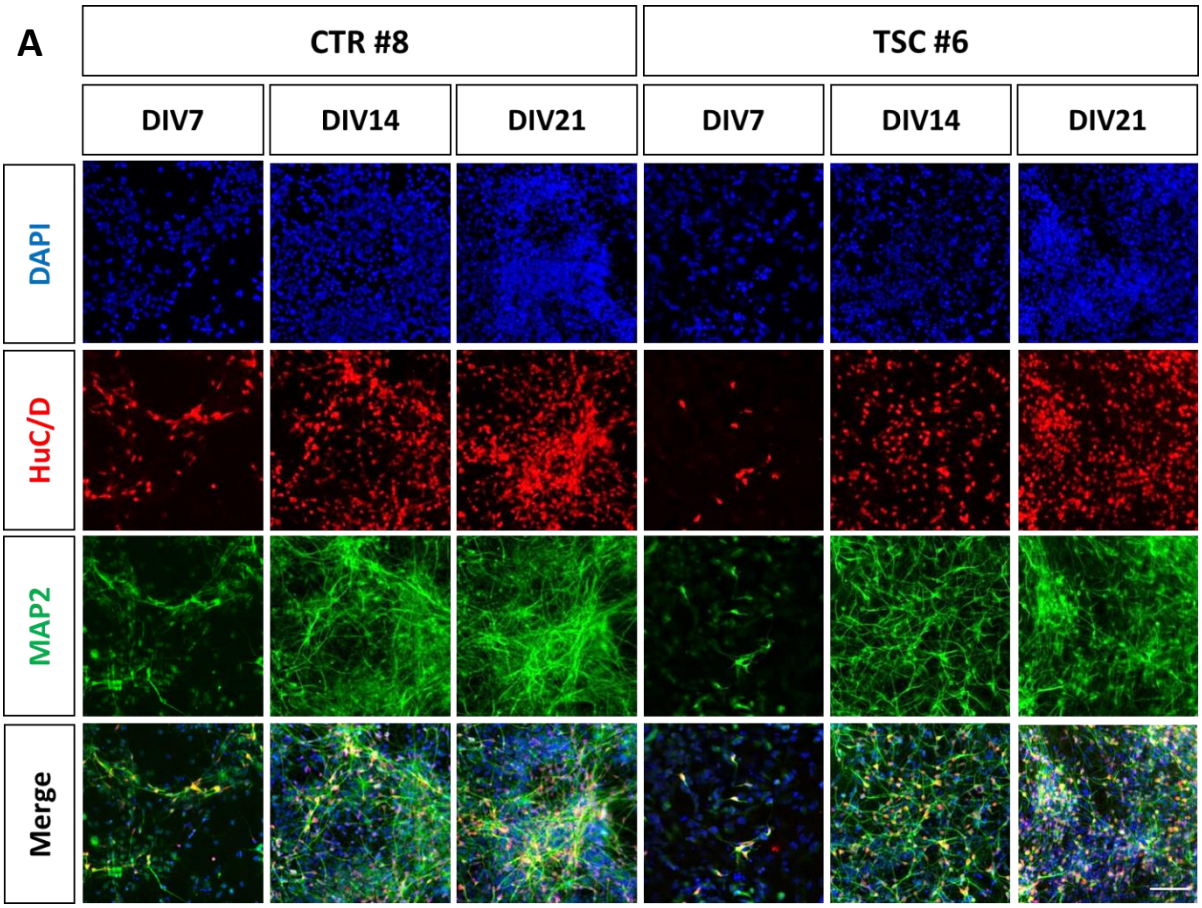
A
CTR #8
TSC #6
DIV7
DIV14
DIV21
DIV7
DIV14
DIV21
DAPI
HuC/D
MAP2
Merge

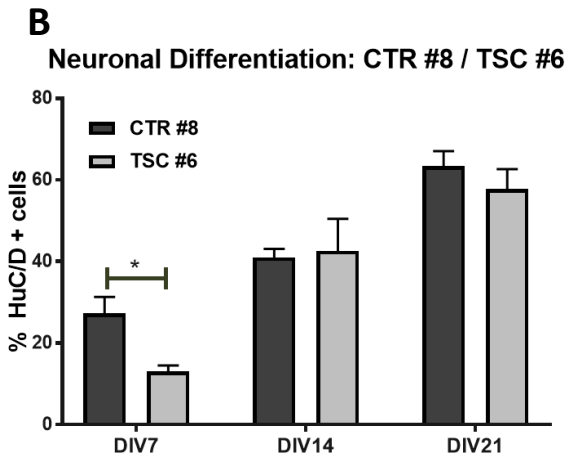
B
Neuronal Differentiation: CTR #8 / TSC #6
% HuC/D + cells
CTR #8
TSC #6
*
DIV7
DIV14
DIV21

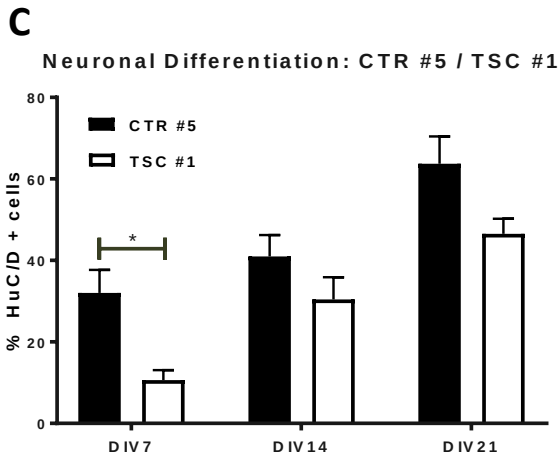
C
Neuronal Differentiation: CTR #5 / TSC #1
% HuC/D + cells
CTR #5
TSC #1
*
DIV7
DIV14
DIV21

Figure 22. (A) Representative confocal images of DIV7, 14, and 21 neuronal cultures generated from TSC patient and control NPC lines. An increasing proportion of cells express the neuron-specific markers HuC/D and MAP2 over the time course of differentiation. Nuclei are counterstained with DAPI. (B-C) Automated high content analysis of randomized image fields show a steadily increasing percentage of HuC/D+ cells during the time course of differentiation for TSC patient and control cultures in both subject sets. However, at DIV7 TSC patient cultures showed a significantly lower percentage of HuC/D+ cells than control in both subject sets (*$p<0.05$, $n = 4$ independent differentiations). The percentage of HuC/D+ neurons in TSC cultures was not significantly altered at DIV14 or DIV21 in either subject set ($n = 3$ independent differentiations). Significance at each time point was determined via multiple unpaired *t* tests corrected using the Holm-Sidak method where $\alpha = 0.05$. Data are plotted as mean values ± SEM. Scale bar = 100μm.

number of cells counterstained with a nuclear stain in both sets of patient and control cultures. Multiple randomized fields were captured for each time point of differentiation and the data obtained from multiple experiments using three independent NPC lines per subject were then pooled together. We found that the percentage of neurons increased through the course of differentiation in both patient and control cell lines from 7 to 21 days *in vitro* (DIV) (Figure 22B-C). However, the percentage of neurons was significantly reduced in both patient cultures compared to controls at DIV7. This effect was transient and was largely abolished by later time points in one patient (TSC #6), whereas in the other patient cultures (TSC #1) values appeared lower than control at DIV14 and DIV21, although this difference was not statistically significant at these later time points (Figure 22B-C). These data suggest that *TSC2* heterozygous mutations could cause a delay or disruption in the process of neuronal differentiation.

To further investigate this possibility, we performed Western blotting analysis of early neuronal marker protein expression in DIV7 neuronal cultures. Total levels of the proteins Doublecortin (DCX) and βIII TUBULIN (TUJ1) were significantly reduced in both patient cultures compared to controls after seven days of differentiation (Figure 23A-C). These findings confirmed that patient cultures likely contained fewer post-mitotic, differentiated neurons at a relatively early time point in the process of neuronal differentiation. Moreover, these data support our earlier RNA-Seq findings which indicated that groups of gene transcripts related to neuronal differentiation and maturation were affected in *TSC2* heterozygous neural progenitors.

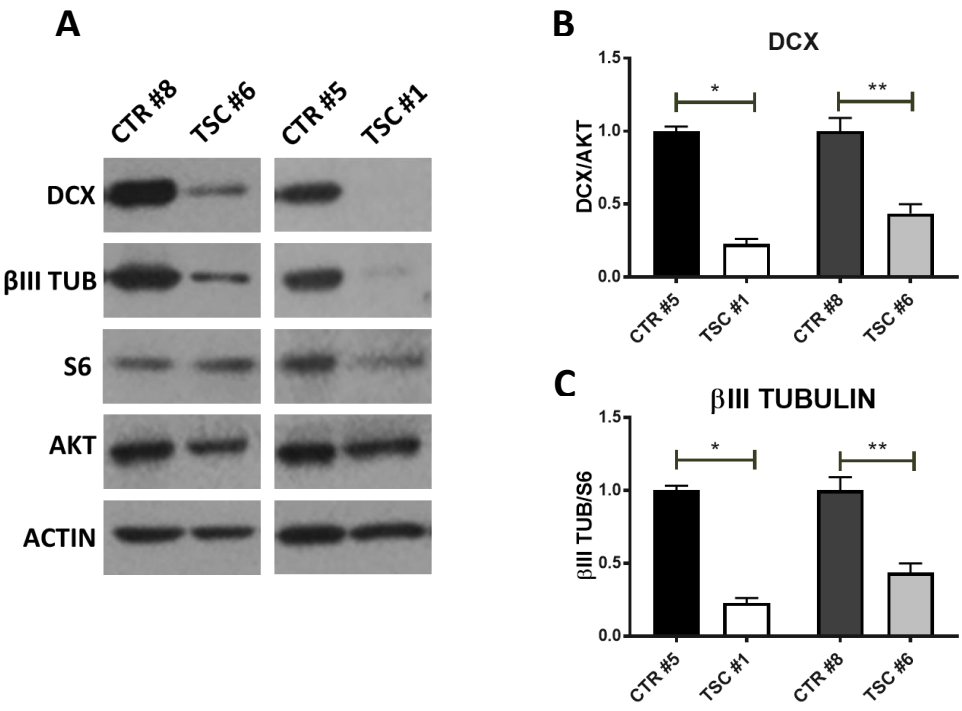

Figure 23. (A) Western blotting of DIV7 differentiating neuronal cultures show reduced levels of early neuronal markers DCX and βIII-TUBULIN in TSC patient samples from both subject sets. (B-C) Quantification of Western blot data normalized to internal controls. The decrease in DCX and βIII-TUB levels were significant in both patient groups compared to controls (*$p<0.05$, **$p<0.01$, $n = 5$ independent differentiations for CTR #8 and TSC #6, $n = 4$ for CTR #5 and TSC #1). Significance was determined via unpaired nonparametric *t* tests (Mann-Whitney). Data are plotted as mean values ± SEM.

NPC-derived neuronal cultures are heterogeneous and express inhibitory markers

During the process of cortical development most newly generated excitatory neurons are produced in the walls lining the ventricular system of the embryonic brain. These newly generated neurons migrate radially towards the apical surface of the developing brain to form the cortical plate. As subsequent waves of migrating neurons arrive at the apical surface of the developing brain they bypass neurons which migrated earlier, giving rise to the cortex's characteristic layered architecture through inside-out process. Most interneurons, however are produced from progenitor cells in the lateral, medial and caudal ganglionic eminences (LGE, MGE and CGE, respectively) and migrate tangentially into the cerebral cortex (Kriegstein and Noctor, 2004). Given the differences in origination of excitatory and inhibitory neuronal subtypes we next sought to characterize the make-up of neuronal cultures generated from iPSC-derived NPCs *in vitro* in order to determine if these neural progenitor cultures produced primarily excitatory or inhibitory neurons. After two weeks of neuronal induction cultures were fixed and stained for the inhibitory neuronal marker glutamate decarboxylase isoform 67 (GAD67) and the pan-neuronal dendritic marker MAP2. Cultures of both *TSC2* genotypes produced heterogenous populations of neurons, with approximately 25-35% of MAP2 positive post-mitotic neurons co-staining for the inhibitory neuronal marker GAD67 (Figure 24A-B). We observed a mild ~25% reduction in the total fraction of GAD67 positive inhibitory neurons in *TSC2* heterozygous cultures, although this difference was not significant (Figure 24B). Moreover, these data show that protocols for generating specific neuronal sub-types *in vitro* may be required to better elucidate the effects of TSC2 haploinsufficiency on specific populations of neurons.

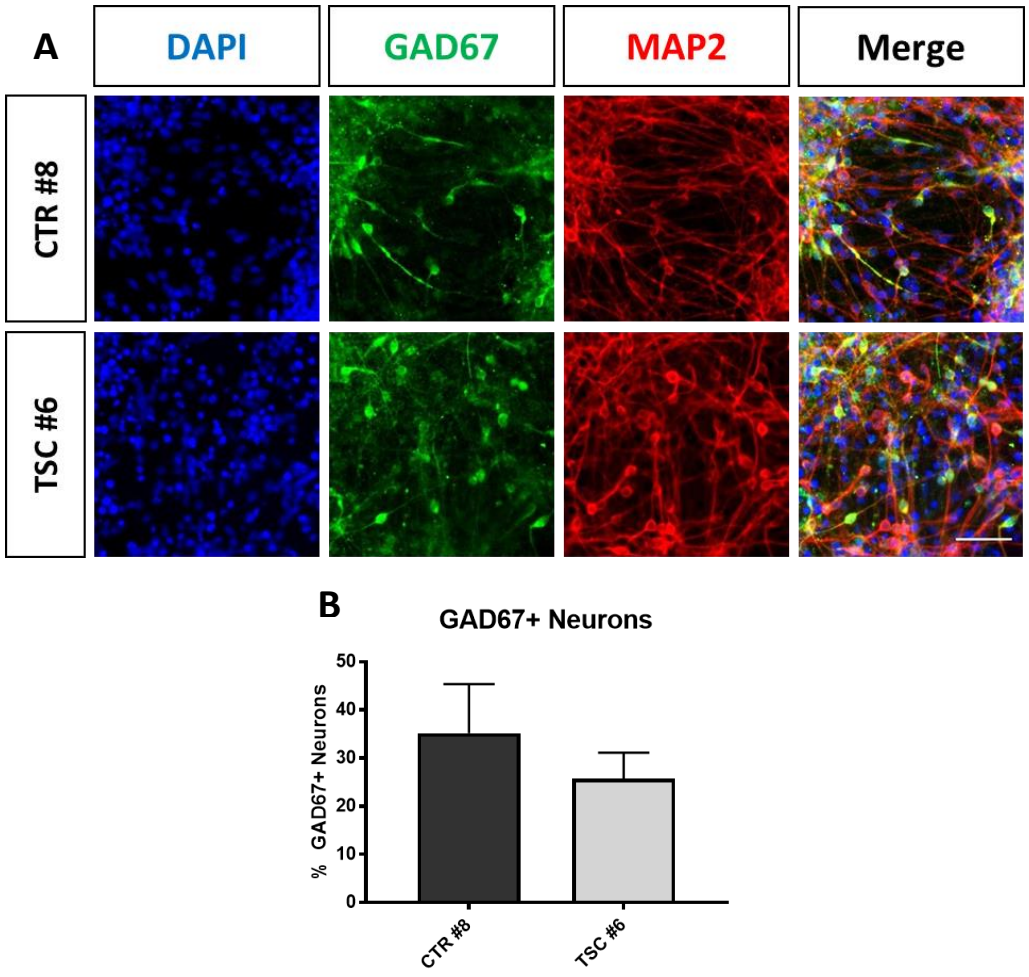

Figure 24. (A) Representative immunofluorescence images of DIV14 neuronal cultures from one TSC patient and control set (TSC #6 and CTR #8) stained for the inhibitory neuronal marker GAD67 and pan-neuronal marker MAP2. Cells are counterstained with DAPI nuclear stain. (B) Image quantification of GAD67+ neurons as a proportion of total MAP2+ neurons. Approximately 25-35% of neurons in cultures of both genotypes were GAD67+. A decrease in TSC patient GAD67+ inhibitory neurons was not significant ($p = 0.19$, $n = 5$ independent differentiations). Data are plotted as mean values ± SEM. Scale bar = 50µm.

AKT inhibition mimics the differentiation delay of TSC patient NPCs

In order to identify signaling alterations which may underlie the delayed neuronal differentiation phenotype observed in *TSC2* heterozygous cells we utilized a pharmacological approach focusing on PI3K/AKT and mTORC1 signaling. First, we utilized the rapamycin-analog RAD001 to suppress mTORC1 activity. NPC lines from one individual with TSC and significantly elevated mTORC1 activity (TSC #6) and control (CTR #8) were treated with 5μM RAD001 or DMSO vehicle control for 48 hours. Consistent with previous Western blot experiments we found that DMSO vehicle-treated NPC cultures derived from the *TSC2* deficient individual expressed significantly higher levels of phosphorylated S6 and reduced levels of phosphorylated AKT Thr308 compared to DMSO-treated control cells. RAD001 treatment successfully abolished elevated phosphorylated S6 levels in patient cultures, and reduced levels of phosphorylated S6 protein in control cells but did not significantly affect phospho-AKT levels in either subject group (Figure 25A-C). Next, we used the AKT inhibitor MK2206 and the PI3K inhibitor LY294002 to reduce AKT activity in control progenitor cells from both unaffected subjects. NPCs from control lines were treated for 24 hours with 1μM MK2206, 10μM LY294002 or DMSO vehicle control. Western blot analysis revealed that both drugs significantly reduced levels of phospho-AKT Thr308 protein in both control subjects as compared to DMSO vehicle-treated samples and reduced levels of downstream phosphor-S6, as expected (Figure 25D-F).

To test the role of mTORC1 activity in neuronal differentiation we incubated patient and control NPCs with 5μM RAD001 or DMSO, whereas to probe AKT activity we incubated control cell lines with 1μM MK2206 or 10μM LY294002. NPCs were induced to differentiate into neurons in the continuous presence of these inhibitors. After seven days neuronal cultures were immunostained with antibodies against the post-mitotic neuronal marker HuC/D, and the extent of

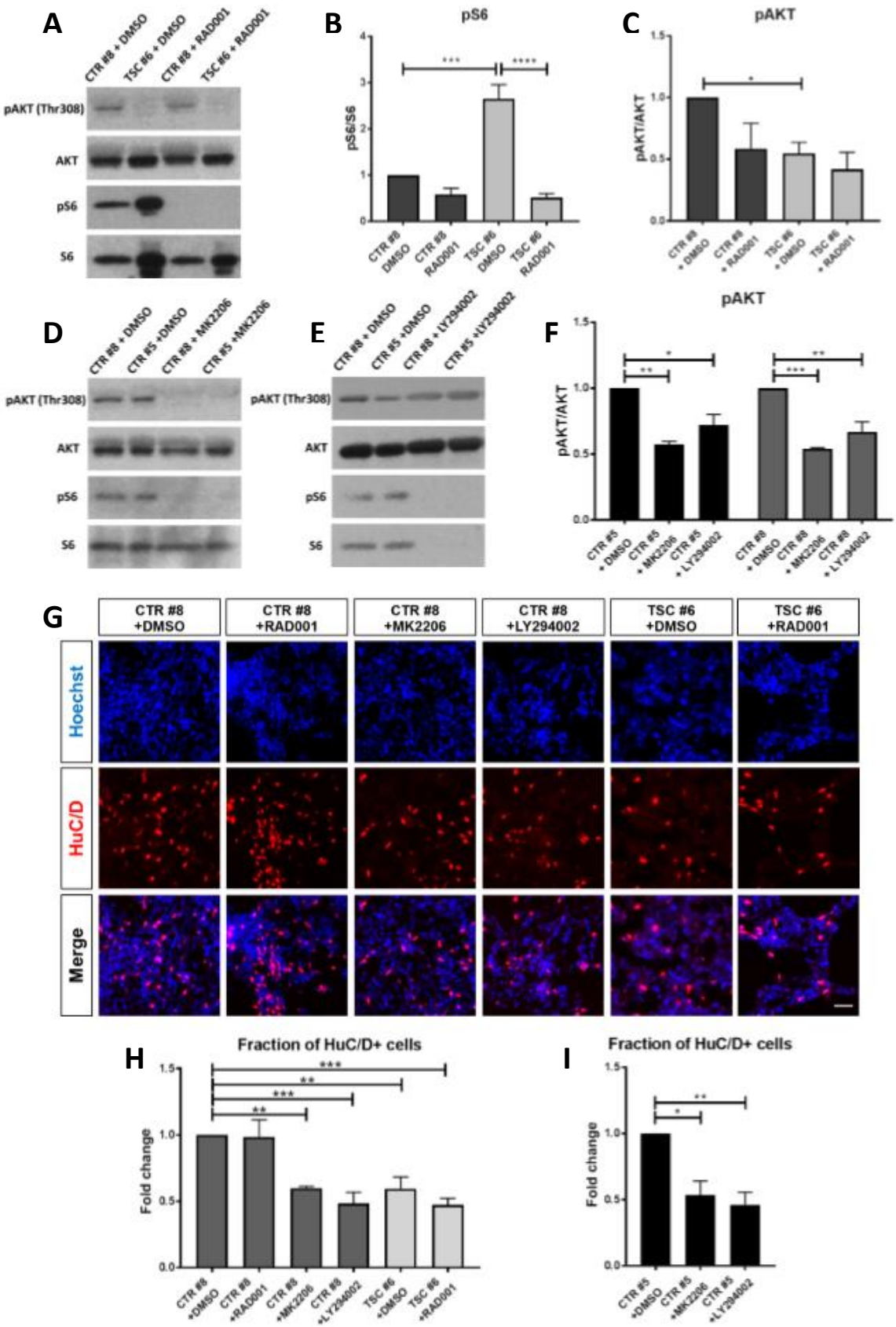
A
CTR #8 + DMSO
TSC #6 + DMSO
CTR #8 + RAD001
TSC #6 + RAD001
pAKT (Thr308)
AKT
pS6
S6
B
pS6
pS6/S6
CTR #8 DMSO
CTR #8 RAD001
TSC #6 DMSO
TSC #6 RAD001
C
pAKT
pAKT/AKT
D
CTR #8 + DMSO
CTR #5 +DMSO
CTR #8 + MK2206
CTR #5 +MK2206
E
CTR #8 + DMSO
CTR #5 +DMSO
CTR #8 + LY294002
CTR #5 +LY294002
F
pAKT
pAKT/AKT
G
CTR #8 +DMSO
CTR #8 +RAD001
CTR #8 +MK2206
CTR #8 +LY294002
TSC #6 +DMSO
TSC #6 +RAD001
Hoechst
HuC/D
Merge
H
Fraction of HuC/D+ cells
Fold change
I
Fraction of HuC/D+ cells
Fold change

Figure 25. (A) Western blot analysis of phospho-AKT (Thr308) and phospho-S6 in control and TSC NPCs treated with 5 µM RAD001 or 0.1% DMSO for 48 hours. (B-C) Quantification of Western blot data for the RAD001 treatment. Significantly increased phospho-S6 levels in TSC +DMSO compared to CTR +DMSO samples were suppressed by RAD001 treatment, whereas significantly lower levels of phospho-AKT were unaffected (*$p<0.05$, ***$p<0.001$, ****$p<0.0001$, n = 6 DMSO-treated independent cultures, n = 3 RAD001-treated cultures). Significance was determined via one-way ANOVA with Tukey's post-hoc analysis. (D) Western blot analysis of phospho-AKT (Thr308) and phospho-S6 in control NPCs treated with 1 µM MK2206, 10 µM LY294002 or 0.1% DMSO for 24 hours. (E) Quantification of Western blot data for MK2206 and LY294002 treatment. Both subject groups show significantly attenuated phospho-AKT levels in MK2206-treated as well as LY294002-treated cultures compared to DMSO controls (*$p<0.05$, **$p<0.01$, ***$p<0.001$, n = 3 independent cultures per subject). Significance was determined via one-way ANOVA with Dunnett's multiple comparisons tests. (F) Representative confocal images of DIV7 neuronal cultures from one TSC patient and control pair (CTR #8 and TSC #6) treated with 0.1% DMSO, 5 µM RAD001, 1 µM MK2206 or 10 µM LY294002. Cultures were immunostained for the pan-neuronal marker HuC/D and counterstained with Hoechst nuclear stain. (G-H) Automated high content analysis of treated culture images. The fraction of HuC/D+ cells was significantly reduced in TSC+DMSO compared to CTR+DMSO cultures, however treatment with RAD001 did not rescue the defect. The fraction of HuC/D+ cells was similarly reduced in CTR+MK2206 and CTR+LY294002 cultures but was not altered in CTR+RAD001 cultures ($p<0.05$**$p<0.01$, ***$p<0.001$,). n = 6 independent differentiations (CTR #8 and TSC #6 +DMSO, n = 4 (CTR #8 and TSC #6 +RAD001), n = 3 (CTR #8 and CTR#5 +MK2206 and +LY294002). The fraction of HuC/D+ cells was normalized to the internal control

in each set (CTR +DMSO) and expressed as fold change. Significance was determined via one-way ANOVA with Dunnett's multiple comparisons test, comparing the mean of each column to each control CTR +DMSO. Data are plotted as mean values ± SEM. Scale bar = 50μm.

neuronal differentiation was determined in each subject group by measuring the fraction of HuC/D positive cells in a large sample set via high content analysis of microscopy images. The data obtained from four independent experiments confirmed that DMSO-treated TSC cultures produce significantly fewer neurons than DMSO-treated controls at DIV7 of differentiation as previously noted for untreated cultures. However, treatment with the Rapamycin analog RAD001 failed to correct the neuronal differentiation defect observed in patient cells and did not alter the differentiation of control cells despite its effectiveness in suppressing mTORC1 activity (Figure 25G-H). However, both MK2206 and LY294002 treatments significantly reduced the fraction of HuC/D positive cells at DIV7 of differentiation in control cultures derived from both unaffected individuals, mimicking the phenotype of *TSC2* haploinsufficient cell lines (Figure 25G-I). Together, these data suggest that PI3K/AKT signaling deficits in *TSC2* heterozygous neural progenitors, rather than mTORC1 hyperactivity directly, may underlie changes in the process of neural differentiation. Somewhat surprisingly, we had previously observed only mild attenuation of AKT signaling in two-week-old differentiating neuronal cultures. However, this discrepancy may result from dynamic changes to AKT activity over the course of differentiation in *TSC2* heterozygous cultures which we were unable to detect after fourteen days of differentiation. It may also be possible that AKT signaling defects were ameliorated through the process of neuronal differentiation in *TSC2* heterozygous culture, and that this restoration correlates to the transient nature of differentiative defects in heterozygous cells. Moreover, deficits in PI3K/AKT signaling in NPCs might impair neural progenitor cultures from the outset of differentiation, impairing the onset of neurogenesis and which the later restoration of AKT signaling would be unable to restore.

To further investigate the role of PI3K/AKT signaling in neuronal differentiation and its possible effects in restoring differentiation defects observed in TSC2 heterozygous cells we next

attempted to use the small molecule AKT activator SC79 to restore phospho-AKT levels in TSC patient cells. Treatment with 5ug/mL SC79 for 48 hours restored levels of phospho-AKT Thr308 protein and in fact increased these levels above those measured in a matched control line treated with a DMSO vehicle. Additionally, SC79 treatment increased phospho-AKT levels in genotypically normal control lines (Figure 26A-C). However, increasing levels of phospho-AKT had no effect on neuronal differentiation as observed between SC79 and DMSO-vehicle treated control lines (Figure 26D-E), suggesting that increasing AKT activity does not have an inductive effect on neuronal differentiation. Moreover, patient lines treated with SC79 continued to display reduced tendencies to differentiate, with only mild improvements compared to DMSO treated lines (Figure 26D-E). These findings indicate that enhanced PI3K/AKT signaling is in and of itself not sufficient to increase neuronal differentiation. While deficiencies in AKT signaling may negatively impact the generation of new neurons, the over-activation of this pathway had no effect on neurogenesis. This suggests that AKT may play a permissive, but not inductive role during differentiation. Indeed, tight regulation of PI3K/AKT signaling is likely necessary to ensure neuronal formation proceeds normally where either under or over-active AKT may be detrimental during the process of neuronal differentiation.

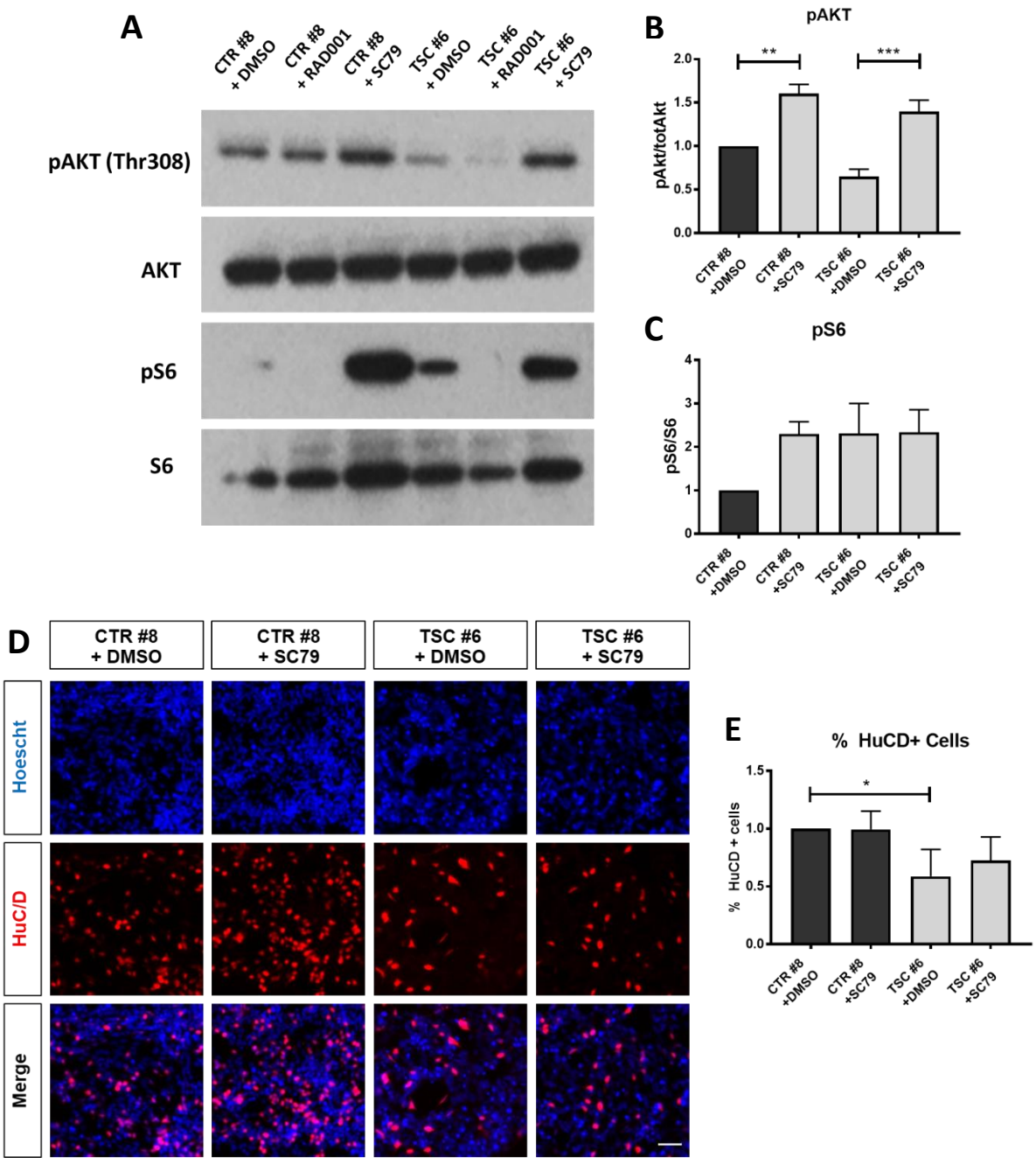
A
CTR #8 + DMSO
CTR #8 + RAD001
CTR #8 + SC79
TSC #6 + DMSO
TSC #6 + RAD001
TSC #6 + SC79
pAKT (Thr308)
AKT
pS6
S6
B
pAKT
pAkt/totAkt
**
***
CTR #8 +DMSO
CTR #8 +SC79
TSC #6 +DMSO
TSC #6 +SC79
C
pS6
pS6/S6
D
CTR #8 + DMSO
CTR #8 + SC79
TSC #6 + DMSO
TSC #6 + SC79
Hoescht
HuC/D
Merge
E
% HuCD+ Cells
% HuCD + cells
*

Figure 26. (A) Western blotting analysis of phospho-AKT (Thr308) and phospho-S6 in 0.1% DMSO and 5µg/mL SC79 48hr treated control and TSC patient samples from one subject pair (CTR #8 and TSC #6). (B-C) Western blot quantification shows SC79 effectively increases phospho-AKT levels in control and TSC patient NPCs compared to DMSO treatment (**$p<0.01$, ***$p<0.001$, $n = 4$ independent cultures). Significance was determined via one-way ANOVA with Tukey's post-hoc analysis. (D) Representative confocal images of TSC patient and control DIV7 neuronal cultures treated with 0.1% DMSO or 5µg/mL SC79. Cultures were stained for the post-mitotic neuronal marker HuC/D and counterstained with Hoechst nuclear stain (E) Automated high-content analysis of confocal images shows a decrease in the proportion of HuC/D+ neurons in DMSO treated TSC patient cultures is not rescued by SC79 treatment. SC79 had no effect on neuronal content in control cultures. $n = 4$ independent differentiations. Data are plotted as mean values ± SEM. Scale bar = 50µm.

Chapter 4: Discussion

In this study, we have successfully used a human iPSC model system to produce primitive, lineage restricted neural progenitors and neurons *in vitro* in order to examine the effects of *TSC2* haploinsufficiency on brain development, supporting the concept of using iPSC-based studies as a viable model for exploring human genetic and neurodevelopmental disease. These neural progenitor cells produced *in vitro* displayed general characteristics of those found *in vivo* including expression of NPC markers NESTIN, SOX2 and PAX6 as well as exhibiting the capacity to fully differentiate into post-mitotic neurons. Neurons produced from our NPC cultures exhibited stereotypical morphologies and expressed common neuronal markers such as βIII TUBULIN, MAP2 and HuC/D, and were observed to form primitive synaptic puncta after four weeks of differentiation, further confirming the neuronal identity of cells differentiated from reprogrammed iPSC cultures. These NPC cultures produced an heterogenous mix of neurons, with ~25% of observed neurons expressing the inhibitory marker GAD67. This suggests that our culture methods were not particularly specific and instead produced less guided differentiation outcomes.

Our findings using this cell culture system demonstrate that human heterozygous *TSC2* NPCs are abnormal despite lacking certain characteristics such as hypertrophy which are observed in LOH cells or lesion tissue. The most salient abnormality in TSC2 heterozygous neural progenitors appears to be their inability to promptly and efficiently differentiate into neurons in response to induction with appropriate growth factors. At the molecular level, this cellular phenotype likely results from the suppression of PI3K/AKT signaling activity, which in turn results from a negative feedback mechanism that is triggered by a modest upregulation of mTORC1 activity. Our data suggest that *TSC2* heterozygosity in neural progenitor cells may be sufficient to alter brain development and function in TSC patients. These findings may also explain why surgical excision

of TSC lesions does not restore cognitive and behavioral function. However, these findings do not dispute the notion that lesions are deleterious for brain activity. Furthermore, it is possible that microscopic lesions or undetected, dispersed homozygous null cells with impaired functionality may contribute to overall TSC symptomology as well (Marcotte et al., 2012; Sosunov et al., 2015).

The molecular signaling phenotype in *TSC2* haploinsufficient neural progenitors is consistent with defects previously reported in homozygous TSC models. *TSC2* heterozygous NPCs exhibited increased mTORC1 activation and decreased PI3K/AKT activation, similar to homozygous models. However, mTORC1 activation was modest as measured by relative levels of phospho-S6 compared to observations often reported in homozygous null *TSC1* or *TSC2* models, as expected for an intermediate haploinsufficient phenotype. Interestingly, while we did not observe any relative increase in phospho-4E-BP1 in *TSC2* heterozygous NPCs we did detect an increase in total 4E-BP1 protein in cell lines from one TSC patient (TSC #1). 4E-BP1 acts as an inhibitor of cap-dependent protein translation which is phosphorylated by mTORC1 to free the translation initiation factor eIF4E. Previous work has indicated that the ratio of total 4E-BP1 to eIF4E protein is an important factor in regulating protein translation, raising the possibility that alterations of 4E-BP1 expression may provide a compensatory mechanism in TSC2 haploinsufficient cells to regulate protein translation when mTORC1 is hyperactive (Alain et al., 2012). However, any potential relationship between 4E-BP1 expression, mTORC1 activity and TSC2 haploinsufficiency is unclear. Furthermore, since this effect was only observed in one individual with TSC it is not possible to definitively state whether it was attributable to the TSC genotype, or whether this may be a factor of individual variation in 4E-BP1/eIF4E signaling between patients. Indeed, given the variability observed within the TSC patient population as a whole, it would not

be surprising to find varying levels of affectedness when assaying the cellular phenotypes of patients with differing mutations and severity of TSC symptoms.

While mTORC1 activity in TSC2 heterozygous cells was less pronounced than in previously characterized LOH or null cells it did appear sufficient to elicit a classic negative feedback pathway leading to the reduction of IRS1 expression and the suppression of downstream PI3K and AKT signaling activity. This dysregulation of the PI3K/AKT/mTORC1 signaling axis was consistent and robust, but it was not accompanied by increased cell growth or proliferation, which typically correlate with high mTORC1 activity in *TSC1* or *TSC2* null cells. Surprisingly, we observed normal soma size in TSC patient neurons, and no significant effect on NPC proliferation in *TSC2* heterozygous NPC cultures. Phosphorylation of a marker downstream from AKT likewise showed only mild, and not significant alterations. This may be due to effects on PI3K/AKT signaling in TSC2 heterozygous cell lines persists near a functional threshold in NPCs where the remaining AKT activity preserves normal cellular function. Alterations in cellular phenotype might also result from the accumulated effect of multiple downstream pathways and would otherwise remain undetectable unless assaying a wide range of downstream factors which this study did not undertake. These cellular phenotypes contrast with previous reports that described increased proliferation in TSC patient-derived NPCs. One study reported not only increased cell count and BrdU incorporation in NPCs cultures, but also increased neuronal soma size in *TSC2* heterozygous cell lines (Li et al., 2017). These data were obtained comparing cells derived from only one TSC patient to cells obtained from unrelated unaffected controls. Another study also reported increased KI67 labeling in *TSC2* heterozygous cells. However, these neural progenitor cells were specifically differentiated into cerebellar progenitor sub-types (Sundberg et al., 2018). Reasons for such discrepancies are presently unclear, but they likely reflect technical differences in neuronal

progenitor cell type, specific induction protocols or time points of analysis. Consistent with this latest study (Sundberg et al., 2018), we did not detect a significant reduction of *TSC2* haploinsufficient NPC cell viability in our short-term culture system, although a modest increase in cell death was noted in both patient-derived cells. Increased cell death occurs in some models of TSC or mTOR pathway activation (Ozcan et al., 2008; Wu et al., 2009), and it was also observed in *TSC2* deficient reprogrammed human stem cells (Armstrong et al., 2017). Further studies are required to determine whether the long-term survival of patient NPCs or neurons is affected, possibly as a result of reduced AKT activity, which is well known to promote survival in many systems (Brunet et al., 1999; Manning and Toker, 2017; Pap and Cooper, 1998).

One of the primary findings of this study is that the progression of lineage restricted neural progenitors differentiating into neurons was perturbed in *TSC2* heterozygous cell lines. This finding was very similar in cell lines from both TSC patients and is consistent with previous research utilizing genome-edited human iPSC lines which showed transiently reduced propensity of heterozygous and homozygous null *TSC2* lines to undergo neuronal differentiation (Costa et al., 2016). Similar observations were also produced during studies using TSC2 knockdown techniques (Soucek et al., 1998). These data were supported by RNA-Seq analyses, which identified a set of gene transcripts that were depleted in TSC patient NPCs and associated with functional groupings consistent with diminished or delayed neuronal differentiation. Additionally, a non-significant trend towards reduced differentiation of inhibitory neurons was also observed in TSC2 haploinsufficient cultures, which might suggest this differentiation defect could affect specific sub populations of neurons. Interestingly, one recent study of cerebellar progenitors demonstrated a reduction in mature Purkinje cells generated from TSC patient cell lines, supporting this concept (Sundberg et al., 2018). We further showed that the differentiation delay of *TSC2* heterozygous

cells could be mimicked by reducing AKT activity in control cell lines, strongly implicating this kinase in the differentiation process. The disruption of neuronal differentiation could have far reaching effects on brain development, particularly the alteration of cortical development. The formation of cortical layers and functional circuitries depend on the appropriate spatial and temporal regulation of neural progenitor proliferation, migration and differentiation (Dehay and Kennedy, 2007; Kwan et al., 2012; Noctor et al., 2004). Subtle alterations to these processes could disrupt the organization and connectivity of neurons in the cortex or subcortical regions. Indeed, *TSC1* and *TSC2* deficiencies and increased mTOR activity can cause neuronal migration defects and cortical malformations in animal models (Carson et al., 2012; Hanai et al., 2017; Zhou et al., 2011). Abnormalities in neuronal morphology, branching and connection, as well as synaptic activity have also been observed in *TSC2* haploinsufficient human neurons (Costa et al., 2016; Li et al., 2017; Sundberg et al., 2018). Moreover, axonal projection, synaptic and behavioral abnormalities have been reported in heterozygous mouse models (Ehninger et al., 2008; Nie et al., 2010; Tavazoie et al., 2005). Together with the neurodevelopmental abnormality reported here, these defects could contribute to the profound neurological deficits observed in TSC, including cognitive and behavioral abnormalities.

Despite the detectable increase of mTORC1 activity in our patient-derived NPCs, and the many documented beneficial effects of rapamycin and rapamycin analogs on TSC mouse models or patients (Carson et al., 2012; Crowell et al., 2015a; Franz et al., 2006; Meikle et al., 2008; Zeng et al., 2008), we found that RAD001, a widely used rapamycin analog, while effectively suppressing mTORC1 activity in *TSC2* haploinsufficient neural progenitors did not rescue the observed neuronal differentiation defect. However, the inhibition of PI3K and its downstream target AKT in control lines mimicked the patient phenotype. These data suggest that AKT signaling may play

a more prominent role in TSC neuropathology than previously thought. Indeed, previous studies indicate that AKT activity is critical for progression of neuronal differentiation, including inhibitory neuronal differentiation (Lopez-Carballo et al., 2002; Oishi et al., 2009; Otaegi et al., 2006; Souza et al., 2011; Vojtek et al., 2003; Yuan et al., 2015; Zhang et al., 2017; Zhang et al., 2014). AKT appears to play a permissive role in cell fate determination, but this role may be highly context-dependent as AKT has also been shown to maintain pluripotency and proliferation (Fishwick et al., 2010; Watanabe et al., 2006). Likewise, our data showed that stimulating AKT granted no added inductive effect on neuronal differentiation. Instead, tight regulation of PI3K/AKT activity appears to be necessary to support neuronal differentiation. It is also worth noting that there are three different isoforms of the AKT protein, and the specific contribution of each to TSC pathology is undefined (Manning and Toker, 2017). Furthermore, levels of phospho-AKT were not significantly, but not significantly affected in later differentiating neuronal cultures, suggesting that AKT signaling in TSC2 haploinsufficient cells may be highly dynamic throughout the process of differentiation. This seems to correlate with our observation that differentiation defects seemed to affect primarily earlier time points and was likewise less pronounced later during differentiation. However, the exact relationship between AKT signaling and neuronal differentiation remains largely undefined and will require additional research to fully explain.

Upstream components of the AKT pathway which respond to growth stimuli have also been shown to be required for differentiation, and insulin signaling specifically appears to play a role in regulating neuronal differentiation (Brooker et al., 2000; Nieto-Estevez et al., 2016; Vicario-Abejon et al., 2003). Our observation that IRS1 is strongly downregulated in patient NPCs suggests that neurodevelopmental defects in TSC may also result from the suppression of key growth signaling factors such as insulin growth factor (IGF) or other IRS1-dependent stimuli. Together,

these data show that proper regulation of PI3K/AKT activity is necessary for neuronal differentiation and fate determination, and its downregulation may be a mechanism underlying neurodevelopmental abnormalities in TSC2 deficient cells. Moreover, the recognition that PI3K/AKT dysregulation may contribute to the overall TSC disease phenotype opens this feedback pathway up as a potential target of future therapeutics. Certain beneficial effects may be derived from treatments that take into account not just mTORC1 hyperactivity, but also the proper restoration of the full upstream component of PI3K/AKT/mTORC1 signaling. Previous work involving both human brain tissue and iPSC models derived from TSC patients has shown neuronal defects including functional defects in mature TSC neurons, and these defects were observed along with overactive mTORC1 which raises the possibility that upstream PI3K/AKT dysregulation of some kind may persist in mature neurons. Although pharmaceutical intervention may not be feasible at the appropriate embryonic time points needed to correct abnormal brain development in TSC, there remains the further possibility that other disease phenotypes mediated by IRS1/PI3K/AKT signaling may persist in more mature, adult cells, and addressing these upstream components of the TSC pathway might still be advantageous in some situations. It is interesting to note that we also detected a significant decrease of AKT phosphorylation in patient cells not only at the Thr308 (a PI3K/PDK-dependent site) phosphorylation site, but also at Ser473, a target of mTORC2, a different mTOR-containing kinase complex that could also play a role in neuronal differentiation. This finding suggests that mTORC2 activity may be downregulated in TSC NPCs as well, a possibility that was not addressed here but warrants further investigation.

One limitation of this study is that the data were obtained from only two sets of patient and control individuals; one set (CTR #5 and TSC #1) consists of a well-matched set of siblings of the same gender and similar age, whereas the other (CTR #8 and TSC #6) consists of two individuals

of similar age, but different gender and from different families. Also, no isogenic control lines were used to confirm the observed TSC2 haploinsufficient phenotypes. Despite these limitations, the fact that we observed similar cellular and molecular defects in cell lines derived from both patients suggest that the phenotypes are due to heterozygous *TSC2* mutations and not to genetic background or cell line variability. This does not rule out the possibility that these phenotypes could be isolated or restricted to a certain subset of other individuals with TSC. Further research is still needed to fully elucidate the consequences of *TSC2* heterozygosity, the role of PI3K/AKT signaling in brain development and neuronal differentiation, and the role of these kinases in the TSC pathophysiology of individuals throughout the spectrum of TSC.

Summary of Findings:

iPSCs from TSC patients carrying heterozygous mutations in *TSC2* and matched controls were capable of differentiation into lineage restricted neural progenitor cells and neurons.

TSC2 heterozygous NPCs exhibited levels of cellular proliferation and viability similar to controls, however TSC2 haploinsufficient NPCs were shown to have elevated mTORC1 activity as measured by levels of phospho-S6, and levels of phospho-AKT and total IRS1 were likewise reduced indicating the presence of feedback signaling resulting from over-active mTORC1.

Neurons produced from TSC2 heterozygous NPCs were not hypertrophic but did appear to have a reduced capacity to differentiate, although this defect appeared to be largely transient as differentiation progressed.

Treatment of TSC2 heterozygous NPCs with RAD001 did not restore early deficits in neuron generation, but treatment of control cell lines with AKT inhibitors phenocopied the TSC2 heterozygous differentiation phenotype, suggesting AKT plays a role in supporting the process of neuronal differentiation.

Future Directions:

Considering this study's limitations in characterizing only two TSC patients additional work could be undertaken to add more patients to characterize a broader spectrum of potential TSC cellular and molecular phenotypes. This may be especially useful to compare cellular and molecular phenotypes of different individual with TSC who present symptoms of varying intensity. The addition of more subjects could also occur in conjunction with the addition of isogenic mutant cell lines which could confirm the observed phenotypes produced from varying TSC-causing mutations. Isogenic mutant lines generated via gene-editing techniques such as zinc-finger nuclease arrays, TALEN or the CRISPR/Cas9 system for genome editing have been used to reproduce disease-causing mutations in a wide variety of genes and cell types including in neurons generated from iPSCs (Dow, 2015; Gaj et al., 2013; Heidenreich and Zhang, 2016; Zhang et al., 2018). Cell lines with edited mutant TSC2 have previously been reported on and have been shown to possess similar phenotypes to patient derived cell lines (Costa et al., 2016; Sundberg et al., 2018). For the purposes of our future studies it would be beneficial to both recapitulate TSC disease phenotypes in edited mutant cell lines, but also to rescue this phenotype by correcting the TSC-causing mutation. Genome edited corrections of TSC mutations achieved through the insertion of normal donor templates via homology directed repair (HDR) would both further confirm the disease etiology of *TSC2* mutations, but also provide a novel therapeutic approach for the treatment of TSC. While CRISPR/Cas9 editing of mammalian embryos to generate transgenic animals has been demonstrated it may also be possible to utilize gene editing systems for in vivo gene therapy in adults (Dai et al., 2016; Yin et al., 2016). However, these technologies are relatively new and will require further refinements and testing before widespread application in humans.

Our findings regarding the role of AKT in mediating differentiation suggest that this kinase provides a supporting effect during neurogenesis and proper regulation of its activity is required for differentiation to proceed normally. However, a more thorough investigation of AKT's role in this process is necessary. Specifically, it should be established how AKT supports neuronal differentiation either through regulating the expression of pro-neural genes or through supporting neuronal survival. It also must be explained why AKT inhibition appears to attenuate neuronal differentiation, but stimulation of AKT has no inductive effect, although this may be due to technical issues surrounding our SC79 treatments. More effective dosing taking into full account the potential for toxicity in neural progenitor cultures would be needed to optimize these experiments. Transcriptome analysis of gene expression during AKT stimulation and inhibition may provide useful data to help explain AKT's possible role in the regulation of pro-neural genes, including specific neuronal subtypes such as inhibitory neurons. Likewise, tracking cell death through differentiation under the same conditions of AKT activation would be useful to show what effect AKT's pro-survival role plays in supporting newly generated neurons. Additionally, more work should be conducted into the signaling abnormalities present in TSC2 heterozygous NPCs and their effects on other downstream pathways. In this study we explored only one candidate pathway in FOXO3a, however other downstream factors may also play a role in mediating TSC disease phenotype, and further molecular biological studies or transcriptome analysis will be needed to fully describe these potential downstream effects. These investigations should also consider possible novel compensatory mechanisms and feedback signaling besides the already highlighted S6K/IRS1 pathway. Evidence that total levels of 4E-BP1 are altered in at least some TSC patients raises the possibility that other such compensatory pathways may be active in cells with dysregulated mTORC1 signaling.

Continuing interest should also be paid to establishing additional details surrounding the characteristics of *TSC2* heterozygous neurons. This study only briefly characterized that TSC2 haploinsufficient neurons did not express hypertrophy, unlike their LOH counterparts. However, a more thorough characterization should be conducted to describe more detailed morphological and functional effects. Specifically, dendritic branching and length, axon and synapse formation should all be assayed to determine if TSC2 deficient neurons express an abnormal phenotype at this stage of development. Functional assays using electrophysiological techniques will be required to establish whether *TSC2* heterozygous neurons are electrically abnormal. Some evidence has already been published to this extent suggesting TSC2 haploinsufficent neurons display certain electrical abnormalities, however more detailed characterizations in patient derived cell lines are still needed. A complete study of the PI3K/AKT/mTORC1 pathway in neurons at a later stage of neuronal development should also be conducted to determine whether defects detected in NPCs persist into the mature neurons, and whether rescuing these molecular defects would have any beneficial effect on potentially abnormal *TSC2* heterozygous neuronal phenotypes. It may also be useful to utilize different differentiation protocols for the generation of specific neuronal sub types. Our data was generating using a protocol which generated neurons through a relatively loosely guided process of differentiation, resulting in the production of neurons of different sub types in a heterogenous culture. More guided protocols should be adapted to produce specific neuronal subtypes in order to study these cell types individually. Previous work showing defects in Purkinje cells raises the prospect that other neuronal subtypes might be differentially affected, and that *TSC2* heterozygosity may more acutely impact neurons of certain sub types over others (Sundberg et al., 2018).

Lastly, while this and other studies have focused on the phenotype of TSC2 heterozygous cells alone, it would also be useful to consider the effect of *TSC2* LOH cells on adjacent heterozygous neurons. White previous studies utilizing gene editing techniques have successfully produced neurons with a *TSC2* null genotype, the effect these abnormal cells might have on relatively less affected heterozygous cells has not been explored. It may be possible to co-culture heterozygous neurons along with LOH cells expressing a reporter such as GFP in order to differentiate them from surrounding haploinsufficient cells. Then a functional analysis could be undertaken to determine if these abnormal TSC2 null cells have any effect on the surrounding tissue. This could answer questions surrounding the effect of small microtubers and other sub-lesion abnormalities observed in some TSC brains. Indeed, some evidence exists to suggest that peri-tuber regions are electrophysiologically or otherwise abnormal (Boer et al., 2008b; Ruppe et al., 2014). Confirming these findings could aid in explaining the relationship between cortical tubers and other abnormal lesions in the TSC brain.

Bibliography

Alain, T., Morita, M., Fonseca, B.D., Yanagiya, A., Siddiqui, N., Bhat, M., Zammit, D., Marcus, V., Metrakos, P., Voyer, L.A., Gandin, V., Liu, Y., Topisirovic, I., Sonenberg, N., 2012. eIF4E/4E-BP ratio predicts the efficacy of mTOR targeted therapies. Cancer Res 72, 6468-6476.

Alfaiz, A.A., Micale, L., Mandriani, B., Augello, B., Pellico, M.T., Chrast, J., Xenarios, I., Zelante, L., Merla, G., Reymond, A., 2014. TBC1D7 mutations are associated with intellectual disability, macrocrania, patellar dislocation, and celiac disease. Hum Mutat 35, 447-451.

Arai, Y., Takashima, S., Becker, L.E., 2000. CD44 expression in tuberous sclerosis. Pathobiology 68, 87-92.

Armstrong, L.C., Westlake, G., Snow, J.P., Cawthon, B., Armour, E., Bowman, A.B., Ess, K.C., 2017. Heterozygous loss of TSC2 alters p53 signaling and human stem cell reprogramming. Hum Mol Genet 26, 4629-4641.

Astrinidis, A., Senapedis, W., Coleman, T.R., Henske, E.P., 2003. Cell cycle-regulated phosphorylation of hamartin, the product of the tuberous sclerosis complex 1 gene, by cyclin-dependent kinase 1/cyclin B. J Biol Chem 278, 51372-51379.

Au, K.S., Williams, A.T., Roach, E.S., Batchelor, L., Sparagana, S.P., Delgado, M.R., Wheless, J.W., Baumgartner, J.E., Roa, B.B., Wilson, C.M., Smith-Knuppel, T.K., Cheung, M.Y., Whittemore, V.H., King, T.M., Northrup, H., 2007. Genotype/phenotype correlation in 325 individuals referred for a diagnosis of tuberous sclerosis complex in the United States. Genet Med 9, 88-100.

Baybis, M., Yu, J., Lee, A., Golden, J.A., Weiner, H., McKhann, G., 2nd, Aronica, E., Crino, P.B., 2004. mTOR cascade activation distinguishes tubers from focal cortical dysplasia. Ann Neurol 56, 478-487.

Benvenuto, G., Li, S., Brown, S.J., Braverman, R., Vass, W.C., Cheadle, J.P., Halley, D.J., Sampson, J.R., Wienecke, R., DeClue, J.E., 2000. The tuberous sclerosis-1 (TSC1) gene product hamartin suppresses cell growth and augments the expression of the TSC2 product tuberin by inhibiting its ubiquitination. Oncogene 19, 6306-6316.

Boer, K., Jansen, F., Nellist, M., Redeker, S., van den Ouweland, A.M., Spliet, W.G., van Nieuwenhuizen, O., Troost, D., Crino, P.B., Aronica, E., 2008a. Inflammatory processes in cortical tubers and subependymal giant cell tumors of tuberous sclerosis complex. Epilepsy Res 78, 7-21.

Boer, K., Troost, D., Jansen, F., Nellist, M., van den Ouweland, A.M., Geurts, J.J., Spliet, W.G., Crino, P., Aronica, E., 2008b. Clinicopathological and immunohistochemical findings in an autopsy case of tuberous sclerosis complex. Neuropathology 28, 577-590.

Bourneville, D.-M., Brissaud, E., 1880. Sclerose tubereuse der circonvolutions cerebrales: idiotie et epilepsie hemiplegique. Archives de neurologie, Paris 1, 81-91.

Bray, N.L., Pimentel, H., Melsted, P., Pachter, L., 2016. Near-optimal probabilistic RNA-seq quantification. Nat Biotechnol 34, 525-527.

Brooker, G.J., Kalloniatis, M., Russo, V.C., Murphy, M., Werther, G.A., Bartlett, P.F., 2000. Endogenous IGF-1 regulates the neuronal differentiation of adult stem cells. J Neurosci Res 59, 332-341.

Brown, E.J., Albers, M.W., Shin, T.B., Ichikawa, K., Keith, C.T., Lane, W.S., Schreiber, S.L., 1994. A mammalian protein targeted by G1-arresting rapamycin-receptor complex. Nature 369, 756-758.

Brugarolas, J., Lei, K., Hurley, R.L., Manning, B.D., Reiling, J.H., Hafen, E., Witters, L.A., Ellisen, L.W., Kaelin, W.G., Jr., 2004. Regulation of mTOR function in response to hypoxia by REDD1 and the TSC1/TSC2 tumor suppressor complex. Genes Dev 18, 2893-2904.

Brunet, A., Bonni, A., Zigmond, M.J., Lin, M.Z., Juo, P., Hu, L.S., Anderson, M.J., Arden, K.C., Blenis, J., Greenberg, M.E., 1999. Akt promotes cell survival by phosphorylating and inhibiting a Forkhead transcription factor. Cell 96, 857-868.

Brunn, G.J., Williams, J., Sabers, C., Wiederrecht, G., Lawrence, J.C., Jr., Abraham, R.T., 1996. Direct inhibition of the signaling functions of the mammalian target of rapamycin by the phosphoinositide 3-kinase inhibitors, wortmannin and LY294002. EMBO J 15, 5256-5267.

Burgering, B.M., Coffer, P.J., 1995. Protein kinase B (c-Akt) in phosphatidylinositol-3-OH kinase signal transduction. Nature 376, 599-602.

Burnett, P.E., Barrow, R.K., Cohen, N.A., Snyder, S.H., Sabatini, D.M., 1998. RAFT1 phosphorylation of the translational regulators p70 S6 kinase and 4E-BP1. Proc Natl Acad Sci U S A 95, 1432-1437.

Caban, C., Khan, N., Hasbani, D.M., Crino, P.B., 2017. Genetics of tuberous sclerosis complex: implications for clinical practice. Appl Clin Genet 10, 1-8.

Cambiaghi, M., Cursi, M., Magri, L., Castoldi, V., Comi, G., Minicucci, F., Galli, R., Leocani, L., 2013. Behavioural and EEG effects of chronic rapamycin treatment in a mouse model of tuberous sclerosis complex. Neuropharmacology 67, 1-7.

Capo-Chichi, J.M., Tcherkezian, J., Hamdan, F.F., Decarie, J.C., Dobrzeniecka, S., Patry, L., Nadon, M.A., Mucha, B.E., Major, P., Shevell, M., Bencheikh, B.O., Joober, R., Samuels, M.E., Rouleau, G.A., Roux, P.P., Michaud, J.L., 2013. Disruption of TBC1D7, a subunit of the TSC1-TSC2 protein complex, in intellectual disability and megalencephaly. J Med Genet 50, 740-744.

Carson, R.P., Van Nielen, D.L., Winzenburger, P.A., Ess, K.C., 2012. Neuronal and glia abnormalities in Tsc1-deficient forebrain and partial rescue by rapamycin. Neurobiol Dis 45, 369-380.

Cass, H., Sekaran, D., Baird, G., 2006. Medical investigation of children with autistic spectrum disorders. Child Care Health Dev 32, 521-533.

Castro, A.F., Rebhun, J.F., Clark, G.J., Quilliam, L.A., 2003. Rheb binds tuberous sclerosis complex 2 (TSC2) and promotes S6 kinase activation in a rapamycin- and farnesylation-dependent manner. J Biol Chem 278, 32493-32496.

Chambers, S.M., Tchieu, J., Studer, L., 2013. Build-a-brain. Cell Stem Cell 13, 377-378.
Chan, J.A., Zhang, H., Roberts, P.S., Jozwiak, S., Wieslawa, G., Lewin-Kowalik, J., Kotulska, K., Kwiatkowski, D.J., 2004. Pathogenesis of tuberous sclerosis subependymal giant cell astrocytomas: biallelic inactivation of TSC1 or TSC2 leads to mTOR activation. J Neuropathol Exp Neurol 63, 1236-1242.

Cheadle, J.P., Reeve, M.P., Sampson, J.R., Kwiatkowski, D.J., 2000. Molecular genetic advances in tuberous sclerosis. Hum Genet 107, 97-114.

Chevere-Torres, I., Maki, J.M., Santini, E., Klann, E., 2012. Impaired social interactions and motor learning skills in tuberous sclerosis complex model mice expressing a dominant/negative form of tuberin. Neurobiol Dis 45, 156-164.

Chiu, M.I., Katz, H., Berlin, V., 1994. RAPT1, a mammalian homolog of yeast Tor, interacts with the FKBP12/rapamycin complex. Proc Natl Acad Sci U S A 91, 12574-12578.

Chu-Shore, C.J., Major, P., Camposano, S., Muzykewicz, D., Thiele, E.A., 2010. The natural history of epilepsy in tuberous sclerosis complex. Epilepsia 51, 1236-1241.

Chun, Y.S., Byun, K., Lee, B., 2011. Induced pluripotent stem cells and personalized medicine: current progress and future perspectives. Anat Cell Biol 44, 245-255.

Collier, S.J., 1989. Immunosuppressive drugs. Curr Opin Immunol 2, 854-858.

Costa, V., Aigner, S., Vukcevic, M., Sauter, E., Behr, K., Ebeling, M., Dunkley, T., Friedlein, A., Zoffmann, S., Meyer, C.A., Knoflach, F., Lugert, S., Patsch, C., Fjeldskaar, F., Chicha-Gaudimier, L., Kiialainen, A., Piraino, P., Bedoucha, M., Graf, M., Jessberger, S., Ghosh, A., Bischofberger, J., Jagasia, R., 2016. mTORC1 Inhibition Corrects Neurodevelopmental and Synaptic Alterations in a Human Stem Cell Model of Tuberous Sclerosis. Cell Rep 15, 86-95.

Crino, P.B., 2004. Molecular pathogenesis of tuber formation in tuberous sclerosis complex. J Child Neurol 19, 716-725.

Crino, P.B., 2011. mTOR: A pathogenic signaling pathway in developmental brain malformations. Trends Mol Med 17, 734-742.

Crino, P.B., 2013. Evolving neurobiology of tuberous sclerosis complex. Acta Neuropathol 125, 317-332.

Crino, P.B., Aronica, E., Baltuch, G., Nathanson, K.L., 2010a. Biallelic TSC gene inactivation in tuberous sclerosis complex. Neurology 74, 1716-1723.

Crino, P.B., Mehta, R., Winters, H.V., 2010b. Pathogenesis of TSC in the Brain. In: Kwiatkowski, D.J., Whittemore, V.H., Thiele, E.A. (Eds.), Tuberous Sclerosis Complex: Genes, Clinical Features and Therapeutics. Wiley-Blackwell, pp. 161-185.

Crino, P.B., Trojanowski, J.Q., Dichter, M.A., Eberwine, J., 1996. Embryonic neuronal markers in tuberous sclerosis: single-cell molecular pathology. Proc Natl Acad Sci U S A 93, 14152-14157.

Cross, D.A., Alessi, D.R., Cohen, P., Andjelkovich, M., Hemmings, B.A., 1995. Inhibition of glycogen synthase kinase-3 by insulin mediated by protein kinase B. Nature 378, 785-789.

Crowell, B., Lee, G.H., Nikolaeva, I., Dal Pozzo, V., D'Arcangelo, G., 2015a. Complex Neurological Phenotype in Mutant Mice Lacking Tsc2 in Excitatory Neurons of the Developing Forebrain. eNeuro 2.

Dai, W.J., Zhu, L.Y., Yan, Z.Y., Xu, Y., Wang, Q.L., Lu, X.J., 2016. CRISPR-Cas9 for in vivo Gene Therapy: Promise and Hurdles. Mol Ther Nucleic Acids 5, e349.

de Vries, P.J., Hunt, A., Bolton, P.F., 2007. The psychopathologies of children and adolescents with tuberous sclerosis complex (TSC): a postal survey of UK families. Eur Child Adolesc Psychiatry 16, 16-24.

de Vries, P.J., Prather, P.A., 2007. The tuberous sclerosis complex. N Engl J Med 356, 92; author reply 93-94.

de Vries, P.J., Whittemore, V.H., Leclezio, L., Byars, A.W., Dunn, D., Ess, K.C., Hook, D., King, B.H., Sahin, M., Jansen, A., 2015. Tuberous sclerosis associated neuropsychiatric disorders (TAND) and the TAND Checklist. Pediatr Neurol 52, 25-35.

Dehay, C., Kennedy, H., 2007. Cell-cycle control and cortical development. Nat Rev Neurosci 8, 438-450.

DeYoung, M.P., Horak, P., Sofer, A., Sgroi, D., Ellisen, L.W., 2008. Hypoxia regulates TSC1/2-mTOR signaling and tumor suppression through REDD1-mediated 14-3-3 shuttling. Genes Dev 22, 239-251.

Dibble, C.C., Elis, W., Menon, S., Qin, W., Klekota, J., Asara, J.M., Finan, P.M., Kwiatkowski, D.J., Murphy, L.O., Manning, B.D., 2012. TBC1D7 is a third subunit of the TSC1-TSC2 complex upstream of mTORC1. Mol Cell 47, 535-546.

DiMario, F.J., Jr., 2004. Brain abnormalities in tuberous sclerosis complex. J Child Neurol 19, 650-657.

Dimos, J.T., Rodolfa, K.T., Niakan, K.K., Weisenthal, L.M., Mitsumoto, H., Chung, W., Croft, G.F., Saphier, G., Leibel, R., Goland, R., Wichterle, H., Henderson, C.E., Eggan, K., 2008. Induced pluripotent stem cells generated from patients with ALS can be differentiated into motor neurons. Science 321, 1218-1221.

Dolmetsch, R., Geschwind, D.H., 2011. The human brain in a dish: the promise of iPSC-derived neurons. Cell 145, 831-834.

Dow, L.E., 2015. Modeling Disease In Vivo With CRISPR/Cas9. Trends Mol Med 21, 609-621.
Ehninger, D., Han, S., Shilyansky, C., Zhou, Y., Li, W., Kwiatkowski, D.J., Ramesh, V., Silva, A.J., 2008. Reversal of learning deficits in a Tsc2+/- mouse model of tuberous sclerosis. Nat Med 14, 843-848.

Eker, R., 1954. Familial renal adenomas in Wistar rats; a preliminary report. Acta Pathol Microbiol Scand 34, 554-562.

Erol, I., Savas, T., Sekerci, S., Yazici, N., Erbay, A., Demir, S., Saygi, S., Alkan, O., 2015. Tuberous sclerosis complex; single center experience. Turk Pediatri Ars 50, 51-60.

Espuny-Camacho, I., Michelsen, K.A., Gall, D., Linaro, D., Hasche, A., Bonnefont, J., Bali, C., Orduz, D., Bilheu, A., Herpoel, A., Lambert, N., Gaspard, N., Peron, S., Schiffmann, S.N., Giugliano, M., Gaillard, A., Vanderhaeghen, P., 2013. Pyramidal neurons derived from human pluripotent stem cells integrate efficiently into mouse brain circuits in vivo. Neuron 77, 440-456.

Ess, K.C., Kamp, C.A., Tu, B.P., Gutmann, D.H., 2005. Developmental origin of subependymal giant cell astrocytoma in tuberous sclerosis complex. Neurology 64, 1446-1449.

European Chromosome 16 Tuberous Sclerosis, C., 1993. Identification and characterization of the tuberous sclerosis gene on chromosome 16. Cell 75, 1305-1315.

Fatehullah, A., Tan, S.H., Barker, N., 2016. Organoids as an in vitro model of human development and disease. Nat Cell Biol 18, 246-254.

Feliciano, D.M., Su, T., Lopez, J., Platel, J.C., Bordey, A., 2011. Single-cell Tsc1 knockout during corticogenesis generates tuber-like lesions and reduces seizure threshold in mice. J Clin Invest 121, 1596-1607.

Finkbeiner, S., 2000. CREB couples neurotrophin signals to survival messages. Neuron 25, 11-14.

Fishwick, K.J., Li, R.A., Halley, P., Deng, P., Storey, K.G., 2010. Initiation of neuronal differentiation requires PI3-kinase/TOR signalling in the vertebrate neural tube. Dev Biol 338, 215-225.

Franke, T.F., Kaplan, D.R., Cantley, L.C., Toker, A., 1997. Direct regulation of the Akt proto-oncogene product by phosphatidylinositol-3,4-bisphosphate. Science 275, 665-668.

Franke, T.F., Yang, S.I., Chan, T.O., Datta, K., Kazlauskas, A., Morrison, D.K., Kaplan, D.R., Tsichlis, P.N., 1995. The protein kinase encoded by the Akt proto-oncogene is a target of the PDGF-activated phosphatidylinositol 3-kinase. Cell 81, 727-736.

Franz, D.N., Krueger, D.A., Balko, G., 2010. Subependymal Giant Cell Astrocytomas. In: Kwiatkowski, D.J., Whittemore, V.H., Thiele, E.A. (Eds.), Tuberous Sclerosis Complex: Genes, Clinical Features, and Therapeutics. Wiley-Blackwell, pp. 211-228.

Franz, D.N., Leonard, J., Tudor, C., Chuck, G., Care, M., Sethuraman, G., Dinopoulos, A., Thomas, G., Crone, K.R., 2006. Rapamycin causes regression of astrocytomas in tuberous sclerosis complex. Ann Neurol 59, 490-498.

Frech, M., Andjelkovic, M., Ingley, E., Reddy, K.K., Falck, J.R., Hemmings, B.A., 1997. High affinity binding of inositol phosphates and phosphoinositides to the pleckstrin homology domain of RAC/protein kinase B and their influence on kinase activity. J Biol Chem 272, 8474-8481.

Fryer, A.E., Chalmers, A., Connor, J.M., Fraser, I., Povey, S., Yates, A.D., Yates, J.R., Osborne, J.P., 1987. Evidence that the gene for tuberous sclerosis is on chromosome 9. Lancet 1, 659-661.

Gai, Z., Chu, W., Deng, W., Li, W., Li, H., He, A., Nellist, M., Wu, G., 2016. Structure of the TBC1D7-TSC1 complex reveals that TBC1D7 stabilizes dimerization of the TSC1 C-terminal coiled coil region. J Mol Cell Biol.

Gaj, T., Gersbach, C.A., Barbas, C.F., 3rd, 2013. ZFN, TALEN, and CRISPR/Cas-based methods for genome engineering. Trends Biotechnol 31, 397-405.

Gan, B., Sahin, E., Jiang, S., Sanchez-Aguilera, A., Scott, K.L., Chin, L., Williams, D.A., Kwiatkowski, D.J., DePinho, R.A., 2008. mTORC1-dependent and -independent regulation of stem cell renewal, differentiation, and mobilization. Proc Natl Acad Sci U S A 105, 19384-19389.

Gao, X., Pan, D., 2001. TSC1 and TSC2 tumor suppressors antagonize insulin signaling in cell growth. Genes Dev 15, 1383-1392.

Gao, X., Zhang, Y., Arrazola, P., Hino, O., Kobayashi, T., Yeung, R.S., Ru, B., Pan, D., 2002. Tsc tumour suppressor proteins antagonize amino-acid-TOR signalling. Nat Cell Biol 4, 699-704.

Garami, A., Zwartkruis, F.J., Nobukuni, T., Joaquin, M., Roccio, M., Stocker, H., Kozma, S.C., Hafen, E., Bos, J.L., Thomas, G., 2003. Insulin activation of Rheb, a mediator of mTOR/S6K/4E-BP signaling, is inhibited by TSC1 and 2. Mol Cell 11, 1457-1466.

Gentleman, R.C., Carey, V.J., Bates, D.M., Bolstad, B., Dettling, M., Dudoit, S., Ellis, B., Gautier, L., Ge, Y., Gentry, J., Hornik, K., Hothorn, T., Huber, W., Iacus, S., Irizarry, R., Leisch, F., Li, C., Maechler, M., Rossini, A.J., Sawitzki, G., Smith, C., Smyth, G., Tierney, L., Yang, J.Y., Zhang, J., 2004. Bioconductor: open software development for computational biology and bioinformatics. Genome Biol 5, R80.

Gillberg, I.C., Gillberg, C., Ahlsen, G., 1994. Autistic behaviour and attention deficits in tuberous sclerosis: a population-based study. Dev Med Child Neurol 36, 50-56.

Goh, S., Butler, W., Thiele, E.A., 2004. Subependymal giant cell tumors in tuberous sclerosis complex. Neurology 63, 1457-1461.

Goodman, M., Lamm, S.H., Engel, A., Shepherd, C.W., Houser, O.W., Gomez, M.R., 1997. Cortical tuber count: a biomarker indicating neurologic severity of tuberous sclerosis complex. J Child Neurol 12, 85-90.

Goorden, S.M., van Woerden, G.M., van der Weerd, L., Cheadle, J.P., Elgersma, Y., 2007. Cognitive deficits in Tsc1+/- mice in the absence of cerebral lesions and seizures. Ann Neurol 62, 648-655.

Goparaju, S.K., Kohda, K., Ibata, K., Soma, A., Nakatake, Y., Akiyama, T., Wakabayashi, S., Matsushita, M., Sakota, M., Kimura, H., Yuzaki, M., Ko, S.B., Ko, M.S., 2017. Rapid differentiation of human pluripotent stem cells into functional neurons by mRNAs encoding transcription factors. Sci Rep 7, 42367.

Goto, J., Talos, D.M., Klein, P., Qin, W., Chekaluk, Y.I., Anderl, S., Malinowska, I.A., Di Nardo, A., Bronson, R.T., Chan, J.A., Vinters, H.V., Kernie, S.G., Jensen, F.E., Sahin, M., Kwiatkowski, D.J., 2011. Regulable neural progenitor-specific Tsc1 loss yields giant cells with organellar dysfunction in a model of tuberous sclerosis complex. Proc Natl Acad Sci U S A 108, E1070-1079.

Goto, K., Imamura, K., Komatsu, K., Mitani, K., Aiba, K., Nakatsuji, N., Inoue, M., Kawata, A., Yamashita, H., Takahashi, R., Inoue, H., 2017. Simple Derivation of Spinal Motor Neurons from ESCs/iPSCs Using Sendai Virus Vectors. Mol Ther Methods Clin Dev 4, 115-125.

Grabole, N., Zhang, J.D., Aigner, S., Ruderisch, N., Costa, V., Weber, F.C., Theron, M., Berntenis, N., Spleiss, O., Ebeling, M., Yeo, G.W., Jagasia, R., Kiialainen, A., 2016. Genomic analysis of the molecular neuropathology of tuberous sclerosis using a human stem cell model. Genome Med 8, 94.

Grajkowska, W., Kotulska, K., Jurkiewicz, E., Matyja, E., 2010. Brain lesions in tuberous sclerosis complex. Review. Folia Neuropathol 48, 139-149.

Gunhanlar, N., Shpak, G., van der Kroeg, M., Gouty-Colomer, L.A., Munshi, S.T., Lendemeijer, B., Ghazvini, M., Dupont, C., Hoogendijk, W.J.G., Gribnau, J., de Vrij, F.M.S., Kushner, S.A., 2017. A simplified protocol for differentiation of electrophysiologically mature neuronal networks from human induced pluripotent stem cells. Mol Psychiatry.

Hanai, S., Sukigara, S., Dai, H., Owa, T., Horike, S.I., Otsuki, T., Saito, T., Nakagawa, E., Ikegaya, N., Kaido, T., Sato, N., Takahashi, A., Sugai, K., Saito, Y., Sasaki, M., Hoshino, M., Goto, Y.I., Koizumi, S., Itoh, M., 2017. Pathologic Active mTOR Mutation in Brain Malformation with Intractable Epilepsy Leads to Cell-Autonomous Migration Delay. Am J Pathol 187, 1177-1185.

Hara, K., Maruki, Y., Long, X., Yoshino, K., Oshiro, N., Hidayat, S., Tokunaga, C., Avruch, J., Yonezawa, K., 2002. Raptor, a binding partner of target of rapamycin (TOR), mediates TOR action. Cell 110, 177-189.

Harrington, L.S., Findlay, G.M., Gray, A., Tolkacheva, T., Wigfield, S., Rebholz, H., Barnett, J., Leslie, N.R., Cheng, S., Shepherd, P.R., Gout, I., Downes, C.P., Lamb, R.F., 2004. The TSC1-2 tumor suppressor controls insulin-PI3K signaling via regulation of IRS proteins. J Cell Biol 166, 213-223.

Hartman, N.W., Lin, T.V., Zhang, L., Paquelet, G.E., Feliciano, D.M., Bordey, A., 2013. mTORC1 targets the translational repressor 4E-BP2, but not S6 kinase 1/2, to regulate neural stem cell self-renewal in vivo. Cell Rep 5, 433-444.

Heidenreich, M., Zhang, F., 2016. Applications of CRISPR-Cas systems in neuroscience. Nat Rev Neurosci 17, 36-44.

Heitman, J., Movva, N.R., Hall, M.N., 1991. Targets for cell cycle arrest by the immunosuppressant rapamycin in yeast. Science 253, 905-909.

Helliwell, S.B., Wagner, P., Kunz, J., Deuter-Reinhard, M., Henriquez, R., Hall, M.N., 1994. TOR1 and TOR2 are structurally and functionally similar but not identical phosphatidylinositol kinase homologues in yeast. Mol Biol Cell 5, 105-118.

Henske, E.P., Wessner, L.L., Golden, J., Scheithauer, B.W., Vortmeyer, A.O., Zhuang, Z., Klein-Szanto, A.J., Kwiatkowski, D.J., Yeung, R.S., 1997. Loss of tuberin in both subependymal giant cell astrocytomas and angiomyolipomas supports a two-hit model for the pathogenesis of tuberous sclerosis tumors. Am J Pathol 151, 1639-1647.

Hernandez, O., Way, S., McKenna, J., 3rd, Gambello, M.J., 2007. Generation of a conditional disruption of the Tsc2 gene. Genesis 45, 101-106.

Hiratani, K., Haruta, T., Tani, A., Kawahara, J., Usui, I., Kobayashi, M., 2005. Roles of mTOR and JNK in serine phosphorylation, translocation, and degradation of IRS-1. Biochem Biophys Res Commun 335, 836-842.

Hirose, T., Scheithauer, B.W., Lopes, M.B., Gerber, H.A., Altermatt, H.J., Hukee, M.J., VandenBerg, S.R., Charlesworth, J.C., 1995. Tuber and subependymal giant cell astrocytoma associated with tuberous sclerosis: an immunohistochemical, ultrastructural, and immunoelectron and microscopic study. Acta Neuropathol 90, 387-399.

Hodges, A.K., Li, S., Maynard, J., Parry, L., Braverman, R., Cheadle, J.P., DeClue, J.E., Sampson, J.R., 2001. Pathological mutations in TSC1 and TSC2 disrupt the interaction between hamartin and tuberin. Hum Mol Genet 10, 2899-2905.

Hu, B.Y., Weick, J.P., Yu, J., Ma, L.X., Zhang, X.Q., Thomson, J.A., Zhang, S.C., 2010. Neural differentiation of human induced pluripotent stem cells follows developmental principles but with variable potency. Proc Natl Acad Sci U S A 107, 4335-4340.

Hu, Y., Qu, Z.Y., Cao, S.Y., Li, Q., Ma, L., Krencik, R., Xu, M., Liu, Y., 2016. Directed differentiation of basal forebrain cholinergic neurons from human pluripotent stem cells. J Neurosci Methods 266, 42-49.

Huang da, W., Sherman, B.T., Zheng, X., Yang, J., Imamichi, T., Stephens, R., Lempicki, R.A., 2009. Extracting biological meaning from large gene lists with DAVID. Curr Protoc Bioinformatics Chapter 13, Unit 13 11.

Huang, J., Manning, B.D., 2008. The TSC1-TSC2 complex: a molecular switchboard controlling cell growth. Biochem J 412, 179-190.

Huang, J., Manning, B.D., 2009. A complex interplay between Akt, TSC2 and the two mTOR complexes. Biochem Soc Trans 37, 217-222.

Hunt, A., Shepherd, C., 1993. A prevalence study of autism in tuberous sclerosis. J Autism Dev Disord 23, 323-339.

Huttenlocher, P.R., Wollmann, R.L., 1991. Cellular neuropathology of tuberous sclerosis. Ann N Y Acad Sci 615, 140-148.

Inoki, K., Li, Y., Xu, T., Guan, K.L., 2003a. Rheb GTPase is a direct target of TSC2 GAP activity and regulates mTOR signaling. Genes Dev 17, 1829-1834.

Inoki, K., Li, Y., Zhu, T., Wu, J., Guan, K.L., 2002. TSC2 is phosphorylated and inhibited by Akt and suppresses mTOR signalling. Nat Cell Biol 4, 648-657.

Inoki, K., Zhu, T., Guan, K.L., 2003b. TSC2 mediates cellular energy response to control cell growth and survival. Cell 115, 577-590.

Jacinto, E., Facchinetti, V., Liu, D., Soto, N., Wei, S., Jung, S.Y., Huang, Q., Qin, J., Su, B., 2006. SIN1/MIP1 maintains rictor-mTOR complex integrity and regulates Akt phosphorylation and substrate specificity. Cell 127, 125-137.

Jacinto, E., Loewith, R., Schmidt, A., Lin, S., Ruegg, M.A., Hall, A., Hall, M.N., 2004. Mammalian TOR complex 2 controls the actin cytoskeleton and is rapamycin insensitive. Nat Cell Biol 6, 1122-1128.

Jaeschke, A., Hartkamp, J., Saitoh, M., Roworth, W., Nobukuni, T., Hodges, A., Sampson, J., Thomas, G., Lamb, R., 2002. Tuberous sclerosis complex tumor suppressor-mediated S6 kinase inhibition by phosphatidylinositide-3-OH kinase is mTOR independent. J Cell Biol 159, 217-224.

James, S.R., Downes, C.P., Gigg, R., Grove, S.J., Holmes, A.B., Alessi, D.R., 1996. Specific binding of the Akt-1 protein kinase to phosphatidylinositol 3,4,5-trisphosphate without subsequent activation. Biochem J 315 (Pt 3), 709-713.

Jansen, F.E., van Huffelen, A.C., Algra, A., van Nieuwenhuizen, O., 2007. Epilepsy surgery in tuberous sclerosis: a systematic review. Epilepsia 48, 1477-1484.

Jay, V., Edwards, V., Musharbash, A., Rutka, J.T., 1998. Cerebellar pathology in tuberous sclerosis. Ultrastruct Pathol 22, 331-339.

Jewell, J.L., Guan, K.L., 2013. Nutrient signaling to mTOR and cell growth. Trends Biochem Sci 38, 233-242.

Johnson, M.W., Miyata, H., Vinters, H.V., 2002. Ezrin and moesin expression within the developing human cerebrum and tuberous sclerosis-associated cortical tubers. Acta Neuropathol 104, 188-196.

Joinson, C., O'Callaghan, F.J., Osborne, J.P., Martyn, C., Harris, T., Bolton, P.F., 2003. Learning disability and epilepsy in an epidemiological sample of individuals with tuberous sclerosis complex. Psychol Med 33, 335-344.

Kaidanovich-Beilin, O., Woodgett, J.R., 2011. GSK-3: Functional Insights from Cell Biology and Animal Models. Front Mol Neurosci 4, 40.

Kandt, R.S., Haines, J.L., Smith, M., Northrup, H., Gardner, R.J., Short, M.P., Dumars, K., Roach, E.S., Steingold, S., Wall, S., et al., 1992. Linkage of an important gene locus for tuberous sclerosis to a chromosome 16 marker for polycystic kidney disease. Nat Genet 2, 37-41.

Khwaja, O.S., Sahin, M., 2011. Translational research: Rett syndrome and tuberous sclerosis complex. Curr Opin Pediatr 23, 633-639.

Kim, D.H., Sarbassov, D.D., Ali, S.M., King, J.E., Latek, R.R., Erdjument-Bromage, H., Tempst, P., Sabatini, D.M., 2002. mTOR interacts with raptor to form a nutrient-sensitive complex that signals to the cell growth machinery. Cell 110, 163-175.

Kim, D.H., Sarbassov, D.D., Ali, S.M., Latek, R.R., Guntur, K.V., Erdjument-Bromage, H., Tempst, P., Sabatini, D.M., 2003. GbetaL, a positive regulator of the rapamycin-sensitive pathway required for the nutrient-sensitive interaction between raptor and mTOR. Mol Cell 11, 895-904.

Kim, S.K., Wang, K.C., Cho, B.K., Jung, H.W., Lee, Y.J., Chung, Y.S., Lee, J.Y., Park, S.H., Kim, Y.M., Choe, G., Chi, J.G., 2001. Biological behavior and tumorigenesis of subependymal giant cell astrocytomas. J Neurooncol 52, 217-225.

Klippel, A., Kavanaugh, W.M., Pot, D., Williams, L.T., 1997. A specific product of phosphatidylinositol 3-kinase directly activates the protein kinase Akt through its pleckstrin homology domain. Mol Cell Biol 17, 338-344.

Knudson, A.G., Jr., 1971. Mutation and cancer: statistical study of retinoblastoma. Proc Natl Acad Sci U S A 68, 820-823.

Kobayashi, T., Minowa, O., Kuno, J., Mitani, H., Hino, O., Noda, T., 1999. Renal carcinogenesis, hepatic hemangiomatosis, and embryonic lethality caused by a germ-line Tsc2 mutation in mice. Cancer Res 59, 1206-1211.

Kobayashi, T., Minowa, O., Sugitani, Y., Takai, S., Mitani, H., Kobayashi, E., Noda, T., Hino, O., 2001. A germ-line Tsc1 mutation causes tumor development and embryonic lethality that are similar, but not identical to, those caused by Tsc2 mutation in mice. Proc Natl Acad Sci U S A 98, 8762-8767.

Kobayashi, T., Mitani, H., Takahashi, R., Hirabayashi, M., Ueda, M., Tamura, H., Hino, O., 1997. Transgenic rescue from embryonic lethality and renal carcinogenesis in the Eker rat model by introduction of a wild-type Tsc2 gene. Proc Natl Acad Sci U S A 94, 3990-3993.

Koh, S., Jayakar, P., Dunoyer, C., Whiting, S.E., Resnick, T.J., Alvarez, L.A., Morrison, G., Ragheb, J., Prats, A., Dean, P., Gilman, J., Duchowny, M.S., 2000. Epilepsy surgery in children with tuberous sclerosis complex: presurgical evaluation and outcome. Epilepsia 41, 1206-1213.

Kohn, A.D., Kovacina, K.S., Roth, R.A., 1995. Insulin stimulates the kinase activity of RAC-PK, a pleckstrin homology domain containing ser/thr kinase. EMBO J 14, 4288-4295.

Kozlowski, P., Roberts, P., Dabora, S., Franz, D., Bissler, J., Northrup, H., Au, K.S., Lazarus, R., Domanska-Pakiela, D., Kotulska, K., Jozwiak, S., Kwiatkowski, D.J., 2007. Identification of 54 large deletions/duplications in TSC1 and TSC2 using MLPA, and genotype-phenotype correlations. Hum Genet 121, 389-400.

Kriegstein, A.R., Noctor, S.C., 2004. Patterns of neuronal migration in the embryonic cortex. Trends Neurosci 27, 392-399.

Kubo, Y., Kikuchi, Y., Mitani, H., Kobayashi, E., Kobayashi, T., Hino, O., 1995. Allelic loss at the tuberous sclerosis (Tsc2) gene locus in spontaneous uterine leiomyosarcomas and pituitary adenomas in the Eker rat model. Jpn J Cancer Res 86, 828-832.

Kwan, K.Y., Sestan, N., Anton, E.S., 2012. Transcriptional co-regulation of neuronal migration and laminar identity in the neocortex. Development 139, 1535-1546.

Kwiatkowska, J., Wigowska-Sowinska, J., Napierala, D., Slomski, R., Kwiatkowski, D.J., 1999. Mosaicism in tuberous sclerosis as a potential cause of the failure of molecular diagnosis. N Engl J Med 340, 703-707.

Kwiatkowski, D.J., 2010a. Genetics of Tuberous Sclerosis Complex. In: Kwiatkowski, D.J., Whittemore, V.H., Thiele, E.A. (Eds.), Tuberous Sclerosis Complex: Genes, Clinical Features, and Therapeutics. Wiley-Blackwell, pp. 29-60.

Kwiatkowski, D.J., 2010b. Rat and Mouse Models of Tuberous Sclerosis. In: Kwiatkowski, D.J., Whittemore, V.H., Thiele, E.A. (Eds.), Tuberous Sclerosis Complex: Genes, Clinical Features, and Therapeutics. Wiley-Blackwell, pp. 117-143.

Kwiatkowski, D.J., Zhang, H., Bandura, J.L., Heiberger, K.M., Glogauer, M., el-Hashemite, N., Onda, H., 2002. A mouse model of TSC1 reveals sex-dependent lethality from liver hemangiomas, and up-regulation of p70S6 kinase activity in Tsc1 null cells. Hum Mol Genet 11, 525-534.

Lam, E.W., Brosens, J.J., Gomes, A.R., Koo, C.Y., 2013. Forkhead box proteins: tuning forks for transcriptional harmony. Nat Rev Cancer 13, 482-495.

Lancaster, M.A., Corsini, N.S., Wolfinger, S., Gustafson, E.H., Phillips, A.W., Burkard, T.R., Otani, T., Livesey, F.J., Knoblich, J.A., 2017. Guided self-organization and cortical plate formation in human brain organoids. Nat Biotechnol 35, 659-666.

Lancaster, M.A., Knoblich, J.A., 2014. Generation of cerebral organoids from human pluripotent stem cells. Nat Protoc 9, 2329-2340.

Lancaster, M.A., Renner, M., Martin, C.A., Wenzel, D., Bicknell, L.S., Hurles, M.E., Homfray, T., Penninger, J.M., Jackson, A.P., Knoblich, J.A., 2013. Cerebral organoids model human brain development and microcephaly. Nature 501, 373-379.

Laplante, M., Sabatini, D.M., 2013. Regulation of mTORC1 and its impact on gene expression at a glance. J Cell Sci 126, 1713-1719.

Lee, A., Maldonado, M., Baybis, M., Walsh, C.A., Scheithauer, B., Yeung, R., Parent, J., Weiner, H.L., Crino, P.B., 2003. Markers of cellular proliferation are expressed in cortical tubers. Ann Neurol 53, 668-673.

Lee, D.F., Kuo, H.P., Chen, C.T., Hsu, J.M., Chou, C.K., Wei, Y., Sun, H.L., Li, L.Y., Ping, B., Huang, W.C., He, X., Hung, J.Y., Lai, C.C., Ding, Q., Su, J.L., Yang, J.Y., Sahin, A.A., Hortobagyi, G.N., Tsai, F.J., Tsai, C.H., Hung, M.C., 2007. IKK beta suppression of TSC1 links inflammation and tumor angiogenesis via the mTOR pathway. Cell 130, 440-455.

Lee, G.H., D'Arcangelo, G., 2016. New Insights into Reelin-Mediated Signaling Pathways. Front Cell Neurosci 10, 122.

Levine, D., Barnes, P., Korf, B., Edelman, R., 2000. Tuberous sclerosis in the fetus: second-trimester diagnosis of subependymal tubers with ultrafast MR imaging. AJR Am J Roentgenol 175, 1067-1069.

Lewis, J.C., Thomas, H.V., Murphy, K.C., Sampson, J.R., 2004. Genotype and psychological phenotype in tuberous sclerosis. J Med Genet 41, 203-207.

Li, Y., Cao, J., Chen, M., Li, J., Sun, Y., Zhang, Y., Zhu, Y., Wang, L., Zhang, C., 2017. Abnormal Neural Progenitor Cells Differentiated from Induced Pluripotent Stem Cells Partially Mimicked Development of TSC2 Neurological Abnormalities. Stem Cell Reports 8, 883-893.

Li, Y., Corradetti, M.N., Inoki, K., Guan, K.L., 2004. TSC2: filling the GAP in the mTOR signaling pathway. Trends Biochem Sci 29, 32-38.

Liu, L., Cash, T.P., Jones, R.G., Keith, B., Thompson, C.B., Simon, M.C., 2006. Hypoxia-induced energy stress regulates mRNA translation and cell growth. Mol Cell 21, 521-531.

Liu, Y., Liu, H., Sauvey, C., Yao, L., Zarnowska, E.D., Zhang, S.C., 2013. Directed differentiation of forebrain GABA interneurons from human pluripotent stem cells. Nat Protoc 8, 1670-1679.

Loh, Y.H., Hartung, O., Li, H., Guo, C., Sahalie, J.M., Manos, P.D., Urbach, A., Heffner, G.C., Grskovic, M., Vigneault, F., Lensch, M.W., Park, I.H., Agarwal, S., Church, G.M., Collins, J.J., Irion, S., Daley, G.Q., 2010. Reprogramming of T cells from human peripheral blood. Cell Stem Cell 7, 15-19.

Lopez-Carballo, G., Moreno, L., Masia, S., Perez, P., Barettino, D., 2002. Activation of the phosphatidylinositol 3-kinase/Akt signaling pathway by retinoic acid is required for neural differentiation of SH-SY5Y human neuroblastoma cells. J Biol Chem 277, 25297-25304.

Lyczkowski, D.A., Conant, K.D., Pulsifer, M.B., Jarrett, D.Y., Grant, P.E., Kwiatkowski, D.J., Thiele, E.A., 2007. Intrafamilial phenotypic variability in tuberous sclerosis complex. J Child Neurol 22, 1348-1355.

Ma, L., Chen, Z., Erdjument-Bromage, H., Tempst, P., Pandolfi, P.P., 2005. Phosphorylation and functional inactivation of TSC2 by Erk implications for tuberous sclerosis and cancer pathogenesis. Cell 121, 179-193.

Magri, L., Cambiaghi, M., Cominelli, M., Alfaro-Cervello, C., Cursi, M., Pala, M., Bulfone, A., Garcia-Verdugo, J.M., Leocani, L., Minicucci, F., Poliani, P.L., Galli, R., 2011. Sustained activation of mTOR pathway in embryonic neural stem cells leads to development of tuberous sclerosis complex-associated lesions. Cell Stem Cell 9, 447-462.

Major, P., Rakowski, S., Simon, M.V., Cheng, M.L., Eskandar, E., Baron, J., Leeman, B.A., Frosch, M.P., Thiele, E.A., 2009. Are cortical tubers epileptogenic? Evidence from electrocorticography. Epilepsia 50, 147-154.

Manning, B.D., 2010. The Role of Target of Rapamycin Signalin in Tuberous Sclerosis Complex. In: Kwiatkowski, D.J., Whittemore, V.H., Thiele, E.A. (Eds.), Tuberous Sclerosis Complex: Genes, Clinical Features, and Therapeutics. Wiley-Blackwell, pp. 87-115.

Manning, B.D., Cantley, L.C., 2003. United at last: the tuberous sclerosis complex gene products connect the phosphoinositide 3-kinase/Akt pathway to mammalian target of rapamycin (mTOR) signalling. Biochem Soc Trans 31, 573-578.

Manning, B.D., Logsdon, M.N., Lipovsky, A.I., Abbott, D., Kwiatkowski, D.J., Cantley, L.C., 2005. Feedback inhibition of Akt signaling limits the growth of tumors lacking Tsc2. Genes Dev 19, 1773-1778.

Manning, B.D., Tee, A.R., Logsdon, M.N., Blenis, J., Cantley, L.C., 2002. Identification of the tuberous sclerosis complex-2 tumor suppressor gene product tuberin as a target of the phosphoinositide 3-kinase/akt pathway. Mol Cell 10, 151-162.

Manning, B.D., Toker, A., 2017. AKT/PKB Signaling: Navigating the Network. Cell 169, 381-405.

Maquat, L.E., 2002. Nonsense-mediated mRNA decay. Curr Biol 12, R196-197.

Marchetto, M.C., Brennand, K.J., Boyer, L.F., Gage, F.H., 2011. Induced pluripotent stem cells (iPSCs) and neurological disease modeling: progress and promises. Hum Mol Genet 20, R109-115.

Marcotte, L., Aronica, E., Baybis, M., Crino, P.B., 2012. Cytoarchitectural alterations are widespread in cerebral cortex in tuberous sclerosis complex. Acta Neuropathol 123, 685-693.

Marcotte, L., Crino, P.B., 2006. The neurobiology of the tuberous sclerosis complex. Neuromolecular Med 8, 531-546.

Mariani, J., Simonini, M.V., Palejev, D., Tomasini, L., Coppola, G., Szekely, A.M., Horvath, T.L., Vaccarino, F.M., 2012. Modeling human cortical development in vitro using induced pluripotent stem cells. Proc Natl Acad Sci U S A 109, 12770-12775.

Martin, K.R., Zhou, W., Bowman, M.J., Shih, J., Au, K.S., Dittenhafer-Reed, K.E., Sisson, K.A., Koeman, J., Weisenberger, D.J., Cottingham, S.L., DeRoos, S.T., Devinsky, O., Winn, M.E., Cherniack, A.D., Shen, H., Northrup, H., Krueger, D.A., MacKeigan, J.P., 2017. The genomic landscape of tuberous sclerosis complex. Nat Commun 8, 15816.

Mayer, K., Ballhausen, W., Leistner, W., Rott, H., 2000. Three novel types of splicing aberrations in the tuberous sclerosis TSC2 gene caused by mutations apart from splice consensus sequences. Biochim Biophys Acta 1502, 495-507.

Meikle, L., Pollizzi, K., Egnor, A., Kramvis, I., Lane, H., Sahin, M., Kwiatkowski, D.J., 2008. Response of a neuronal model of tuberous sclerosis to mammalian target of rapamycin (mTOR) inhibitors: effects on mTORC1 and Akt signaling lead to improved survival and function. J Neurosci 28, 5422-5432.

Meikle, L., Talos, D.M., Onda, H., Pollizzi, K., Rotenberg, A., Sahin, M., Jensen, F.E., Kwiatkowski, D.J., 2007. A mouse model of tuberous sclerosis: neuronal loss of Tsc1 causes dysplastic and ectopic neurons, reduced myelination, seizure activity, and limited survival. J Neurosci 27, 5546-5558.

Miyata, H., Chiang, A.C., Vinters, H.V., 2004. Insulin signaling pathways in cortical dysplasia and TSC-tubers: tissue microarray analysis. Ann Neurol 56, 510-519.

Mizuguchi, M., 2007. Abnormal giant cells in the cerebral lesions of tuberous sclerosis complex. Congenit Anom (Kyoto) 47, 2-8.

Mizuguchi, M., Mori, M., Nozaki, Y., Momoi, M.Y., Itoh, M., Takashima, S., Hino, O., 2004. Absence of allelic loss in cytomegalic neurons of cortical tuber in the Eker rat model of tuberous sclerosis. Acta Neuropathol 107, 47-52.

Mizuguchi, M., Takashima, S., 2001. Neuropathology of tuberous sclerosis. Brain Dev 23, 508-515.

Mizuguchi, M., Yamanouchi, H., Becker, L.E., Itoh, M., Takashima, S., 2002. Doublecortin immunoreactivity in giant cells of tuberous sclerosis and focal cortical dysplasia. Acta Neuropathol 104, 418-424.

Moolten, S.E., 1942. Hamartial Nature of the Tuberous Sclerosis Complex and Its Bearing on the Tumor Problem. Archives of Internal Medicine 69, 589-623.

Muhlebner, A., Iyer, A.M., van Scheppingen, J., Anink, J.J., Jansen, F.E., Veersema, T.J., Braun, K.P., Spliet, W.G., van Hecke, W., Soylemezoglu, F., Feucht, M., Krsek, P., Zamecnik, J., Bien, C.G., Polster, T., Coras, R., Blumcke, I., Aronica, E., 2016a. Specific pattern of maturation and differentiation in the formation of cortical tubers in tuberous sclerosis omplex (TSC): evidence from layer-specific marker expression. J Neurodev Disord 8, 9.

Muhlebner, A., van Scheppingen, J., Hulshof, H.M., Scholl, T., Iyer, A.M., Anink, J.J., van den Ouweland, A.M., Nellist, M.D., Jansen, F.E., Spliet, W.G., Krsek, P., Benova, B., Zamecnik, J., Crino, P.B., Prayer, D., Czech, T., Wohrer, A., Rahimi, J., Hoftberger, R., Hainfellner, J.A., Feucht, M., Aronica, E., 2016b. Novel Histopathological Patterns in Cortical Tubers of Epilepsy Surgery Patients with Tuberous Sclerosis Complex. PLoS One 11, e0157396.

NCBI, N.C.f.B.I., 2018a. TSC1 TSC complex subunit 1 [*Homo sapiens* (human)].

NCBI, N.C.f.B.I., 2018b. TSC2 TSC complex subunit 2 [*Homo Sapiens* (human)].

Nelsen, C.J., Rickheim, D.G., Tucker, M.M., Hansen, L.K., Albrecht, J.H., 2003. Evidence that cyclin D1 mediates both growth and proliferation downstream of TOR in hepatocytes. J Biol Chem 278, 3656-3663.

Nicholas, C.R., Chen, J., Tang, Y., Southwell, D.G., Chalmers, N., Vogt, D., Arnold, C.M., Chen, Y.J., Stanley, E.G., Elefanty, A.G., Sasai, Y., Alvarez-Buylla, A., Rubenstein, J.L., Kriegstein, A.R., 2013. Functional maturation of hPSC-derived forebrain interneurons requires an extended timeline and mimics human neural development. Cell Stem Cell 12, 573-586.

Nie, D., Di Nardo, A., Han, J.M., Baharanyi, H., Kramvis, I., Huynh, T., Dabora, S., Codeluppi, S., Pandolfi, P.P., Pasquale, E.B., Sahin, M., 2010. Tsc2-Rheb signaling regulates EphA-mediated axon guidance. Nat Neurosci 13, 163-172.

Nieto-Estevez, V., Defterali, C., Vicario-Abejon, C., 2016. IGF-I: A Key Growth Factor that Regulates Neurogenesis and Synaptogenesis from Embryonic to Adult Stages of the Brain. Front Neurosci 10, 52.

Niida, Y., Stemmer-Rachamimov, A.O., Logrip, M., Tapon, D., Perez, R., Kwiatkowski, D.J., Sims, K., MacCollin, M., Louis, D.N., Ramesh, V., 2001. Survey of somatic mutations in tuberous sclerosis complex (TSC) hamartomas suggests different genetic mechanisms for pathogenesis of TSC lesions. Am J Hum Genet 69, 493-503.

Noctor, S.C., Martinez-Cerdeno, V., Ivic, L., Kriegstein, A.R., 2004. Cortical neurons arise in symmetric and asymmetric division zones and migrate through specific phases. Nat Neurosci 7, 136-144.

Nojima, H., Tokunaga, C., Eguchi, S., Oshiro, N., Hidayat, S., Yoshino, K., Hara, K., Tanaka, N., Avruch, J., Yonezawa, K., 2003. The mammalian target of rapamycin (mTOR) partner, raptor, binds the mTOR substrates p70 S6 kinase and 4E-BP1 through their TOR signaling (TOS) motif. J Biol Chem 278, 15461-15464.

Northrup, H., Koenig, M.K., Pearson, D.A., Au, K.S., 1993. Tuberous Sclerosis Complex. In: Adam, M.P., Ardinger, H.H., Pagon, R.A., Wallace, S.E., Bean, L.J.H., Stephens, K., Amemiya, A. (Eds.), GeneReviews((R)), Seattle (WA).

O'Callaghan, F.J., Harris, T., Joinson, C., Bolton, P., Noakes, M., Presdee, D., Renowden, S., Shiell, A., Martyn, C.N., Osborne, J.P., 2004. The relation of infantile spasms, tubers, and intelligence in tuberous sclerosis complex. Arch Dis Child 89, 530-533.

Oishi, K., Watatani, K., Itoh, Y., Okano, H., Guillemot, F., Nakajima, K., Gotoh, Y., 2009. Selective induction of neocortical GABAergic neurons by the PDK1-Akt pathway through activation of Mash1. Proc Natl Acad Sci U S A 106, 13064-13069.

Onda, H., Lueck, A., Marks, P.W., Warren, H.B., Kwiatkowski, D.J., 1999. Tsc2(+/-) mice develop tumors in multiple sites that express gelsolin and are influenced by genetic background. J Clin Invest 104, 687-695.

Osborne, J.P., Fryer, A., Webb, D., 1991. Epidemiology of tuberous sclerosis. Ann N Y Acad Sci 615, 125-127.

Otaegi, G., Yusta-Boyo, M.J., Vergano-Vera, E., Mendez-Gomez, H.R., Carrera, A.C., Abad, J.L., Gonzalez, M., de la Rosa, E.J., Vicario-Abejon, C., de Pablo, F., 2006. Modulation of the PI 3-kinase-Akt signalling pathway by IGF-I and PTEN regulates the differentiation of neural stem/precursor cells. J Cell Sci 119, 2739-2748.

Ozcan, U., Ozcan, L., Yilmaz, E., Duvel, K., Sahin, M., Manning, B.D., Hotamisligil, G.S., 2008. Loss of the tuberous sclerosis complex tumor suppressors triggers the unfolded protein response to regulate insulin signaling and apoptosis. Mol Cell 29, 541-551.

Pang, Z.P., Yang, N., Vierbuchen, T., Ostermeier, A., Fuentes, D.R., Yang, T.Q., Citri, A., Sebastiano, V., Marro, S., Sudhof, T.C., Wernig, M., 2011. Induction of human neuronal cells by defined transcription factors. Nature 476, 220-223.

Pap, M., Cooper, G.M., 1998. Role of glycogen synthase kinase-3 in the phosphatidylinositol 3-Kinase/Akt cell survival pathway. J Biol Chem 273, 19929-19932.

Park, S.H., Pepkowitz, S.H., Kerfoot, C., De Rosa, M.J., Poukens, V., Wienecke, R., DeClue, J.E., Vinters, H.V., 1997. Tuberous sclerosis in a 20-week gestation fetus: immunohistochemical study. Acta Neuropathol 94, 180-186.

Patel, P.H., Thapar, N., Guo, L., Martinez, M., Maris, J., Gau, C.L., Lengyel, J.A., Tamanoi, F., 2003. Drosophila Rheb GTPase is required for cell cycle progression and cell growth. J Cell Sci 116, 3601-3610.

Pederson, T.M., Kramer, D.L., Rondinone, C.M., 2001. Serine/threonine phosphorylation of IRS-1 triggers its degradation: possible regulation by tyrosine phosphorylation. Diabetes 50, 24-31.

Pfisterer, U., Kirkeby, A., Torper, O., Wood, J., Nelander, J., Dufour, A., Bjorklund, A., Lindvall, O., Jakobsson, J., Parmar, M., 2011. Direct conversion of human fibroblasts to dopaminergic neurons. Proc Natl Acad Sci U S A 108, 10343-10348.

Pimentel, H., Bray, N.L., Puente, S., Melsted, P., Pachter, L., 2017. Differential analysis of RNA-seq incorporating quantification uncertainty. Nat Methods 14, 687-690.

Plank, T.L., Yeung, R.S., Henske, E.P., 1998. Hamartin, the product of the tuberous sclerosis 1 (TSC1) gene, interacts with tuberin and appears to be localized to cytoplasmic vesicles. Cancer Res 58, 4766-4770.

Potter, C.J., Huang, H., Xu, T., 2001. Drosophila Tsc1 functions with Tsc2 to antagonize insulin signaling in regulating cell growth, cell proliferation, and organ size. Cell 105, 357-368.

Povey, S., Ekong, R., 2018. Leiden Open Variation Database Tuberous sclerosis database.
Prather, P., de Vries, P.J., 2004. Behavioral and cognitive aspects of tuberous sclerosis complex. J Child Neurol 19, 666-674.

Radimerski, T., Montagne, J., Hemmings-Mieszczak, M., Thomas, G., 2002. Lethality of Drosophila lacking TSC tumor suppressor function rescued by reducing dS6K signaling. Genes Dev 16, 2627-2632.

Ramos, F.J., Langlais, P.R., Hu, D., Dong, L.Q., Liu, F., 2006. Grb10 mediates insulin-stimulated degradation of the insulin receptor: a mechanism of negative regulation. Am J Physiol Endocrinol Metab 290, E1262-1266.

Ridler, K., Suckling, J., Higgins, N., Bolton, P., Bullmore, E., 2004. Standardized whole brain mapping of tubers and subependymal nodules in tuberous sclerosis complex. J Child Neurol 19, 658-665.

Roach, E.S., Williams, D.P., Laster, D.W., 1987. Magnetic resonance imaging in tuberous sclerosis. Arch Neurol 44, 301-303.

Rose, V.M., Au, K.S., Pollom, G., Roach, E.S., Prashner, H.R., Northrup, H., 1999. Germ-line mosaicism in tuberous sclerosis: how common? Am J Hum Genet 64, 986-992.

Roux, P.P., Ballif, B.A., Anjum, R., Gygi, S.P., Blenis, J., 2004. Tumor-promoting phorbol esters and activated Ras inactivate the tuberous sclerosis tumor suppressor complex via p90 ribosomal S6 kinase. Proc Natl Acad Sci U S A 101, 13489-13494.

Ruppe, V., Dilsiz, P., Reiss, C.S., Carlson, C., Devinsky, O., Zagzag, D., Weiner, H.L., Talos, D.M., 2014. Developmental brain abnormalities in tuberous sclerosis complex: a comparative tissue analysis of cortical tubers and perituberal cortex. Epilepsia 55, 539-550.

Sabatini, D.M., Erdjument-Bromage, H., Lui, M., Tempst, P., Snyder, S.H., 1994. RAFT1: a mammalian protein that binds to FKBP12 in a rapamycin-dependent fashion and is homologous to yeast TORs. Cell 78, 35-43.

Sahin, M., Henske, E.P., Manning, B.D., Ess, K.C., Bissler, J.J., Klann, E., Kwiatkowski, D.J., Roberds, S.L., Silva, A.J., Hillaire-Clarke, C.S., Young, L.R., Zervas, M., Mamounas, L.A., Tuberous Sclerosis Complex Working Group to Update the Research, P., 2016. Advances and Future Directions for Tuberous Sclerosis Complex Research: Recommendations From the 2015 Strategic Planning Conference. Pediatr Neurol 60, 1-12.

Sancak, O., Nellist, M., Goedbloed, M., Elfferich, P., Wouters, C., Maat-Kievit, A., Zonnenberg, B., Verhoef, S., Halley, D., van den Ouweland, A., 2005. Mutational analysis of the TSC1 and TSC2 genes in a diagnostic setting: genotype--phenotype correlations and comparison of diagnostic DNA techniques in Tuberous Sclerosis Complex. Eur J Hum Genet 13, 731-741.

Sarbassov, D.D., Ali, S.M., Kim, D.H., Guertin, D.A., Latek, R.R., Erdjument-Bromage, H., Tempst, P., Sabatini, D.M., 2004. Rictor, a novel binding partner of mTOR, defines a rapamycin-insensitive and raptor-independent pathway that regulates the cytoskeleton. Curr Biol 14, 1296-1302.

Saucedo, L.J., Gao, X., Chiarelli, D.A., Li, L., Pan, D., Edgar, B.A., 2003. Rheb promotes cell growth as a component of the insulin/TOR signalling network. Nat Cell Biol 5, 566-571.

Sepp, T., Yates, J.R., Green, A.J., 1996. Loss of heterozygosity in tuberous sclerosis hamartomas. J Med Genet 33, 962-964.

Shah, O.J., Hunter, T., 2006. Turnover of the active fraction of IRS1 involves raptor-mTOR- and S6K1-dependent serine phosphorylation in cell culture models of tuberous sclerosis. Mol Cell Biol 26, 6425-6434.

Shah, O.J., Wang, Z., Hunter, T., 2004. Inappropriate activation of the TSC/Rheb/mTOR/S6K cassette induces IRS1/2 depletion, insulin resistance, and cell survival deficiencies. Curr Biol 14, 1650-1656.

Shaw, R.J., 2009. LKB1 and AMP-activated protein kinase control of mTOR signalling and growth. Acta Physiol (Oxf) 196, 65-80.

Shi, Y., Kirwan, P., Livesey, F.J., 2012a. Directed differentiation of human pluripotent stem cells to cerebral cortex neurons and neural networks. Nat Protoc 7, 1836-1846.

Shi, Y., Kirwan, P., Smith, J., Robinson, H.P., Livesey, F.J., 2012b. Human cerebral cortex development from pluripotent stem cells to functional excitatory synapses. Nat Neurosci 15, 477-486, S471.

Shimobayashi, M., Hall, M.N., 2014. Making new contacts: the mTOR network in metabolism and signalling crosstalk. Nat Rev Mol Cell Biol 15, 155-162.

Smalley, S.L., Tanguay, P.E., Smith, M., Gutierrez, G., 1992. Autism and tuberous sclerosis. J Autism Dev Disord 22, 339-355.

Sofer, A., Lei, K., Johannessen, C.M., Ellisen, L.W., 2005. Regulation of mTOR and cell growth in response to energy stress by REDD1. Mol Cell Biol 25, 5834-5845.

Soldner, F., Hockemeyer, D., Beard, C., Gao, Q., Bell, G.W., Cook, E.G., Hargus, G., Blak, A., Cooper, O., Mitalipova, M., Isacson, O., Jaenisch, R., 2009. Parkinson's disease patient-derived induced pluripotent stem cells free of viral reprogramming factors. Cell 136, 964-977.

Sosunov, A.A., McGovern, R.A., Mikell, C.B., Wu, X., Coughlin, D.G., Crino, P.B., Weiner, H.L., Ghatan, S., Goldman, J.E., McKhann, G.M., 2nd, 2015. Epileptogenic but MRI-normal perituberal tissue in Tuberous Sclerosis Complex contains tuber-specific abnormalities. Acta Neuropathol Commun 3, 17.

Sosunov, A.A., Wu, X., Weiner, H.L., Mikell, C.B., Goodman, R.R., Crino, P.D., McKhann, G.M., 2nd, 2008. Tuberous sclerosis: a primary pathology of astrocytes? Epilepsia 49 Suppl 2, 53-62.

Soucek, T., Holzl, G., Bernaschek, G., Hengstschlager, M., 1998. A role of the tuberous sclerosis gene-2 product during neuronal differentiation. Oncogene 16, 2197-2204.

Souza, B.R., Romano-Silva, M.A., Tropepe, V., 2011. Dopamine D2 receptor activity modulates Akt signaling and alters GABAergic neuron development and motor behavior in zebrafish larvae. J Neurosci 31, 5512-5525.

Stan, R., McLaughlin, M.M., Cafferkey, R., Johnson, R.K., Rosenberg, M., Livi, G.P., 1994. Interaction between FKBP12-rapamycin and TOR involves a conserved serine residue. J Biol Chem 269, 32027-32030.

Stein, J.L., de la Torre-Ubieta, L., Tian, Y., Parikshak, N.N., Hernandez, I.A., Marchetto, M.C., Baker, D.K., Lu, D., Hinman, C.R., Lowe, J.K., Wexler, E.M., Muotri, A.R., Gage, F.H., Kosik, K.S., Geschwind, D.H., 2014. A quantitative framework to evaluate modeling of cortical development by neural stem cells. Neuron 83, 69-86.

Stenson, P.D., Mort, M., Ball, E.V., Evans, K., Hayden, M., Heywood, S., Hussain, M., Phillips, A.D., Cooper, D.N., 2017. The Human Gene Mutation Database: towards a comprehensive repository of inherited mutation data for medical research, genetic diagnosis and next-generation sequencing studies. Hum Genet 136, 665-677.

Stocker, H., Hafen, E., 2000. Genetic control of cell size. Curr Opin Genet Dev 10, 529-535.

Stocker, H., Radimerski, T., Schindelholz, B., Wittwer, F., Belawat, P., Daram, P., Breuer, S., Thomas, G., Hafen, E., 2003. Rheb is an essential regulator of S6K in controlling cell growth in Drosophila. Nat Cell Biol 5, 559-565.

Stranahan, A.M., Erion, J.R., Wosiski-Kuhn, M., 2013. Reelin signaling in development, maintenance, and plasticity of neural networks. Ageing Res Rev 12, 815-822.

Sundberg, M., Tochitsky, I., Buchholz, D.E., Winden, K., Kujala, V., Kapur, K., Cataltepe, D., Turner, D., Han, M.J., Woolf, C.J., Hatten, M.E., Sahin, M., 2018. Purkinje cells derived from TSC patients display hypoexcitability and synaptic deficits associated with reduced FMRP levels and reversed by rapamycin. Mol Psychiatry.

Takahashi, D.K., Dinday, M.T., Barbaro, N.M., Baraban, S.C., 2004. Abnormal cortical cells and astrocytomas in the Eker rat model of tuberous sclerosis complex. Epilepsia 45, 1525-1530.

Takahashi, K., Tanabe, K., Ohnuki, M., Narita, M., Ichisaka, T., Tomoda, K., Yamanaka, S., 2007. Induction of pluripotent stem cells from adult human fibroblasts by defined factors. Cell 131, 861-872.

Talos, D.M., Kwiatkowski, D.J., Cordero, K., Black, P.M., Jensen, F.E., 2008. Cell-specific alterations of glutamate receptor expression in tuberous sclerosis complex cortical tubers. Ann Neurol 63, 454-465.

Taniguchi, C.M., Emanuelli, B., Kahn, C.R., 2006. Critical nodes in signalling pathways: insights into insulin action. Nat Rev Mol Cell Biol 7, 85-96.

Tapon, N., Ito, N., Dickson, B.J., Treisman, J.E., Hariharan, I.K., 2001. The Drosophila tuberous sclerosis complex gene homologs restrict cell growth and cell proliferation. Cell 105, 345-355.

Tavazoie, S.F., Alvarez, V.A., Ridenour, D.A., Kwiatkowski, D.J., Sabatini, B.L., 2005. Regulation of neuronal morphology and function by the tumor suppressors Tsc1 and Tsc2. Nat Neurosci 8, 1727-1734.

Tee, A.R., Anjum, R., Blenis, J., 2003a. Inactivation of the tuberous sclerosis complex-1 and -2 gene products occurs by phosphoinositide 3-kinase/Akt-dependent and -independent phosphorylation of tuberin. J Biol Chem 278, 37288-37296.

Tee, A.R., Fingar, D.C., Manning, B.D., Kwiatkowski, D.J., Cantley, L.C., Blenis, J., 2002. Tuberous sclerosis complex-1 and -2 gene products function together to inhibit mammalian target of rapamycin (mTOR)-mediated downstream signaling. Proc Natl Acad Sci U S A 99, 13571-13576.

Tee, A.R., Manning, B.D., Roux, P.P., Cantley, L.C., Blenis, J., 2003b. Tuberous sclerosis complex gene products, Tuberin and Hamartin, control mTOR signaling by acting as a GTPase-activating protein complex toward Rheb. Curr Biol 13, 1259-1268.

Thiele, E.A., 2010. Managing and understanding epilepsy in tuberous sclerosis complex. Epilepsia 51 Suppl 1, 90-91.

Thier, M., Worsdorfer, P., Lakes, Y.B., Gorris, R., Herms, S., Opitz, T., Seiferling, D., Quandel, T., Hoffmann, P., Nothen, M.M., Brustle, O., Edenhofer, F., 2012. Direct conversion of fibroblasts into stably expandable neural stem cells. Cell Stem Cell 10, 473-479.

Tiscornia, G., Vivas, E.L., Izpisua Belmonte, J.C., 2011. Diseases in a dish: modeling human genetic disorders using induced pluripotent cells. Nat Med 17, 1570-1576.

Tsai, P.T., Hull, C., Chu, Y., Greene-Colozzi, E., Sadowski, A.R., Leech, J.M., Steinberg, J., Crawley, J.N., Regehr, W.G., Sahin, M., 2012. Autistic-like behaviour and cerebellar dysfunction in Purkinje cell Tsc1 mutant mice. Nature 488, 647-651.

Tschuluun, N., Wenzel, H.J., Schwartzkroin, P.A., 2007. Irradiation exacerbates cortical cytopathology in the Eker rat model of tuberous sclerosis complex, but does not induce hyperexcitability. Epilepsy Res 73, 53-64.

Uhlmann, E.J., Wong, M., Baldwin, R.L., Bajenaru, M.L., Onda, H., Kwiatkowski, D.J., Yamada, K., Gutmann, D.H., 2002. Astrocyte-specific TSC1 conditional knockout mice exhibit abnormal neuronal organization and seizures. Ann Neurol 52, 285-296.

Vadlakonda, L., Dash, A., Pasupuleti, M., Anil Kumar, K., Reddanna, P., 2013. The Paradox of Akt-mTOR Interactions. Front Oncol 3, 165.

Valencia, I., Legido, A., Yelin, K., Khurana, D., Kothare, S.V., Katsetos, C.D., 2006. Anomalous inhibitory circuits in cortical tubers of human tuberous sclerosis complex associated with refractory epilepsy: aberrant expression of parvalbumin and calbindin-D28k in dysplastic cortex. J Child Neurol 21, 1058-1063.

van der Vos, K.E., Coffer, P.J., 2011. The extending network of FOXO transcriptional target genes. Antioxid Redox Signal 14, 579-592.

van Eeghen, A.M., Teran, L.O., Johnson, J., Pulsifer, M.B., Thiele, E.A., Caruso, P., 2013. The neuroanatomical phenotype of tuberous sclerosis complex: focus on radial migration lines. Neuroradiology 55, 1007-1014.

van Slegtenhorst, M., de Hoogt, R., Hermans, C., Nellist, M., Janssen, B., Verhoef, S., Lindhout, D., van den Ouweland, A., Halley, D., Young, J., Burley, M., Jeremiah, S., Woodward, K., Nahmias, J., Fox, M., Ekong, R., Osborne, J., Wolfe, J., Povey, S., Snell, R.G., Cheadle, J.P., Jones, A.C., Tachataki, M., Ravine, D., Sampson, J.R., Reeve, M.P., Richardson, P., Wilmer, F., Munro, C., Hawkins, T.L., Sepp, T., Ali, J.B., Ward, S., Green, A.J., Yates, J.R., Kwiatkowska, J., Henske, E.P., Short, M.P., Haines, J.H., Jozwiak, S., Kwiatkowski, D.J., 1997. Identification of the tuberous sclerosis gene TSC1 on chromosome 9q34. Science 277, 805-808.

van Slegtenhorst, M., Nellist, M., Nagelkerken, B., Cheadle, J., Snell, R., van den Ouweland, A., Reuser, A., Sampson, J., Halley, D., van der Sluijs, P., 1998. Interaction between hamartin and tuberin, the TSC1 and TSC2 gene products. Hum Mol Genet 7, 1053-1057.

Vezina, C., Kudelski, A., Sehgal, S.N., 1975. Rapamycin (AY-22,989), a new antifungal antibiotic. I. Taxonomy of the producing streptomycete and isolation of the active principle. J Antibiot (Tokyo) 28, 721-726.

Vicario-Abejon, C., Yusta-Boyo, M.J., Fernandez-Moreno, C., de Pablo, F., 2003. Locally born olfactory bulb stem cells proliferate in response to insulin-related factors and require endogenous insulin-like growth factor-I for differentiation into neurons and glia. J Neurosci 23, 895-906.

Vierbuchen, T., Ostermeier, A., Pang, Z.P., Kokubu, Y., Sudhof, T.C., Wernig, M., 2010. Direct conversion of fibroblasts to functional neurons by defined factors. Nature 463, 1035-1041.

Vignoli, A., La Briola, F., Peron, A., Turner, K., Vannicola, C., Saccani, M., Magnaghi, E., Scornavacca, G.F., Canevini, M.P., 2015. Autism spectrum disorder in tuberous sclerosis complex: searching for risk markers. Orphanet J Rare Dis 10, 154.

Vincent, E.E., Elder, D.J., Thomas, E.C., Phillips, L., Morgan, C., Pawade, J., Sohail, M., May, M.T., Hetzel, M.R., Tavare, J.M., 2011. Akt phosphorylation on Thr308 but not on Ser473 correlates with Akt protein kinase activity in human non-small cell lung cancer. Br J Cancer 104, 1755-1761.

Vojtek, A.B., Taylor, J., DeRuiter, S.L., Yu, J.Y., Figueroa, C., Kwok, R.P., Turner, D.L., 2003. Akt regulates basic helix-loop-helix transcription factor-coactivator complex formation and activity during neuronal differentiation. Mol Cell Biol 23, 4417-4427.

von der Brelie, C., Waltereit, R., Zhang, L., Beck, H., Kirschstein, T., 2006. Impaired synaptic plasticity in a rat model of tuberous sclerosis. Eur J Neurosci 23, 686-692.

Vries, P.J.d., 2010. Neurodevelopmental, Psychiatric and Cognitive Aspects of Tuberous Sclerosis Complex. In: Kwiatkowski, D.J., Whittemore, V.H., Thiele, E.A. (Eds.), Tuberous Sclerosis Complex: Genes, Clinical Features and Therapeutics. Wiley-Blackwell, pp. 229-267.

Wang, Y., Greenwood, J.S., Calcagnotto, M.E., Kirsch, H.E., Barbaro, N.M., Baraban, S.C., 2007. Neocortical hyperexcitability in a human case of tuberous sclerosis complex and mice lacking neuronal expression of TSC1. Ann Neurol 61, 139-152.

Watanabe, S., Umehara, H., Murayama, K., Okabe, M., Kimura, T., Nakano, T., 2006. Activation of Akt signaling is sufficient to maintain pluripotency in mouse and primate embryonic stem cells. Oncogene 25, 2697-2707.

Webb, A.E., Brunet, A., 2014. FOXO transcription factors: key regulators of cellular quality control. Trends Biochem Sci 39, 159-169.

Wienecke, R., Konig, A., DeClue, J.E., 1995. Identification of tuberin, the tuberous sclerosis-2 product. Tuberin possesses specific Rap1GAP activity. J Biol Chem 270, 16409-16414.

Wiznitzer, M., 2004. Autism and tuberous sclerosis. J Child Neurol 19, 675-679.

Wong, M., Roper, S.N., 2016. Genetic animal models of malformations of cortical development and epilepsy. J Neurosci Methods 260, 73-82.

Wortmann, S.B., Reimer, A., Creemers, J.W., Mullaart, R.A., 2008. Prenatal diagnosis of cerebral lesions in Tuberous sclerosis complex (TSC). Case report and review of the literature. Eur J Paediatr Neurol 12, 123-126.

Wu, Y.T., Tan, H.L., Huang, Q., Ong, C.N., Shen, H.M., 2009. Activation of the PI3K-Akt-mTOR signaling pathway promotes necrotic cell death via suppression of autophagy. Autophagy 5, 824-834.

Wullschleger, S., Loewith, R., Hall, M.N., 2006. TOR signaling in growth and metabolism. Cell 124, 471-484.

Xiao, G.H., Shoarinejad, F., Jin, F., Golemis, E.A., Yeung, R.S., 1997. The tuberous sclerosis 2 gene product, tuberin, functions as a Rab5 GTPase activating protein (GAP) in modulating endocytosis. J Biol Chem 272, 6097-6100.

Yamanouchi, H., Ho, M., Jay, V., Becker, L.E., 1997. Giant cells in cortical tubers in tuberous sclerosis showing synaptophysin-immunoreactive halos. Brain Dev 19, 21-24.

Yan, Y., Shin, S., Jha, B.S., Liu, Q., Sheng, J., Li, F., Zhan, M., Davis, J., Bharti, K., Zeng, X., Rao, M., Malik, N., Vemuri, M.C., 2013. Efficient and rapid derivation of primitive neural stem cells and generation of brain subtype neurons from human pluripotent stem cells. Stem Cells Transl Med 2, 862-870.

Yang, Q., Inoki, K., Ikenoue, T., Guan, K.L., 2006. Identification of Sin1 as an essential TORC2 component required for complex formation and kinase activity. Genes Dev 20, 2820-2832.

Yeung, R.S., Katsetos, C.D., Klein-Szanto, A., 1997. Subependymal astrocytic hamartomas in the Eker rat model of tuberous sclerosis. Am J Pathol 151, 1477-1486.

Yeung, R.S., Xiao, G.H., Everitt, J.I., Jin, F., Walker, C.L., 1995. Allelic loss at the tuberous sclerosis 2 locus in spontaneous tumors in the Eker rat. Mol Carcinog 14, 28-36.

Yeung, R.S., Xiao, G.H., Jin, F., Lee, W.C., Testa, J.R., Knudson, A.G., 1994. Predisposition to renal carcinoma in the Eker rat is determined by germ-line mutation of the tuberous sclerosis 2 (TSC2) gene. Proc Natl Acad Sci U S A 91, 11413-11416.

Yin, H., Song, C.Q., Dorkin, J.R., Zhu, L.J., Li, Y., Wu, Q., Park, A., Yang, J., Suresh, S., Bizhanova, A., Gupta, A., Bolukbasi, M.F., Walsh, S., Bogorad, R.L., Gao, G., Weng, Z., Dong, Y., Koteliansky, V., Wolfe, S.A., Langer, R., Xue, W., Anderson, D.G., 2016. Therapeutic genome editing by combined viral and non-viral delivery of CRISPR system components in vivo. Nat Biotechnol 34, 328-333.

Yu, D.X., Marchetto, M.C., Gage, F.H., 2013. Therapeutic translation of iPSCs for treating neurological disease. Cell Stem Cell 12, 678-688.

Yu, Y., Li, S., Xu, X., Li, Y., Guan, K., Arnold, E., Ding, J., 2005. Structural basis for the unique biological function of small GTPase RHEB. J Biol Chem 280, 17093-17100.

Yuan, H., Chen, R., Wu, L., Chen, Q., Hu, A., Zhang, T., Wang, Z., Zhu, X., 2015. The regulatory mechanism of neurogenesis by IGF-1 in adult mice. Mol Neurobiol 51, 512-522.

Zacharek, S.J., Xiong, Y., Shumway, S.D., 2005. Negative regulation of TSC1-TSC2 by mammalian D-type cyclins. Cancer Res 65, 11354-11360.

Zeng, L.H., Xu, L., Gutmann, D.H., Wong, M., 2008. Rapamycin prevents epilepsy in a mouse model of tuberous sclerosis complex. Ann Neurol 63, 444-453.

Zhang, H., Cicchetti, G., Onda, H., Koon, H.B., Asrican, K., Bajraszewski, N., Vazquez, F., Carpenter, C.L., Kwiatkowski, D.J., 2003a. Loss of Tsc1/Tsc2 activates mTOR and disrupts PI3K-Akt signaling through downregulation of PDGFR. J Clin Invest 112, 1223-1233.

Zhang, H.H., Lipovsky, A.I., Dibble, C.C., Sahin, M., Manning, B.D., 2006. S6K1 regulates GSK3 under conditions of mTOR-dependent feedback inhibition of Akt. Mol Cell 24, 185-197.

Zhang, J., Gao, Z., Yin, J., Quon, M.J., Ye, J., 2008. S6K directly phosphorylates IRS-1 on Ser-270 to promote insulin resistance in response to TNF-(alpha) signaling through IKK2. J Biol Chem 283, 35375-35382.

Zhang, X., He, X., Li, Q., Kong, X., Ou, Z., Zhang, L., Gong, Z., Long, D., Li, J., Zhang, M., Ji, W., Zhang, W., Xu, L., Xuan, A., 2017. PI3K/AKT/mTOR Signaling Mediates Valproic Acid-Induced Neuronal Differentiation of Neural Stem Cells through Epigenetic Modifications. Stem Cell Reports 8, 1256-1269.

Zhang, X., Zhang, L., Cheng, X., Guo, Y., Sun, X., Chen, G., Li, H., Li, P., Lu, X., Tian, M., Qin, J., Zhou, H., Jin, G., 2014. IGF-1 promotes Brn-4 expression and neuronal differentiation of neural stem cells via the PI3K/Akt pathway. PLoS One 9, e113801.

Zhang, Y., Gao, X., Saucedo, L.J., Ru, B., Edgar, B.A., Pan, D., 2003b. Rheb is a direct target of the tuberous sclerosis tumour suppressor proteins. Nat Cell Biol 5, 578-581.

Zhang, Y., Sastre, D., Wang, F., 2018. CRISPR/Cas9 Genome Editing: A Promising Tool for Therapeutic Applications of Induced Pluripotent Stem Cells. Curr Stem Cell Res Ther 13, 243-251.

Zhao, X.Y., Li, W., Lv, Z., Liu, L., Tong, M., Hai, T., Hao, J., Guo, C.L., Wang, X., Wang, L., Zeng, F., Zhou, Q., 2010. Efficient and rapid generation of induced pluripotent stem cells using an alternative culture medium. Cell Res 20, 383-386.

Zheng, X.F., Florentino, D., Chen, J., Crabtree, G.R., Schreiber, S.L., 1995. TOR kinase domains are required for two distinct functions, only one of which is inhibited by rapamycin. Cell 82, 121-130.

Zhou, J., Shrikhande, G., Xu, J., McKay, R.M., Burns, D.K., Johnson, J.E., Parada, L.F., 2011. Tsc1 mutant neural stem/progenitor cells exhibit migration deficits and give rise to subependymal lesions in the lateral ventricle. Genes Dev 25, 1595-1600.

Zhu, Y., Li, H., Zhou, L., Wu, J.Y., Rao, Y., 1999. Cellular and molecular guidance of GABAergic neuronal migration from an extracortical origin to the neocortex. Neuron 23, 473-485.